Cape Peninsula
University of Technology

ADSORPTION OF PERFLUORINATED WATER CONTAMINANTS ON MICROPOROUS *AGAVE SISALANA* ACTIVATED CARBON FIBRE

by

Serge Mapan Imwer

Thesis submitted in fulfilment of the requirements for the degree

Magister Technologiae: Chemical Engineering

in the Faculty of Engineering

at the

Cape Peninsula University of Technology

Supervisor: Dr. S.K.O. Ntwampe

Co-Supervisor: Prof. M.S. Sheldon

Cape Town

2014

DECLARATION

I, **Serge Mapan Imwer**, declare that the contents of this thesis represent my own work, and that the thesis has not previously been submitted for academic examination towards any qualification. Furthermore, it represents my own opinions and not necessarily those of the Cape Peninsula University of Technology and the National Research Foundation of South Africa.

Signed **Date**

ABSTRACT

An awareness campaign on the harmful effects of Perfluorinated compounds (PFCs), especially Perfluorooctanoic acid (PFOA) and Perfluorooctane sulfonate (PFOS) has been conducted to inform the general public about the impact of these organic compounds on humans and biota. These compounds have been shown to be potential carcinogens, as indicated by the United States Environmental Protection Agency (USEPA) and the Organization for Economic Co-operation and Development . A major concern about these chemicals is that they have been widely used in consumer products and have been detected in food and drinking water. They have been determined to be resistant to biological degradation, owing to their unique chemical and physical properties (fluorine atoms that have substituted hydrogen atoms in their chemical structure). Owing to their characteristics of being highly soluble in water, they cannot be removed from water using ordinary purification processes. Studies have been conducted to evaluate the removal of PFOA and PFOS from water using different methods. Among these methods, it has been proved that adsorption is a suitable method with the best adsorbent identified as activated carbon (AC). AC can be found in many forms, including as a fibre. The use of AC for the removal of PCFs can be augmented with sonication and electro-chemical methods for rapid absorption of these compounds. The aim of this study was to remove these contaminants using a microporous AC fibre (ACF) made from an indigenous plant, *Agave sisalana,* which is widely available across sub-Saharan Africa, by using electro-physico-chemical methods. ACF has the following advantages when compared with granulated and/or powdered AC: it has a slightly larger reactive surface area; small quantities can be used; it is easily handled; it retains its shape under stress, thus does not require additional filtration to remove particulate residue; and can be regenerated easily.

The manufacturing process of the ACF was done in several steps: 1) harvesting of the *A. sisalana* leaves, stripping them to obtain wet fibre by scrapping using traditional methods, 2) chemical activation using NaOH, KOH, $ZnCl_2$ and H_3PO_4, employing a spraying method instead of soaking, which was followed by drying, and 3) carbonisation in a furnace at the required temperature. The use of activation reagents involved the determination of an appropriate concentration, with optimum concentrations determined as 0.54M, 0.625M, 1.59M and 0.73M for NaOH, KOH, $ZnCl_2$ and H_3PO_4, respectively. Apart from the fibre activation, temperature and activation time were also important parameters that were optimised. A response surface methodology was used to design a set of experiments that provided the optimum temperature and activation time. From the input variables, the Expert design soft-

ware generated experimental runs (n = 13) for each fibre activation reagent used with a temperature range of 450°C to 933°C being assessed for carbonisation time of between 17 to 208 minutes. ACF activated with KOH (0.54 M) and characterised by micropores with the highest surface area achieved being 1285.8 m^2/g in comparison with Granular activated carbon (Ounas *et al.*, 2009) with an average surface area range of 1000 to 1100 m^2/g. This surface area was measured using Dubinin-Astakhov isotherm with CO_2 at 273 K. The physical characteristics of the ACF were analysed using a Scanning Electron Microscope to ascertain the integrity of the fibres.

PFOA and PFOS were analysed using a solid phase extraction (SPE) method followed by analysis using a liquid chromatography/tandem mass spectrometer (SPE-LC/MS/MS). The water sample volume used for extraction was 60 mL. The instrument used was an HPLC - Ultimate 3000 Dionex HPLC system and MS model - Amazon SL Ion Trap, with the following MS/MS operational conditions and ion mode: MS Interface → ESI; dry temp → 350°C; nebulising pressure → 60 psi; dry gas flow → 10 L/min; ionisation mode → negative; capillary voltage → +4500V; end plate offset → −500V, while the separation column was a Waters Sunfire C18, 5 µm, 4.6 × 150 mm column (supplier: Waters, Dublin, Ireland), with an operational temperature of 30°C.

Initially, adsorption studies (n = 48) using sonication (20 kHz) in batch systems indicated efficient removal of PFOA and PFOS within 120 min, with numerous samples (n = 14) achieving complete removal for both PFOA and PFOS. The minimum removal rates observed were 65.55% for PFOA and 95.92% for PFOS. From the ACF samples in which highest removal rates were achieved, a number (n = 3) of the ACF samples were selected for surface characterisation. Based on the sonication in the previous experiments, an electro-physico-chemical adsorption regime was designed, to facilitate the rapid adsorption of PFOS and PFOA from contaminated drinking water in an electrolytic cell. In these experiments, simultaneous sonication and electrolysis were used. A comparison was made between ACF produced in this study and the commercial activated carbon. The result revealed that adsorption of PFOA and PFOS on ACF was a monolayer adsorption type phenomenon and had the best fit using a Freundlich isotherm compared with the Langmuir isotherm. Adsorption of PFOA and PFOS on the commercial AC presented a multilayer adsorption type of isotherm fit with the Langmuir isotherm having the best fit compared with the Freundlich isotherm.

ACKNOWLEDGMENTS

I would like to take this opportunity to thank all individuals and institutions that have contributed to the completion of this study.

- First and foremost, Jesus Christ, for giving me the courage and strength to complete this study.
- My supervisors, Dr. Karabo S. Ntwampe, and Prof. Marshall Sheldon, for their expertise, tireless support, and research strategies they provided.
- The technical officers of the Department of Chemical Engineering and the Faculty of Applied Sciences, Hannelene Small, Alwyn Bester and Lorna Marshall, for their assistance when needed.
- The librarian officers Lara Skelly, Nathan Kalam and Rolf Proske at the Postgraduate Research Information Support Centre for their support, technical advises and willingness to assist when needed during the preparation of this thesis.
- My colleagues, Dr. Debbie de Jager, Dr. James Doughari, Thando Ndlovu, Lukhanyo Mekuto, Innocentia Erdogan, Bruno Santos, John Mudumbi, Lizzy Muedi, Aime Mume, Patrick Waka, Rita Abaajeh, Luc Ilunga, Mwema Wanjiya, Steve Tshilumbu, Butteur Mulumba, Marc Tshibangu, Jim Chiyen, Joseph Kapuku and all other colleagues, for their encouragement and for providing such an enthusiastic learning research environment.
- The National Research Foundation for financial support of this research.
- My wife, Gina Mujinga Tshilenge. Your support at all stages of this study is appreciated.
- Last but not least, the Mapan family, Arsene, Cyrin, Stephy-Renaud, Olga, Mireille, Paul and Olivier, whose love, support and encouragement, have made everything possible. It means more to me than I can express in words. I love you all and am extremely fortunate to have you. I share this with you!

DEDICATION

To my parents

Faustin Mapan Ipamakom Yiriyo

and

Madeleine Mutani Mubembel

TABLE OF CONTENTS

LIST OF FIGURES

LIST OF TABLES

LIST OF SYMBOLS

		Units
A	Koble–Corrigan parameter 1	-
B	Koble–Corrigan parameter 2	-
B_{DR}	Dubinin–Radushkevich isotherm constant	[mol^2/kJ^2]
B_1	Temkin constant related to the heat of adsorption	-
C_{BET}	BET adsorption	m^2/kg
C_e	Equilibrium concentration of the adsorbate	[mg/L]
C_s	Adsorbate monolayer saturation concentration	[mg/L]
E	Gaussian energy distribution	[kJ/mol]
K_F	Freundlich constant, distribution coefficient and represents the quantity of adsorbate adsorbed onto the adsorbent for a unit equilibrium concentration	[mg/g[L/mg]^n]
K_{FH}	Flory–Huggins isotherm constant indicative of the equilibrium constant	-
K_R	Redlich–Peterson constant 2	[L/g]
K_T	Equilibrium binding function constant	[L/mol]
L	The nucleus slit width	[µm]
N	Amount of adsorbed	[mg/L]
P	Equilibrium pressure	[kPa]
P_s	Vapour pressure	[kPa]
Q	Sorption capacity	-
Q_o	Langmuir constant related to adsorption capacity	-
R	Ideal gas constant	[J/mol °C]
T	Temperature	[°C]

V	Maximum adsorption velocity	$[s^{-1}]$
W	The amount of gas adsorbed	[L/g]
W_0	Volume of micropores	$[m^3/g]$
a_K	Khan model exponent	-
a_R	Radke–Prausnitz model constant 1	[L/g]
a_{RP}	Redlich–Peterson constant 1	[L/mg]
b	Langmuir constants related to the rate of adsorption	$[mg^{-1}]$
b*	Sip Isotherm parameter 2,	$[kPa^{-1}]$
b_K	Khan model constant	-
b_T	Toth's model exponent 2	-
d	Interlayer spacing	m
n	Freundlich constant, indicates the favourability of the adsorption process	-
n*	Sip isotherm parameter 3,	-
nh	Hill coefficient	-
n_T	Toth's model exponent 1	-
q_e	Amount of adsorbate adsorbed per unit mass of adsorbate	[mg/g]
q_m	Sip isotherm parameter 1,	[mmol/g]
q_s	Theoretical isotherm saturation capacity	[mg/g]
r	Inverse of distance from the surface	m^{-1}
r_R	Radke–Prausnitz model constant 2	-
s	The substrate/contaminant concentration	[mg/L]
v	Primary adsorption velocity	s^{-1}
z	The distance of adsorbate molecule from the surface atom in a slit wall	[m]

x_{FH}	Constant indicative of the isotherm adsorption exponent	-
ΔG°	Gibbs energy	[J/°C]
α	Frenkel–Halsey–Hill isotherm constant	[Jm^r/mole]
β	Redlich–Peterson constant 3	-
β_R	Radke–Prausnitz model exponent 3	-
σ	the distance from surface atom at zero interaction energy	[m]
θ	Degree of the surface coverage	-
$\mathcal{E}$	The potential energy of interaction	J
$\mathcal{E}^*$	potential energy minimum	J

GLOSSARY

- **Absorption**: Penetration of molecules into the bulk of a solid or liquid, forming either a solution or compound. Absorption can be a chemical process or a physical process.
- **Adsorption** - a method widely used in industry to accumulate molecules of a known compound/substance on a defined film or a surface of a solid.
- **Adsorbent**: A substance that collects molecules of another substance on its surface.
- **Desorption**: Desorption is a phenomenon whereby a substance is released from or through a surface.
- **Perfluorinated compounds/polyfluoroalkyl compounds (PFCs)** - synthetic fluorinated organic compounds used in some consumer products and industrial applications. The chemical structure of PFCs consists of a hydrophobic alkyl chain and a hydrophilic functional group. This gives these compounds desirable unique physical and chemical properties such as high thermal and chemical stability; water and fat repellent properties; and low surface free energy.
- **Perfluorooctanoic acid/perfluorooctanoate (PFOA)** - a synthetic, stable perfluorinated carboxylic acid and fluorosurfactant. [CAS number is 335-67-1].
- **Perfluorooctane sulfonate/perfluorooctanesulfonic acid (PFOS)** -a man-made fluorosurfactant and global pollutant [CAS number is 1763-23-1].
- **Mesoporous** - materials or any solid with a porous structure in which the pore diameter sizes are in the range of 2 to 50 nm.
- **Microporous** - materials or any solid with a porous structure in which the pore diameter sizes are <1.42 nm.
- **Activated carbon (AC)** - forms of carbon that has been processed to be highly porous and has large surface area available for adsorption or chemical reactions.
- **Granular activated carbon** – a granular form of activated carbon which has been retained on a 50-mesh sieve size (0.297 mm).
- **Activated carbon fibre (ACF)** – activated carbon made from a fibrous raw material.
- ***Agave sisalana*** – a tropical plant which is cultivated for its fibres that are extracted from the leaves.
- **Sorbate**: a material that has been or is capable of being taken up by another substance by either absorption or adsorption material.
- **Sorbent**: insoluble materials or mixtures of materials used to recover liquids through the mechanism of absorption, or adsorption, or both.

- **Sorption**: A general term used to encompass the processes of absorption, adsorption, ion exchange, and chemisorptions.
- **Chemisorption:** is a sub-class of adsorption, driven by a chemical reaction occurring at the exposed surface. A new chemical species is generated at the adsorbant surface.
- **Telomerization :** chem polymerization in the presence of a chain transfer agent to yield a series of products of low molecular weight
- **Fluorination:** A chemical reaction that introduces fluorine into a compound.

ABBREVIATIONS

ACF:	Activated carbon fibre
GAC:	Granular activated carbon
OECD:	Organisation for Economic Co-operation and Development
PAC:	Powdered activated carbon
PFAS:	Perfluoroalkyl sulfonates
PFC:	Perfluorinated compound
PFCA:	Perlfuorocarboxylate acid
PFOA:	Perfluorooctanoic acid
PFOS:	Perfluorooctane sulfonate
USEPA:	US Environmental Protection Agency

CHAPTER ONE
INTRODUCTION

1.1 Background to the research

Perfluorooctanoic acid (PFOA) and perfluorooctane sulfonate (PFOS) are inert chemical compounds that have been determined to be bio-accumulative, persistent and major environmental pollutants in water. They have been used in many industrial processes and are found in Teflon-based cookware, drinking tap water and various media (Herrera & Alvarez, 2008). As these compounds are highly soluble in water, they contaminate environmental water sources, that is, ground water, surface water and river water (Yu *et al.*, 2009). PFOA and PFOS have been reported to be harmful to humans, and determined to be potential carcinogens (Organisation Economic co-operation and Development (OECD), 2002). Owing to their detrimental effect on humans, research on PFCs as environmental contaminants has being documented worldwide in recent years because of their extensive use in lubricants, surfactants, fire retardants, adhesives, paper-coats, refrigerants, propellants and agrochemicals. The Organisation for Economic Co-operation and Development issued a hazard assessment for PFOS and PFOA, including their salts, during the year 2002. In 2003, the US Environmental Protection Agency (USEPA) issued a preliminary risk assessment report which focused on the toxicity associated with exposure to perfluorinated compounds (PFCs), in particular PFOA and PFOS and their salts. Furthermore, the USEPA gave a directive to the manufacturers in 2006 to decrease PFOA emissions and content in products by 95% before 2010 with the aim of complete eradication by 2015 (Wang *et al.*, 2008). This was a legislative measure to reduce the associated harmful effects of these compounds on humans.

The unique properties of PFOA and PFOS, which make them suitable for various industrial applications and non-biodegradability, are the lack of carbon-hydrogen (C–H) bonds in their structure, which are replaced by carbon-fluorine (C–F) bonds (Renner, 2001; Qiu, 2007). As a result, these compounds are thermodynamically stable, which makes them non-biodegradable.

Their presence in the environment has been reported in several countries and recently in South Africa (Mudumbi, 2012). For example, in a study conducted in the USA, the presence of PFOA in potable water in Washington and Virginia was determined to be in the range of 1.9 to 4.9 ng PFOA/L (Bartell *et al.*, 2010), with the median PFOA concentration in human sera being 8.75 ng PFOA/L (range 4 to 21 ng PFOA/L) (Steenland *et al.*, 2010), indicating a possible continuous exposure or ingestion. Similarly, the presence of PFOS and PFOA was detected and quantified in tap water in China, with the concentration range of

<0.1 to 14.8 ng/L and <0.1 to 45 ng/L for PFOS and PFOA, respectively (Jin *et al*., 2009). A similar survey was done in South Africa (SA), where the presence of PFOS and PFOA in maternal serum and cord blood of South African women was determined in a range of 0.5 to 16 ng/mL and 0.4 to 8.5 ng/mL, respectively (Hanssen *et al.*, 2010). This prompted a study to assess PFOA and PFOS concentrations in the drinking water of the Western Cape, South Africa (Booi, 2013). The results indicated a widespread contaminate of PFOA and PFOS in drinking water, including river water used to irrigate agricultural produce (Mudumbi, 2012). The major concern about PFOA and PFOS present in drinking water is that they do have harmful effects on animals and humans. It has also been reported that exposure to higher concentrations of PFOA and PFOS is directly related to thyroid diseases. Furthermore, PFOS has been positively identified to have carcinogenic effects (OECD, 2002; Melzer *et al*., 2010). Several methods for water purification and recycling have been proposed and used with a varying degree of success for contaminant removal. The most important tertiary treatment methods are: reverse osmosis (RO), electrodialysis, ion exchange and electrolysis. However, most of these methods have been determined to be ineffective when used to eradicate PFOS and PFOA. These methods incur high operational and infrastructural investment costs which result in associated costs of 10 to 450 USD (~ 105.9 to 4765.5 ZAR) per million litres of water treated. The cost of treated water by adsorption varies from 10 to 200 USD to ~ 105.9 to 2118 ZAR) per million litres (Ali & Gupta, 2007); this means that adsorption processes are faster, less expensive and can be widely used, even in areas in which there is a lack of water treatment infrastructure (Jain *et al.*, 2002; Ali & Gupta, 2007) – a situation commonly found in rural South Africa. Furthermore, the application of conventional treatments for the removal of anionic PFC surfactants from aqueous steams in these areas is restricted by technical and/or economic constraints (Herrera & Alvarez, 2008), and adsorption using a readily available bioresource, offers the best possible solution.

Many studies have published information on the removal of PFOS and PFOA by adsorption. A comparison was made whereby powdered activated carbon (PAC), granulated activated carbon(Ounas *et al.*) (Ounas *et al.*, 2009), and ion exchange resin (AI400) were evaluated for the removal of PFOA and PFOS from water. It was found that the adsorbent size influenced the sorption kinetics with activated carbon (AC) being effective in comparison with ion exchange (Yu *et al.*, 2009). In another study, organo-montmorillonites were also used as sorbents for the removal of PFOS from water and the sorption isotherms showed that the sorption quantity of PFOS onto these montmorillomites was higher compared with metallic-montmorillonites (Zhou *et al.*, 2010). Another comparison was made between granular activated carbon , zeolites and sludge, whereby the adsorption of PFOS and PFOA from aqueous solutions onto GAC was demonstrated to be effective, followed by zeolites and

sludge (Herrera & Alvarez, 2008). The sorbent most frequently used currently is activated carbon and it can be in the form of GAC, PAC or activated carbon fibre (ACF).

Apart from GAC and PAC, ACF can also be used as an adsorbent. The versatility of ACF was demonstrated in a study where silver (Ag) was immobilised onto supporting ACF fibres to create an ACF-Ag fibre, which showed antibacterial activity against *Escherichia coli* and *Staphylococcus aureus*. It has been shown that *Agave sisalana*, viscose and pitch fibres can be used as precursors for ACF (Chen *et al.*, 2005). Additionally, it was demonstrated by Shuixia *et al.* (1998) that *A. sisalana*-based ACF can be an effective biosorbent. The study was based on the adsorption of dyes onto the fibres, as a sustainable way of water treatment for water containing environmental pollutants (Shuixia *et al.*, 1998). For this thesis, a widely available fibrous source, even in rural areas, *Agave sisalana*, was proposed and evaluated as an effective sorbent for the removal of PFOA and PFOS from drinking water, both in its original form and the proposed ACF form.

1.2 Research statement

The use of activated carbon requires filtration after adsorption has taken place; this factor would compromise the use of activated carbon especially on an industrial scale. Therefore, ACF usage would be better because of ease handling and thus does not necessarily require filtration facilities.

The work presented in this thesis was therefore to evaluate a method by which PFOS and PFOA can be removed from contaminated water using activated carbon fibre obtained from an indigenous African plant, that is, *Agave sisalana*. The sisal fibre was transformed into ACF by chemical activation and carbonisation.

1.3 Hypothesis of the research

It was hypothesised that sisal fibres as raw material can be used to produce an ACF sorbent that can effectively adsorb PFOA and PFOS from water. The following questions were addressed during the research study:

1) What will be a suitable activation reagent and its concentration for the production of the sisal ACF?

2) Can sisal fibre and sisal-based ACF be used effectively as an adsorbent for the simultaneous removal of PFOS and PFOA?

3) Can the produced ACF be comparable to the GAC in terms of PFOA and PFOS adsorption capacity?

4) Which of the activating agents will provide ACF with a higher surface area and better PFOA and PFOS removal capabilities?

5) Which adsorption isotherm models are suitable for modelling adsorption kinetics of PFOA and PFOS onto the ACF? That is, which of the isotherm models is suitable for modelling the adsorption of PFOA and PFOS on the ACF?

1.4 Research objectives

The objectives of the present study were to:

1) determine the optimum activation reagent concentration suitable for the sisal fibre;
2) evaluate the adsorption capacity of the sisal-activated carbon fibre (ACF) for PFOA and PFOS removal using different activation reagents;
3) characterise the surface properties of the sisal-ACF with a higher removal of PFOA and PFOS; and
4) model adsorption kinetics of PFOA and PFOS on to the sisal fibre and sisal-based ACF, using available adsorption isotherms for modelling with assisted electro-physico-chemical assisted adsorption for rapid removal of PFOA and PFOS from drinking water.

1.5 Significance of the study

The presence of PFCs in the environment has been noted by several researchers worldwide, including in South Africa. There has been no study on the adsorption of PFOA and PFOS using South African treated drinking water. This includes the removal of PFOS and PFOA using ACF from *Agave sisalana*. This study investigates a cost-effective technique for the removal of PFCs from raw and treated drinking water, from the South African environment.

1.6 Delineation of the thesis

The study focused only on the removal of PFOS and PFOA in PFC-contaminated treated drinking water. The health effects, localisation of PFCs in the pore of the fibre and their source were not covered by this study.

CHAPTER TWO
LITERATURE REVIEW: PERFLUORINATED COMPOUNDS

2.1 Production of fluorinated compounds

Fluorination of organic compounds starts with the use of fluorine gas, which is the most abundant and reactive gas among halogen gases (Qiu, 2007). The compounds used as feedstock have one or more carbon-hydrogen (C-H) bond which is replaced by carbon-fluorine (C-F) bonds, resulting in fluoro-organic compounds. Because of a high electro-negativity of fluorine in comparison with other halogens, the C-F bonds have a stronger polarity, including strength, and is one of the most thermodynamically stable bonds known. The C-F bond gives fluoro-organic compounds many of their unique properties. These chemicals repel water and oils, and can reduce the surface tension of water better than most surfactants. In perfluorinated chemicals, all C-H bonds are replaced by C-F bonds (Renner, 2001; Qiu, 2007); this makes them non-degradable, with a half-life of several years.

2.2 Properties of perfluorinated compounds (PFCs)

This section discusses properties of perfluorinated compounds (PFCs), in particular perfluorooctanoic acid (PFOA) and perflurooctane sulfonate (PFOS) as shown in Table 2.1.

Table 2.1: Physico-chemical properties of PFOA and PFOS (Qiu, 2007; Kunacheva, 2009)

Properties	PFOA	PFOS
Molecular weight	413	499
Chemical formula	$CF_3(CF_2)_6COO^-$	$CF_3(CF_2)_7SO_3^-$
Melting point (°C)	45 - 50	≥400
Boiling point °C (kPa)	189 - 192 (100 kPa)	n/d
Vapour pressure	1.33 kPa (25°C)	$3.31x10^{-7}$ kPa (20°C)
Solubility in pure water (g/L)	3.4	0.57 (in pure water)
Air/water partition coefficient	unknown	$< 2x10^{-6}$
pK_a	2.5	-3.27
pH	2.6 (at 1/g/L)	7 - 8 (salt of PFOS)
Specific gravity	1.70	2.05
Appearance	White powder	White powder

Among several PFCs that have been studied over the years, PFOS [$CF_3(CF_2)_7SO_3^-$] and PFOA [$CF_3(CF_2)_6COO^-$] are among the most commonly found in various environmental matrices, such as water, soil and plants. These two PFCs are completely fluorinated organic compounds and can be produced synthetically or through the degradation of other fluoro-chemical products (Kunacheva, 2009). PFOA and PFOS are distinctive products of their group, perfluorocarboxylates and perfluoroalkyl sulfonates, respectively. These two PFCs are commonly named 'C8s', due to the eight carbon atoms in their structure. Their behaviour as fluoro-surfactants arises from their unique properties owing to the elemental fluorine in their structure. Properties of fluorine, which in turn are embedded into these fluorinated compounds, are as follows (Kissa, 2001):

1) High oxidation potential, since fluorine has an oxidation potential of E_o = -2.65 V.
2) High electro-affinity.
3) High ionisation energy.
4) High electro-negativity of covalently bonded fluorine, as fluorine is a electronegative element.
5) Low dissociation energy.

Inherently, PFCs such as PFOA and PFOS will have some of these properties, as all C-H bonds are replaced by C-F bonds. PFOA and PFOS molecules are built on a PFC chain (see structure in Figure 2.1) and can have a functional group, whereby a carboxylic or sulfonic group can be an affiliate to make PFCs hydrophilic. Owing to the perfluorinated carbon chain with C-F bonds, the bonds protect the PFC molecule from breaking down by oxidative radicals. Furthermore, the hydrophobic functional group-like properties, depending on the PFC molecule, can impart surfactant-like properties, resulting in the combination of hydrophobic and hydrophilic groups which further results in the stability of the compounds under extreme thermal and oxidative conditions (Qiu, 2007).

Perfluoro-octanoate acid	Perfluoro-octane sulfonate
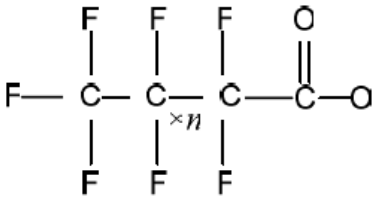	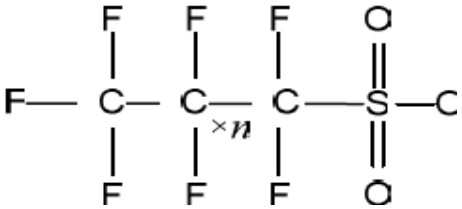
$CF_3(CF_2)_6COO^-$	$CF_3(CF_2)_7SO_3^-$
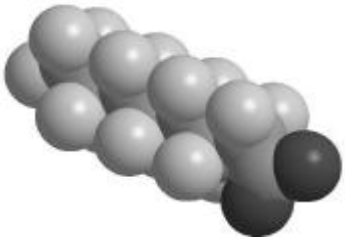	
PFOA	PFOS

Figure 2. 1: Structure of PFOA and PFOS (Qiu, 2007)

The physico-chemical properties of PFOA and PFOS indicate stable chemicals for use in industrial applications (see Figure 2.1 for structural analysis). However, their non-biodegradability, is mainly due to the effect of the cumulative C-F bonds. Overall, PFOA and PFOS are, respectively, surfactant and fluoro-surfactant, and lower the surface tension of water more than any other hydrocarbon surfactants (Kissa 2001; Lemal, 2004, cited in Kunacheva, 2009).

2.3 Production of perfluorinated compounds (PFCs)

Manufacturing processes by which PFCs are formed, use electro-chemical fluorination (ECF) and telomerisation, whereby two major classes of PFCs, namely perfluoroalkyl sulfonates (PFASs) and perlfuorocarboxylate acid (PFCAs), are produced as depicted in Figure 2.2 (Qiu, 2007; Renner, 2001).

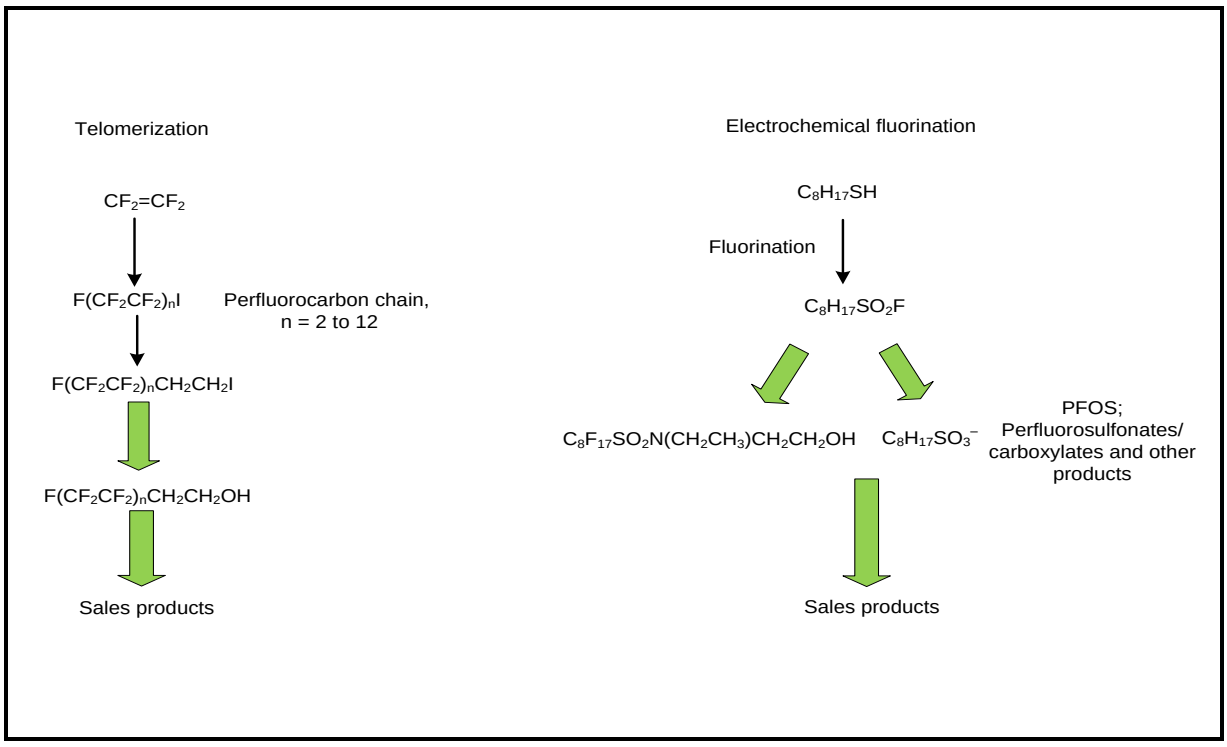

Figure 2.2: Manufacturing processes for PFCs, electrochemical fluorination and telomerisation plant (Renner, 2001)

2.3.1 Producing fluorinated compounds using electrochemical fluorination

In 1945, Dr. Simons developed an electro-chemical fluorination (ECF) method for PFC production at Penn State University. The procedure was then adopted by the 3M Company in their process to produce organofluorine chemicals. Anhydrous hydrofluoric acid is utilised in electrochemical fluorination as a fluorine source (Qiu, 2007; Kissa, 2001; Noel *et al.*, 1997).

The organic substance to be fluorinated is dispersed or dissolved in a hydrogen fluoride solution and a direct electric current of a voltage between 5 and 10 V, current densities of 100 - 200 A/m^2 and electrolyte temperatures of 0 to 20°C are used. Cooling the electrolyte is required to dissipate the heat from the process while, the current is passed through the electrolyte. To recover the hydrogen fluoride in the hydrogen gas escaping from the cell, the gas is cooled down in a condenser, so that the hydrogen fluorine recovered can be redirected to the cell for further use. Hydrogen gas escapes on the cathode, while perfluorination occurs at the anode. The electrochemical fluorination reaction for the production of the perfluoroalkylsulfonyl fluorides is shown in Eq. 2.1:

$$C_nH_{(2n+1)}SO_2F+(2n+1)HF \xrightarrow{n.53.6\ Ah} C_nF_{(2n+1)}SO_2F+(2n+1)H_2 \quad 2.1$$

These perfluoroalkyl sulfonyls are used as raw materials for flame retardants, fire extinguishing agents, textile oleophobising agents, flow improvers for paint systems and emulsifiers for the polymerisation of tetrafluoroethene (Noel *et al.*, 1997).

2.3.2 Producing fluorinated compounds using telomerisation

The raw materials of telomerisation process are perfluoroalkyl iodine and tetrafluoroethylene. The most important among several perfluoroalkyl iodines used in the telomerisation process is pentafluoroethyl iodine. The process is based on the addition of iodine fluoride to tetrafluoroethylene; however, the iodine fluoride is unstable to be isolated and is consequently formed from iodine pentafluoride in situ. Tetrafluoroethylene reacts with iodine pentafluoride and iodine under pressure in the presence of a catalyst like antimony trifluoride, according to the following stoichiometric equation (Kissa, 2001):

$$5CF_2=CF_2+IF_5+2I_2 \xrightarrow{SbF_3} 5CF_3CF_2I \quad 2.2$$

Then, the formed hexafluoro isopropylene reacts with iodine fluoride and iodine to form heptafluoroisopropyl iodide (Kissa, 2001):

$$5CF_3CF=CF_2I + IF_5 + 2I_2 \xrightarrow{SbF_3} 5(CF_3)_2CFI \quad 2.3$$

The heptafluoroisopropyl iodide as a telomerisation agent produces telomers featuring a branched fluorocarbon chain. This telomerisation process was first developed by the Du Pont Company for radical polymerisation of ethylene. Besides PFOS, the telomerisation process can be used to produce Fluorotelomer B alcohol, FTOH ($C_8F_{17}C_2C_2H_4OH$) (Kissa, 2001; Renner, 2001; Parsons *et al.*, 2008).

2.4 Application of perfluorinated compounds

The products produced by either telomerisation or electrofluorination can be used in a diversity of products that can be divided into several categories, such as surface treatment, paper protection and industrial/high-performance chemicals. Table 2.2 shows products and uses of both PFOA and PFOS.

Table 2.2: PFOA and PFOS products and uses (Parsons *et al.*, 2008; Renner, 2001; Kissa, 2001)

PFOA products	Salts	Fluoropolymers	Fluoroelastomers	Other products
		Non-stick cookware and breathable stain-resistant all-weather clothing	Transportation (automotive, aerospace, small engine) Pharmaceutical and food processing Fluid handling and environmental control system Oil, gas and mineral extraction	Alcohols Silanes Alkoxylates Fatty Acid Esters Adipates Urethanes Polyesters Acrylates Copolymers Phosphate Esters
PFOS products	K; Li; DEA; NH_4 salts	Amines; quaternary ammonium salts; amphoterics	Carboxylates Oxazolidinones Amides	
		USES		
	Surfactant in firefighting foam Surfactant for alkaline cleaners Emulsifier in floor polish Mist suppressant for metal plating baths Surfactant for; etching acids, circuit boards pesticide active ingredient and ant bait traps	Mist suppressant for metal plating bath; water/solvent repellent for leather/paper	Antistatic agent in photographic paper; waterproofing casts/wound dressings; pesticide active ingredient	Soil/oil/water repellent for carpet, fabric/upholstery, apparel leather, metal/glass Oil/water repellent for plates, food containers, bags, wraps folding, cartons, containers, carbonless forms, masking papers

For example, in surface treatment applications, PFOS is designed to be used for surface treatment applications, as it is oil, water and soil repellent. It is applied to home furnishings and personal clothes. Other uses in this category are the protection of leather, clothes, fabric (upholstery) and carpets, which are the main products of leather tanneries, textile mills, carpet manufacturers and fibre producers. These attributes make PFOS a suitable agent for paper protection, in particular for the masking of papers, folding cartons, carbonless paper forms and containers, as well as wrappers, paper plates, bags and food containers (Kissa, 2001; Renner, 2001; Qiu, 2007). As a high-performance chemical, PFOS is used in mining, fire-fighting foams and oil-well surfactants, acid suppressants for metal plating and electronic etching baths, electronic chemicals, hydraulic fluid additives, photolithography, floor polishes, alkaline cleaners, photography film, denture cleaners, chemical intermediates, shampoos, coating additives, as well as in insecticides (Kissa, 2001; Organisation Economic co-operation and Development (OECD), 2002; Qiu, 2007).

PFOA is primarily used as a reactive intermediate, while its salts are used in the production of fluoropolymers which are utilised in the manufacture of non-stick cookware and breathable, stain resistant, all-weather clothing (Melzer *et al.*, 2010; Moore, 2010), and fluoroelastomers and in other surfactant uses (Midasch *et al.*, 2007). Furthermore, the principal use of PFOA is in the production of Teflon and its associate products. Additionally, as a stable fluoro-surfactant, its applications are similar to those of PFOS, that is, oil and water repellents in the processing of fabrics and leather, including the manufacture of waxed papers and floor waxes (Ylinen *et al.*, 1985).

2.5 Hazards associated with perfluorinated compounds (PFCs)

For 50 years, PFCs have been produced and used in consumer products before being considered persistent, bioaccumulative and toxic, with possible carcinogenic properties(Renner, 2001; OECD, 2002; Stahl *et al*., 2009).

2.5.1 Bioaccumulation potential of perfluorinated compounds (PFCs)

In a study by Stahl *et al.* (2009), it was shown how perfluorinated compounds, specifically PFOA and PFOS, can be carried over from the soil to edible plants such as wheat, oats, potatoes and maize, whereby they can find a possible route into foodstuffs and as a result into the human body. A study on the biosorption of different concentration levels of PFOS (0.1 to 200 $mg.L^{-1}$) onto wheat seedlings showed that low levels of PFOS may slightly stimulate the growth of the seedlings as well as provoke the synthesis of chlorophyll and soluble protein in the seedlings – a phenomenon associated with surfactant-like properties of

PFOS which can influence the nutrient sorption rates. Higher concentrations of PFOS showed inhibition of root elongation, reduction in the total chlorophyll content in the wheat leaves, and soluble protein in the wheat roots. Furthermore, the antioxidant enzyme activity of wheat seedlings was altered with increasing concentration of PFOS (Huang *et al.*, 2010).

As PFCs have surfactant-like properties, they are soluble in water, thus promoting metal and organic contaminants' sorption rates on plant materials. When present in sources of water where animals consume plant materials in riparian areas, or when present in water-borne plant debris, aquatic animal species such as fish consume the debris, and therefore the PFCs, resulting in their bioaccumulation in these animals. Thus they accumulate along the food chain. The accumulation of PFCs varies depending on the carbon chain length, from C8 to C15. As some of these animals are edible, this can result in PFC accumulation in humans (Whitacre, 2010). This assertion is based on the fact that contagion levels of PFOS were determined to be high in fish-eating animals living in continental areas (Renner, 2001). Similarly, seabird eggs have been found to contain PFCs and are part of traditional food for humans in northern Norway, providing further evidence of how PFCs find their way into the human diet (Verreault *et al.*, 2007).

The accumulation potential of PFCs was also demonstrated in a survey whereby PFOA, PFOS and other PFC concentrations were evaluated in herring gull eggs in two different locations for a period of 20 years, which indicated a cumulative pattern of accumulation, whereby PFOS was the dominant PFC with a concentration up to 42 ng/g wet weight (Verreault *et al.*, 2007). Furthermore, Huang *et al*. (2010) showed that zebra-fish embryos and larvae were accumulating PFOS with minimal elimination being observed. In the study, it was proved that exposure to various PFOS concentrations (0 to 8 mg/L) from 6 to 120 hours post-fertilization for embryos, including larvae, resulted in morphological malformations such as uninflated swim bladder and bent spine, altered spontaneous movement, irregular heart-beat rate and increased cellular death.

2.5.2 Presence of PFOA and PFOS in water

Perfluorocarbons have been used for several decades in various industries because of their properties. PFOA and PFOS are products of groups, perfluorocarboxylates and perfluoroalkyl sulfonates, respectively, among other perfluorinated chemicals. The major route of these pollutants in terms of environmental contamination is through contaminated water sources such as wastewater released by industries using water during manufacturing. Several studies have been done to assess their prevalence in natural water sources such as river-, sea-, and rainwater. Skutlarek *et al*. (2006) carried out a study to quantify the concen-

tration of perfluorinated surfactants in surface and drinking waters, where 12 different perfluorinated surfactants (PFOA and PFOS included) were found in German rivers (the Rhine River and its main tributaries, as well as the Moehne River), canals and drinking waters of the Ruhr catchment area. PFOA concentrations were 9 ng/L, 48 ng/L, 21 ng/L, 22 ng/L, 3640 ng/L, respectively, in the Rhine, Ruhr (Rhine's tributary), Lippe (Rhine's tributary), Emscher (Rhine's tributary) and Moehne Rivers. PFOS concentrations were 26 ng/L, 5 ng/L, 18 ng/L, 193 ng/L, respectively, in the Rhine, Ruhr (Rhine's tributary), Emscher (Rhine's tributary) and Moehne Rivers. The highest concentration of PFCs in drinking water collected from taps in the Ruhr and Moehne area, was 519 ng/L for PFOA (Skutlarek *et al.*, 2006).

In a similar study in China, PFOA and PFOS were found in environmental water samples (river, lake and ground water) and tap water. The highest concentrations for environmental water for PFOA and PFOS were 297.5 ng/L (Yanatze River) and 44.6 ng/L (Hu River), while the highest concentrations for tap water were 45.9 ng/L and 14.8 ng/L, respectively, for PFOA and PFOS sampled from the city of Shenzhen (Jin *et al.*, 2009). For California, where perfluorinated surfactants were found in recycled water from several wastewater plants, it was found that concentrations in the range of 90 to 470 ng/L for PFCs were detected, with PFOA being the predominant PFC followed by PFOS (Plumlee *et al.*, 2008).

Furthermore, Lein *et al*. (2008) conducted a study to survey PFOA and PFOS in surface water of the Yodo River (Japan) in order to develop contamination profiles for the river. It was determined that PFOA and PFOS were present with concentrations varying from 0.4 to 123 ng/L and from 4.2 to 2600 ng/L, respectively. Recently, a study conducted in the Western Cape (South Africa) in the three major rivers in the region, the Eerste, Diep and Salt Rivers, found PFOA and PFOS in higher concentrations than those reported in other countries. PFOA and PFOS were detected in concentrations of 23 and 146 ng/L for the Eerste River, 182 and 314 ng/L for the Diep River and 47 and 390 ng/L for the Salt River (Mudumbi, 2012). Some of this water is used for irrigation purposes, which in turn can result in contamination of agricultural produce intended for human consumption.

2.5.3 Eradication methods for perfluorocarbons in liquid samples

Several studies on the removal of pefluorinated compounds have been carried out internationally. A study on the removal of PFOS and two related PFCs, PFOA and perfluorobutane sulfonate (PFBS) was done in order to remove the contaminant from aqueous solutions and industrial effluents. The objective of the study was initially the elimination of PFOS, using the optimum sorption capacity obtained to make a comparison with alternative sorbents including zeolites. The highest sorption capacities were 1.2 g and 0.52 g per gram of

PAC for PFOA and PFOS, respectively (Yu *et al.*, 2009). In 2010, a study was initiated in order to eliminate PFOS specifically using orgono-montmorillonites with different microstructures. The results showed that the orgono-montmorillonites removed PFOS effectively up to 0.84 g of PFOS per gram from aqueous solutions (Zhou *et al.*, 2010).

In another study initiated in 2011, the adsorption of four PFCs, PFOS, PFOA, perfluorobutane sulfonate (PFBS) and perfluorobutanoate (PFBA) from landfill ground water was studied using granulated activated carbon (Ounas *et al.*, 2009). This study provided evidence that activated carbon adsorbs PFCs relative to the PFCs' chain length. Furthermore, the adsorption was improved with sonication. However, in the same study it was revealed that the effectiveness of the removal process was lower in landfill groundwater than in purified water (Zhao *et al.*, 2011), suggesting competitive sorption kinetics between other pollutants and PFCs. In the same year, another study was done on the adsorption of PFOA and PFOS on alumina, evaluating the influence of pH. The results showed that the adsorption equilibrium was reached after 48 hours and the sorption of PFOA and PFOS on alumina was 0.157 $\mu g/m^2$ and 0.252 $\mu g/m^2$, respectively, at a pH of 4.3 (Wang & Shih, 2011).

Table 2.3 presents recent studies (2012 – 2013) that have been carried out for the removal of PFCs, in particular, PFOS and PFOA. The removal of these PFCs was up to 99% for some processes in a period ranging from 90 min to 33 days. The removability of these PFCs was observed using novel methods as well as conventional methods used in water processing industry.

Table 2.3: Current, significant advances in the removal efficiency of perfluorocarbons (PFCs) using different removal methods/processes (2012 - 2013)

Compounds	Process used	Max. Removal efficiency (loading)	Time to reach equi-librium (min)	References
Adsorption using novel materials				
PFBA, PFPeA, PFHxA, PFOA, PFNA, PFDA, PFHxS, PFOS	Nano-filtration - NF270	>93% removal	47520	(Appleman *et al.*, 2013)
PFOA, PFBA and PFOS	Aminated rice husk (RH)	1.32 g PFOS/g RH	660	(Deng *et al.*, 2013)
PFOS	hexadecyltrimethylammonium bromide (HDTMAB) immobi-lized mesoporous SiO_2 hollow spheres	99%, from 1 mg/L	6000	(Zhou *et al.*, 2013)
Adsorption using conventional methods				
PFOS and PFOA	Oxidation - Ozonation	PFOA - 56% and PFOS - 42%	240	(Lin *et al.*, 2012)
PFOS and PFOA	Coagulation - Alum	<20% of PFOS and PFOA	90	(Xiao *et al.*, 2013)

perfluorobutyric acid (PFBA), perfluoropentanoic acid (PFPeA), perfluorohexanoic acid (PFHxA),perfluorononanoic acid (PFNA), perfluorodecanoic acid (PFDA), perfluorohexane sulfonic acid (PFHxS)

2.5.4 Activated carbon (AC): Applications

Activated carbons are extensively used in water purification processes in the waste-water industry or for removal of contaminants from drinkable water (Phan *et al.*, 2006; Suzuki, 1994). Three types of AC exist: activated carbon powdered (ACP), granular activated carbon(Ounas *et al.*) (Ounas *et al.*, 2009), as well as activated carbon fibre (ACF), which is the focus of this particular study (Phan *et al.*, 2006). The problems faced in the application of adsorption processes in water treatment are the slow rate of intra-particle diffusion for GAC and the complexity of handling in large quantities of ACP, although faster adsorption velocity is observed with ACP (Carrott *et al.*, 2001; Phan *et al.*, 2006). ACF has better adsorption characteristics when compared with ACP and GAC, making it usable on a large scale due to its ease handling. The thin fibre shape of ACF provides speedy intra-particle adsorption kinetics. ACF is therefore useful when designing adsorption units where intra-particle diffusion resistance is an important factor, resulting in significant reduction in the dimensions of the adsorption units (Suzuki, 1994). Because of the above-mentioned reasons, ACF was the preferred sorbent for this study.

2.5.5 Preparation of activated carbons using renewal resources

The manufacture of all types of AC follows the same procedure. Fundamentally, the preparation and manufacture of AC requires two major steps: firstly, the carbonisation of the carbonaceous raw material at a suitable temperature, in the absence of oxygen; and secondly, the activation of the carbonised product (i.e. char), which can be either a physical or chemical activation. Physical activation is a process occurring in two steps and it involves the activation of the consequential char at high temperatures in the presence of suitable oxidising gases such as carbon dioxide (CO_2), nitrogen (N_2), steam, or their mixtures. Activation in the presence of CO_2 is preferred as the activation process can be controlled owing to the slow reaction rate at high temperatures. The ACF obtained by physical activation renders a final product usable as either adsorbents or filters (Baquero *et al.*, 2003; Adinata *et al.*, 2007).

The chemical activation process is performed in a single step, by mixing the feedstock with chemical activating agents, which have both dehydrating and oxidative properties. Chemical activation presents numerous advantages as it is completed in a single step, merging carbonisation and activation, at lower temperatures, which results in the development of better porous structures (Adinata *et al.*, 2007). However, ACFs have thin fibre structure which facilitate the intra-particle adsorption kinetics from different sources (Suzuki, 1994).

Pitch fibre has also been used to produce ACF via steam activation (875°C) with a high BET surface area and was proved to be efficient for the removal of dyes (Tamai *et al.*, 1999).

Coconut shell and palm seeds were used to produce ACF using the zinc chloride ($ZnCl_2$) chemical activation method; thus a high micro- and meso-porosity was observed during this study (Hu *et al.*, 2001). Pitch fibre, sisal, and viscose were used as precursors to produce supported ACFs with chemical activation using phosphoric acid (H_3PO_4) as the activation reagent for a study on antibacterial activity (Chen *et al.*, 2005). Similarly, rubber wood sawdust from *Hevea brasiliensis* was used as the raw material to prepare ACF by chemical activation with H_3PO_4 for the adsorption of Cr(IV) from solution (Karthikeyan *et al.*, 2005). Palm shell was also used to prepare AC by chemical activation with potassium carbonate (K_2CO_3) as the activation reagent (Adinata *et al.*, 2007). Bamboo was used to prepare AC by physico-chemical methods with potassium hydroxide (KOH) as the activation reagent under CO_2 at 850°C for 2 hours (Hameed *et al.*, 2007). Waste tea was used to produce AC, using a chemical type of activation with H_3PO_4 as the chemical reagent (Yagmur *et al.*, 2008).

Hemp fibre (Rosas *et al.*, 2009) and eucalyptus bark (Kongsuwan *et al.*, 2009) were used to produce ACF by chemical activation with H_3PO_4 under N_2 and CO_2, respectively. Piassava fibres have been used to produce AC, using chemical and physical activation processes. The chemical activation was performed with H_3PO_4 and $ZnCl_2$ as the chemical reagents under nitrogen N_2, while physical activation was performed with CO_2 and water vapour (Avelar *et al.*, 2010). Flamboyant pods were used as precursor to prepare AC via chemical activation with sodium hydroxide (NaOH), as the chemical reagent, under N_2 (Vargas *et al.*, 2010; Vargas *et al.*, 2011). *Jatropha curcas* fruit shell has also been used to prepare AC via thermo-chemical activation with NaOH as the chemical activation agent under N_2 (Tongpoothorn *et al.*, 2011).

2.5.6 *Agave sisalana*

Agave sisalana (sisal) is a tropical plant which falls under the genus *Agave*. This plant is principally monocarpic (i.e. reproducing only once after several years and then dying). *A.sisalana* is of considerable ecological (as keystone species) and economic importance as it is used as a raw material for several industries in various countries (Good-Avila *et al.*, 2006). It is an important cordage fibre-yielding plant that is drought resistant and can withstand extreme dry conditions. Fibres are collected from the sisal leaves by manual scraping or using mechanical instruments, and the leaves can be pulped and used (Nikam *et al.*, 2003) – see Table 2.4 for properties of *A. sisalana*.

Table 2.4: Properties of *Agave sisalana (Lu et al., 2014)*

Material	Moisture (%)	Ash content (%)	Volatile matter (%)	Fixed Carbon (%)
Agave sisalana	8.8	4.7	13.1	73.4

2.5.7 Activated carbon fibre (ACF) production and activation reagent selection using

To demonstrate its usability in ACF production, sisal fibre-based activated carbon fibres were prepared using $(NH_4)HPO_4$ solution as a chemical reagent for the activation process (Fu *et al.*, 1995). Furthermore, a study was conducted by the same author, where identical precursors were used with H_3PO_4 as a chemical reagent for the activation process (Fu *et al.*, 2003). Additionally, the sisal fibres were carbonised to produce a silver supported activated carbon fibre (Chen *et al.*, 2005). Sisal waste was also used as a feedstock to produce ACF by a chemical activation process with K_2CO_3 as the activating agent under N_2 flow (Mestre *et al.*, 2011).

Other potential feedstocks for the production of ACF are listed in Table 2.5. Furthermore, all production requirements (i.e. activation reagents, temperature, and surface area characteristics of the ACF) are highlighted. *Agave sisalana* was chosen as the feedstock for this study for the following reasons: *Agave sisalana* is a widely available resource throughout sub-Saharan Africa and can be prepared using mud ovens, which are used to produce charcoal, with and without activation agents. This is, in particular, for application in remote communities that collect their drinking water from contaminated sources such as rivers. In regard to the production of ACF, the selection of chemical reagents was based on previous studies of cellulosic-type materials.

Table 2.5: Potential feedstock for the production of activated carbon fibre (ACF) from cellulosic-type material bioresources

Feedstock	Activation reagent	Surface area (m^2/g)	Roasting time (min.)	Temperature (°C)	Reference
Coconut shell	$ZnCl_2$	2191/2390	120/300	800	(Hu *et al.*, 2001)
Hemp fibre	H_3PO_4	1355	120	550	(Rosas *et al.*, 2009)
[a]Pitch fibre	Steam with metal compounds	1550/1990	35/70	875	(Tamai *et al.*, 1999)
Bamboo	KOH	1896	120	850	(Hameed *et al.*, 2007)
Sisal fibre	H_3PO_4	1186	_	850	(Chen *et al.*, 2005)
Piassava fibre	$ZnCl_2$	1190	180	500	(Avelar *et al.*, 2010)
Euteromorpha prolitera	$ZnCl_2$	1722	30/120/180/240	400 - 700	(Li *et al.*, 2011)
Delonix regia	NaOH	2854	60	761.7	(Vargas *et al.*, 2010; Vargas *et al.*, 2011)
Hevea brasiliensis (sawdust)	H_3PO_4	1673,9	60	400	(Karthikeyan *et al.*, 2005)
Cynara cardunculus	H_3PO_4	2038	60	500	(Benadjemia *et al.*, 2011)
Posidonia oceanica	$ZnCl_2$	1483	120	600	(Dural *et al.*, 2011)
Euphorbia camaldulensis Dehn eucalyptus Bark	H_3PO_4	2933,6	60	500	(Kongsuwan *et al.*, 2009)
Jatropha curcas	NaOH	1873	120	800	(Tongpoothorn *et al.*, 2011)
Palm shell	K_2CO_3	1065	60	800	(Adinata *et al.*, 2007)
Waste tea	H_3PO_4	1157	180	350	(Yagmur *et al.*, 2008)
Sisal	K_2CO_3	1038	60	800	(Mestre *et al.*, 2011)

2.5.8 Electro and physico-chemical assisted adsorption of organic pollutants to sorbents

Numerous processes for water purification and recycling have been applied. The relevant tertiary treatment methods are ion exchange, electrodialysis, electrolysis reverse osmosis and adsorption. Nevertheless, the majority of these processes have been proved inefficient when used to remove PFOS and PFOA. Most of the processes mentioned above are expensive technologies with a cost of 10 to 450 USD per million litres of water treated. However, water treatment cost by adsorption varies in the range of 10 to 200 USD per million litres (Ali & Gupta, 2007). Based on the cost analysis, adsorption can be selected among other processes, as it is a fast, cheap and commonly applied method (Jain *et al.*, 2002; Ali & Gupta, 2007). In addition, the applicability of conventional processes for the removal of anionic PFC surfactants from aqueous solution is limited by economical and/or technical restrictions (Herrera & Alvarez, 2008). The sonication or ultrasound process augments mass transfer and pore diffusion of the adsorption process. However, ultrasound also promotes the desorption process or the regeneration of the adsorbent (Breitbach & Bathen, 2001). Researchers have verified sonication as way of stirring (in comparison with mechanical stirring), to be effective; such as Li Puma *et al*. (2008) in a study conducted to prevent coagulation of the photocatalyst . Additionally, a study conducted on adsorption and desorption of phenol using activated carbon and polymeric resin demonstrated that ultrasound has a positive effects on adsorption and desorption phenomena. For adsorption in batch system, ultrasound was found to operate as a mixer and a driving force for adsorption (Schueller & Yang, 2001).

The decomposition using electrolysis for PFCs particularly PFOA and PFOS have been used as a process of defluorinating PFCs into other by-products. Ochiai *et al.* (2011) were able to decompose PFOA using a boron-doped diamond (BDD) electrode. To verify the decomposition of PFOA, the amount of CO_2 released in the electrolytic cell was monitored by a photo acoustic field. These observations demosntrated that PFOA can be decomposed to CO_2 and F^- by electrolysis, particularly for PFOA saturated samples. A similar study was done by Zhuo *et al*. (2012) where several PFCs were assessed including PFOS using a similar electrolysis unit. It was again observed the decomposition of PFOA along with PFOS, both resulting in a formation of CO_2 and F^- thus certifying the decomposition of PFOA and PFOS (Zhuo *et al.*, 2012). These studies were performed using saturated samples, with no other studies reporting a similar phenomena using low PFC concentrations.

Furthermore, the combination of both sonication and electrolysis for PFOA and PFOS had never been evaluated before. Therefore, it was imperative to assess such a combination, i.e. Electro - physico-chemical adsorption for rapid adsorption of both PFOA and PFOS, simultaneously onto *A. sisalana* ACF.

CHAPTER THREE
SORPTION MODELS: THEORETICAL CONCEPTS

3.1 Introduction

Activated carbon is a useful adsorbent material with applications in a variety of industries. In the water sector, it is used as an adsorbent to remove contaminants under defined conditions (Tzong-Horng, 2011). In this chapter, adsorption models are discussed, so that they can be used in the determination of sorption parameters, such as sorption capacity and the rate of sorption, that is, for the dual adsorption of PFOS and PFOA onto the activated carbon fibre.

3.2 Sorption models

In most cases, adsorption isotherms are presented in a form that describes the retention and release of a substance from an aqueous medium onto a solid-phase at a known and constant pH and temperature to achieve a state of equilibrium. Adsorption equilibrium is a state whereby the adsorbate-containing phase has been in contact with the adsorbent for a sufficient amount of time with the adsorbate concentration in the bulk solution, and a dynamic stability with the interface concentration is established. However, physico-chemical parameters of the adsorbent and adsorbate can influence the degree of adsorption, which is dependent on the affinity of the adsorbent and the surface properties of the adsorbate. Several equilibrium isotherm models have been developed. Among them are those of Langmuir, Brunauer-Emmett-Teller, Freundlich, Redlich-Peterson, Sips, Radke-Prausnitz, Temkin, Flory-Huggins, Koble-Corrigan, Khan, Hill, Toth, and Dubinin-Radushkevich. All these isotherms have been formulated based on approaches which include kinetic and thermodynamic parameters (Foo & Hameed, 2010).

After a literature review of Van Der Waal's adsorption gases principle, Brunauer *et al*. (1940) confirmed the existence of five different types of isotherms from which most adsorption phenomena could be identified (Brunauer *et al.*, 1940). Later on, the above classification was increased to six (Webb & Orr, 1997). However, the said classification is represented with regard to the shape of the plot volume versus pressure as presented in Figure 3.1.

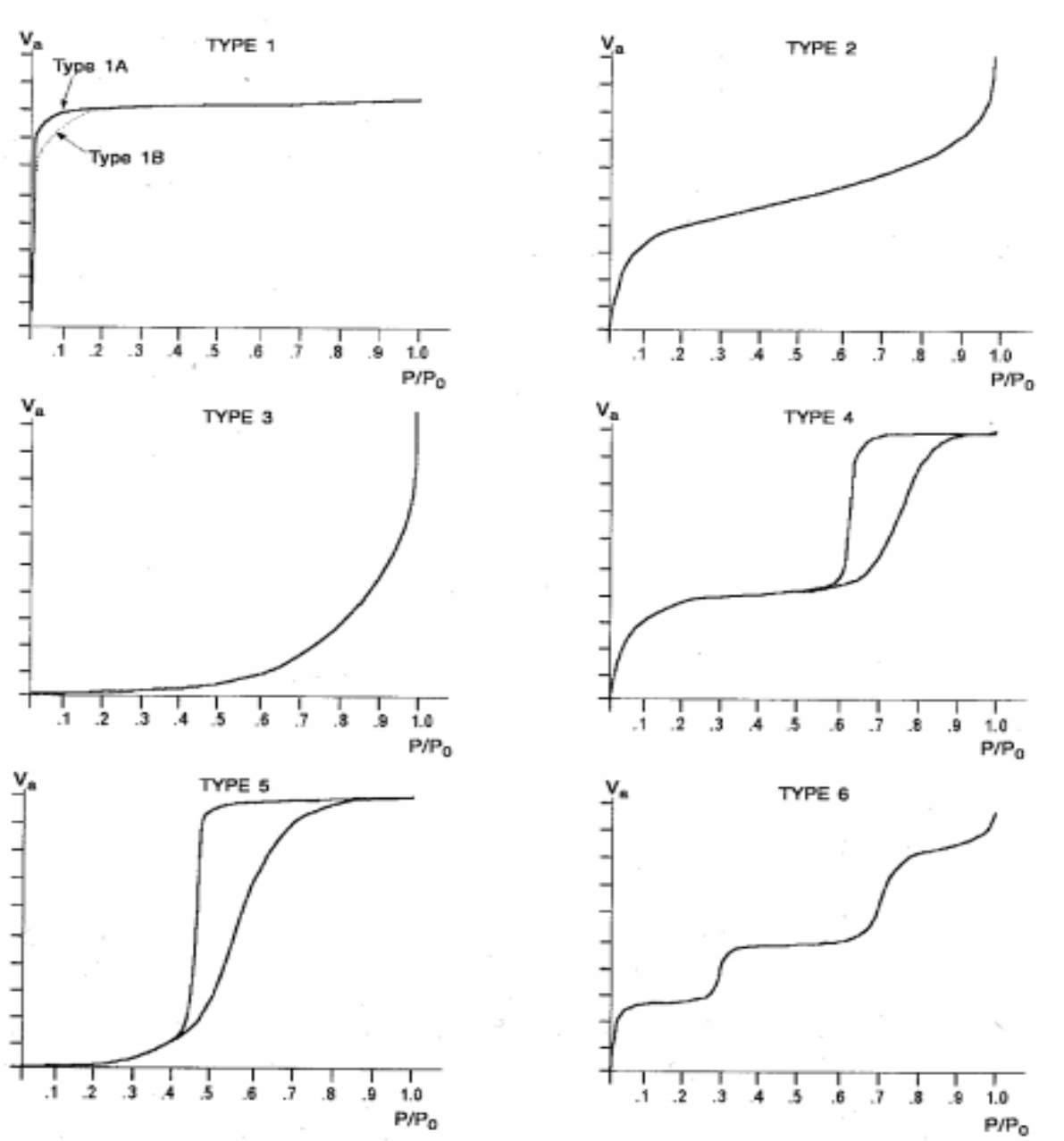

Figure 3.1: The six types of basic adsorption isotherms (Webb & Orr, 1997).

The characteristic of adsorbents with very small pores is represented by Type 1. Nonporous adsorbents and adsorbents that possess large pores can be indicated by Type 2 and 4. The adsorption process under conditions whereby the adsorptive molecules have a superior affinity for a different material than the solid, corresponds to Types 3 and 5 isotherms. On the other hand, these conditions are worthless in pores and surface analysis. Finally, there is the sixth (Type 6) and quite rare type of isotherm which represents a uniform surface and nonporous solid (Brunauer, 1940; Webb, 1997). Examples that can be linked to each type of adsorption while taking place are: Oxygen on charcoal at -183°C (Type 1), nitrogen on iron catalysts at -195°C (Type 2), bromine on silica gel at 79°C (Type 3), benzene

on ferric oxide gel at 50°C (Type 4), and water vapour on charcoal at 100°C (Type 5) (Brunauer *et al.*, 1940).

3.3 Two parameter models

3.3.1 Langmuir isotherm

Initially, the Langmuir isotherm was developed to illustrate gas-solid phase adsorption kinetics onto activated carbon. The isotherm was used in comparison with other models. The basis of this model was founded on a monolayer adsorption, where adsorption can occur at a certain number of defined sites, which are equivalent to and identical with minimal lateral interaction and steric hindrances between the adsorbed molecules, even on sites closest to each other (Hameed *et al.*, 2007; Foo & Hameed, 2010). Homogeneous adsorption was primarily assumed in the derivation of the Langmuir isotherm, with every molecule being posed to have a constant sorption activated energy and enthalpy once the molecule occupies a site, with further adsorption occurring (Foo & Hameed, 2010). The Langmuir isotherm in a linear form is given by Tan *et al*. (2008) and Vargas *et al.* (2011) as:

$$\frac{1}{q_e} = \frac{1}{Q_o} + \frac{1}{bQ_oC_e} \quad , \qquad 3.1$$

where C_e is the equilibrium concentration of the adsorbate, q_e being the amount of adsorbate adsorbed per unit mass of adsorbate. Q_o and b are Langmuir constants related to adsorption capacity and the rate of adsorption, respectively (Hameed *et al.*, 2007; Tan *et al.*, 2007).

3.3.2 Freundlich isotherm

This isotherm was firstly identified as describing non-ideal, reverse adsorption, and not limited to the formation of a monolayer. The Freundlich isotherm can be used as a functional multilayer adsorption model, with non-uniform distribution of the heat of adsorption and adsorbent affinity over a heterogeneous surface (Hameed *et al.*, 2007). The logarithmic form of the Freundlich isotherm is represented by the following equation:

$$\log q_e = \log K_F + \left(\frac{1}{n}\right)\log C_e \qquad 3.2$$

where C_e is the equilibrium concentration of the adsorbate, q_e is the amount adsorbed at equilibrium, while K_F and n are the Freundlich constants. K_F describes the adsorption capac-

ity of the adsorbent, while *n* gives an indication of the favourability of the adsorption process. Furthermore, K_F can be described as the distribution coefficient and represents the quantity of adsorbate adsorbed onto the adsorbent for a unit equilibrium concentration (Hameed *et al.*, 2007). Currently, the Freundlich isotherm is widely used in heterogeneous systems, especially for organic compound adsorption onto highly interactive sites on activated carbon and molecular sieves. The measure of adsorption intensity or surface heterogeneity is the slope $\left(\frac{1}{n}\right)$ which ranges between 0 and 1. When the value of the slope is closer to zero, it indicates a more heterogeneous adsorption process, whereas a value closer to unity implies that a chemisorptic-type process is favoured, while that above unity is an indication of a co-operative adsorption process (Foo & Hameed, 2010)

3.3.3 Dubinin-Radushkevich isotherm

The Dubinin–Radushkevich isotherm is used for the analysis of isotherms of a high degree of rectangularity (Tan *et al.*, 2007). Originally conceived for the adsorption of subcritical vapours onto micropore solids following a pore filling process, it is mostly used for adsorption processes with a Gaussian energy distribution into a heterogeneous surface. The model fit high solute activities and intermediate concentration ranges (Foo & Hameed, 2010). However, the approach was applied to differentiate the chemical and physical adsorption of metals, when significant free energy per molecule of adsorbate is required for the removal of the molecule from its location on the sorption site. This model can be computed by:

$$E = \left[\frac{1}{\sqrt{2B_{DR}}}\right] \qquad 3.3$$

where B_{DR} is the isotherm constant and the parameter *E* can be determined using:

$$E = RT\ln\left[1 + \frac{1}{C_e}\right] \qquad 3.4$$

where *T*, *R* and C_e represent the temperature, the ideal gas constant (8,314 J/mol K) and the adsorbate equilibrium concentration, respectively.

The Dubinin–Radushkevich isotherm is temperature dependent, as when adsorption data are obtained at different temperatures and the adsorption rate is assessed as a function of the logarithm of the quantity adsorbed versus the square of the potential energy.

3.3.4 Dubinin-Astakhov isotherm

The use of microporous carbons has been reported in several studies and is well documented. The approaches to describe adsorption on this material have taken numerous paths. Among the models used to describe adsorption on these types of adsorbents, the Dubinin-Astakhov model has been widely used to describe the process (Amankwah & Schwarz, 1995). This model or method was developed by Dubinin and Radushkevich (Webb & Orr, 1997). The Dubinin-Astakhov model is a theoretical model which is assessed by the theory of volume filling of pores (TVFM) and offers parameters that need to be described (Amankwah & Schwarz, 1995; Gil & Grange, 1996). However, in the case of microporous materials, Dubinin introduced a TVFM concept in 1947, which led to the Dubinin-Radushkevich equation and later to the Dubinin-Astakhov equation. This concept is based on the thermodynamic theory that the amount of adsorbate adsorbed has a unique adsorption potential (Pereira & Faria, 2008).

The general equation of the Dubinin-Astakhov model is given as:

$$W = W_0 \exp\left[-\left(\frac{A}{\beta E_0}\right)^n\right] \quad , \qquad 3.5$$

where W is the quantity adsorbed at a relative pressure, W_0 is the limiting micropore volume, β is the affinity coefficient which is equivalent to 1 when the adsorptive is the reference vapour, A is the adsorption potential, n is the structural heterogeneity parameter, and E_0 is the characteristic energy of the adsorption system. The adsorption potential can be determined by:

$$A = RT\ln P_s/P \quad . \qquad 3.6$$

P_s is the vapour pressure and P is the saturated pressure (Amankwah & Schwarz, 1995).

3.3.5 Horvath-Kawasoe isotherm

Horvath-Kawasoe is a model developed by Horvath and Kawasoe in 1983. This method consists of computing the effective size dimension of pore size distribution of slit-shaped pores of carbon sieve material, from an adsorption isotherm (Gil & Grange, 1997; Cheng & Yang, 1995; Webb & Orr, 1997). The modification of the model by derivation allows the application of the Horvath-Kawasoe model on other pore geometry shapes than slits (Webb & Orr, 1997). The Horvath-Kawasoe isotherm is expressed by:

$$\varepsilon(z) = K\varepsilon^{*}\left[-\left(\frac{\sigma}{z}\right)^{4} + \left(\frac{\sigma}{z}\right)^{10} - \left(\frac{\sigma}{L-z}\right)^{4} + \left(\frac{\sigma}{L-z}\right)^{10}\right] \quad 3.7$$

where ε is the potential energy of interaction, *z* the distance of the adsorbate molecule from the surface atom in slit wall, K is a constant, ε* the potential energy minimum, *σ* the distance from surface atom at zero interaction energy, and *L* the nucleus to nucleus slit width (Webb & Orr, 1997; Gil & Grange, 1997; Gil *et al.*, 2003; Cheng & Yang, 1995).

3.3.6 Temkin isotherm

The Temkin isotherm was firstly developed to describe the adsorption of hydrogen onto platinum electrodes within solutions. This model considered the effects of indirect adsorbate/adsorbate interactions on adsorption kinetics. The effects of indirect adsorbate/adsorbent interaction on adsorption kinetics were considered. This model describes the heat of adsorption (a function of temperature), with the assumption that all the molecules in the adsorbent layer decrease linearly due to the adsorbate adsorbent interactions (Adinata *et al.*, 2007; Foo & Hameed, 2010). The Temkin isotherm is represented as follows:

$$q_e = \left(\frac{RT}{b}\right)\ln(K_T C_e)\,, \quad 3.8$$

which is linearised as:

$$q_e = B_1 \ln K_T + B_1 \ln C_e \quad , \quad 3.9$$

where $B_1 = \frac{RT}{b}$, B_1 is a constant related to the heat of adsorption, q_e is the adsorption capacity at equilibrium (mg g^{-1}), C_e is the equilibrium liquid phase concentration (mg.L^{-1}), and K_T is the equilibrium binding function constant (L.mol^{-1}).

The Temkin isotherm considers the adsorbing species–adsorbent interactions. It was assumed that the adsorption is characterised by a uniform distribution of binding energies (considering the highest binding energy to be on top), while the organisation in the tightly packed structure of the adsorbent is packed in such way that the pore structure of adsorbent is varied, that means, the sites do not have the same orientation. This presumes that all the molecules in the layer decrease linearly with coverage due to adsorbent–adsorbate interactions because of the heat of adsorption. The Temkin isotherm can be used for predicting the

gas phase equilibrium. However, this isotherm cannot represent liquid-phase adsorption isotherms and complex adsorption systems (Mall *et al.*, 2005; Tan *et al.*, 2007).

3.3.7 Flory-Huggins isotherm

The Flory-Huggins isotherm model can express the practicability and spontaneous nature of an adsorption process. But in some cases, the isotherm can be used to determine the degree of surface coverage. For this to happen, *θ* must be evaluated as it quantifies the degree of the surface coverage, with K_{FH} and x_{FH} being constants indicative of the equilibrium constant and the isotherm's adsorption exponent (Oguzie *et al.*, 2004; Oguzie & Ebenso, 2006; Foo & Hameed, 2010). According to Oguzie *et al*. (2004), the isotherm can be represented by Equation 3.10:

$$\text{Log}\left[\frac{\theta}{C}\right]=\log K_{FH} + \chi_{FH}\log(1-\theta) \qquad 3.10$$

However, according to Foo and Hameed (2010), K_{FH} can be used for the calculation of the free Gibbs energy, while the Gibbs energy is expressed using Equation 3.11 as follows:

$$\Delta G°=-RT\ln(K_{FH}) \qquad 3.11$$

3.3.8 Hill isotherm

The equation describing the Hill isotherm model was postulated to illustrate the binding of diverse species onto homogeneous adsorbents. The model presumes that adsorption is a cooperative phenomenon, whereby the ligand aptitude at one site on the macromolecule, can influence binding on the same macromolecule (Foo & Hameed, 2010; Hofmeyr & Cornish-Bowden, 1997). The isotherm is represented by:

$$V=\frac{Vs^{nh}}{K+s^{nh}} \qquad 3.12$$

in which *v* is the preliminary velocity of the reaction, *V* is the maximum velocity, s is the substrate concentration, *K* and *nh* are constants. Furthermore, *nh* is often designated the Hill coefficient (Hofmeyr & Cornish-Bowden, 1997; Atkins, 1973).

3.4 Three parameter models

3.4.1 Redlich–Peterson isotherm

This isotherm features both the Langmuir and Freundlich isotherms. The Redlich–Peterson isotherm is a hybrid isotherm which incorporates three parameters into an empirical equation. The Redlich–Peterson isotherm contains three parameters, K_R, a_{RP}, including β, and can be written as:

$$q_e = \frac{K_R C_e}{1 + a_{RP} C_e^{\beta}} \qquad 3.13$$

in which a_{RP}, K_R, and β are all the Redlich–Peterson constants. The exponent, β, is always positioned between 0 and 1 ;and affects Langmuir and Henry low depending on the value observed (Ng *et al.*, 2002).

The Redlich–Peterson model describes the sorption of the adsorbate onto the adsorbent over the concentration range studied by presenting a linear dependence on concentration in the numerator and an exponential function in the denominator. This is such that it represents the equilibrium on a large concentration range, thus being applicable in homogeneous or heterogeneous systems due to the versatility of the model (Foo & Hameed, 2010; Ng *et al.*, 2002).

3.4.2 Sips isotherm

The Sips isotherm is also a combination of the Langmuir and Freundlich isotherm expressions. It differs from the Redlich–Peterson isotherm in that it was deduced for predicting adsorption dynamics of heterogeneous adsorption systems and avoids the limitation of the increasing adsorbate concentration associated with the Freundlich isotherm model. At high concentrations, it predicts a monolayer adsorption capacity characteristic of the Langmuir isotherm, while at low adsorbate concentrations; it is reduced to the Freundlich isotherm. The operating conditions such as variation of temperature, pH and concentration mostly control the model parameters (Foo & Hameed, 2010). The model is represented as follows:

$$N = \frac{q_m b^* P^{1/n^*}}{1 + b^* P^{1/n^*}} \qquad 3.14$$

in which N is the amount adsorbed, P is the equilibrium pressure, and q_m, b^* and n^* are the isotherm parameters which are numerically determined (Kim *et al.*, 2003; Lee *et al.*, 2006).

3.4.3 Toth isotherm

The Toth isotherm has an additional empirical equation developed to supplement the Langmuir isotherm, based on experimental data and practicality when describing heterogeneous adsorption systems, which satisfy both the high- and low-end boundary concentrations (Ho *et al.*, 2002; Vijayaraghavan *et al.*, 2006; Foo & Hameed, 2010). The Toth isotherm can be represented as:

$$Q = \frac{Q_{max} b_T C_f}{\left[1 + (b_T C_f)^{1/nT}\right]^{nT}} \qquad 3.15$$

where n_T is the Toth model exponent and b_T the Toth model constant. When n_T is unity, the Toth isotherm reduces to the Langmuir sorption model.

Based on the correlation coefficient, root-mean-square error (RMSE) and chi-squared test, the Toth isotherm model describes the sorption kinetics better than most of the three other parameter models (Vijayaraghavan *et al.*, 2006).

3.4.4 Koble-Corrigan isotherm

The Koble-Corrigan isotherm is also one of the three parameter models, and is similar to the Sips isotherm as it also incorporates both the Langmuir and Freundlich isotherm models for representing the equilibrium adsorption data. The Koble–Corrigan isotherm model is represented by the following equation:

$$q_e = \frac{A c_e^n}{1 + B c_e^n}, \qquad 3.16$$

where A, B and n are Koble–Corrigan parameters. An advantage associated with this model is that the three isotherm constants, A, B and n, can be quantified from the linear plot, represented on Eq. 3.17. An optimisation method can be used to fit the isotherm to the experimental data using a trial-and-error method (Han *et al.*, 2005).

$$\frac{1}{q_e} = \frac{1}{A} \cdot \frac{1}{c_e^n} + \frac{B}{A} \qquad 3.17$$

3.4.5 Khan isotherm model

The Khan isotherm model is a universal model recommended for pure solutions. This model can be expressed in its simplified form as follows:

$$Q = \frac{Q_{max} b_K C_f}{(1+b_K C_f)^{a_K}} , \qquad 3.18$$

where b_K is the Khan model constant, a_K the Khan model exponent and Q the sorption capacity (Vijayaraghavan *et al.*, 2006).

3.4.6 Radke–Prausnitz isotherm

The Radke-Prausnitz equation has several important properties which are suitable for use in many adsorption systems. It is represented as follows:

$$Q = \frac{a_K r_R C_f^{\beta_R}}{a_K + r_R C_f^{\beta_{R-1}}} \qquad 3.19$$

where Q is the sorption uptake or the carbon loading in kg adsorbate per kg adsorbent, a_R and r_R are Radke–Prausnitz model constants and β_R the Radke–Prausnitz model exponent (Vijayaraghavan *et al.*, 2006).

3.5 Multi-layer models

3.5.1 Brunauer–Emmett–Teller isotherm

The Brunauer–Emmett–Teller isotherm model is a theoretical equation, most extensively applied in gas–solid equilibrium systems. This isotherm is an extension of the Langmuir adsorption isotherm developed for multilayer adsorption kinetics (Keller & Staudt, 2005). The model represents liquid-solid sorption interactions according to the following equation:

$$q_{e=}\frac{q_s C_{BET} C_e}{(C_s-C_e)[1+(C_{BET}-1)(C_e/C_s)]} \quad 3.20$$

where C_s, q_e, q_s and C_{BET} are adsorbate monolayer saturation concentration, equilibrium adsorption capacity, theoretical isotherm saturation capacity and the BET adsorption (L/mg), respectively. The equation is simplified when the values of $(C_e/C_s)C_{BET}$ and C_{BET} are much bigger than 1 so that:

$$q_{e=}\frac{q_s}{1-(C_s-C_e)} \quad 3.21$$

3.5.2 Frenkel–Halsey–Hill isotherm

Frenkel–Halsey–Hill (FHH) isotherm is another multilayer adsorption, for which the derivation is from the theoretical potential energy and can be presented as:

$$\ln\left(\frac{C_e}{C_s}\right) = -\frac{\alpha}{RT}\left(\frac{q_s}{q_e d}\right)^r \quad 3.22$$

where d, r and α are interlayer spacing(m), inverse power of distance from the surface and α the isotherm constant (Jm^r/mole), respectively.

Similarly to the MacMillan–Teller isotherm, this adsorption model interpretation is based on the inclusion of surface tension effects in the isotherm so that:

$$q_e = q_s\left(\frac{k}{ln(C_n/C_e)}\right)^{1/3} \quad 3.23$$

where k is an isotherm constant. However, when C_s/C_e is within reach of unity, the logarithmic expression might be approximated to (Foo & Hameed, 2010):

$$q_e = q_s \left(\frac{kC_e}{C_s - C_e} \right)^{1/3}$$ 3.24

A summary of the Isotherms in 1) non-linear, and 2) linear forms are presented in Table 3.1. This includes parameters to use when generating a linear graphical presentation for the assessment of model parameters.

Table 3.1: A summary of commonly used adsorption isotherms including examples of where they have been used

Isotherm	Nonlinear form	Linear form	Plot	Uses	Reference
Two parameter models					
Langmuir	$q_e = \frac{Q_o b C_e}{1 + b C_e}$	$\frac{1}{q_e} = \frac{1}{Q_o} + \frac{1}{b Q_o C_e}$	$\frac{1}{q_e}\ vs\ \frac{1}{C_e}$	Fundamental properties of liquid and solid adsorption	(Langmuir, 1916)
Freundlich	$q_e = K_F C_e^{1/n}$	$\log q_e = \log K_F + \frac{1}{n}\log C_e$	$\log q_e\ vs\ \log C_e$	Sorption of solid to solid surfaces	(Hameed *et al.*, 2007)
Dubinin–Radushkeich	$q_e = (q_s) s x p(-k_{ad}\varepsilon^2)$	$ln(q_e) = ln(q_s) - k_{ad}\varepsilon^2$	$ln(q_e)\ vs\ \varepsilon^2$	Sorption of solid to solid surfaces	(Tan *et al.*, 2007)
Tempkin	$q_e = \frac{RT}{b_T} \ln A_T C_e$	$q_e = \frac{RT}{b_T}\ln A_T + \left(\frac{RT}{b_T}\right) \ln C_e$	$q_e\ vs\ lnC_e$	Removal of dye from solution onto bagasse fly ash and activated carbon	(Mall *et al.*, 2005)
Flory–Huggins	$\frac{\theta}{C_o} = K_{FH}(1-\theta)^{n_{FH}}$	$log\left(\frac{\theta}{C_o}\right) = log(K_{FH}) + x_{FH} log(1-\theta)$	$log\left(\frac{\theta}{C_o}\right)\ vs\ log(1-\theta)$	Adsorption of organic compound on steel surfaces	(Oguzie *et al.*, 2004)
Hill	$q_e = \frac{q_{s_H} C_e^{n_H}}{K_D + C_e^{n_H}}$	$log\left(\frac{q_e}{q_{s_H} - q_e}\right) = n_H log(C_e) - log(K_D)$	$log\left(\frac{q_e}{q_{s_H} - q_e}\right)\ vs\ log(C_e)$	Kinetics of allosteric enzymes	(Atkins, 1973)
Three parameter models					
Redich–Peterson	$q_e = \frac{K_R C_e}{1 + a_R C_e^g}$	$ln\left(K_R \frac{C_e}{q_e} - 1\right) = g ln(C_e) + ln(a_R)$	$ln\left(K_R \frac{C_e}{q_e} - 1\right)\ vs\ ln(C_e)$	Sorption of Cu (II) ions onto chitosan	(Ng *et al.*, 2002)
Sips	$q_e = \frac{K_s C_e^{\gamma} S}{1 + a_s C_e^{\beta} S}$	$\beta_s ln(C_e) = -ln\left(\frac{K_s}{q_e}\right) + ln(a_s)$	$ln\left(\frac{K_s}{q_e}\right)\ vs ln(C_e)$	-	(Foo & Hameed, 2010)
Toth	$q_e = \frac{K_T C_e}{(a_T + C_e)^{1/t}}$	$ln\left(\frac{q_e}{K_T}\right) = ln(C_e) - \frac{1}{t} ln(a_T + C_e)$	$ln\left(\frac{q_e}{K_T}\right)\ vs\ ln(C_e)$	Biosorption of nickel onto *Sargassum wightii*	(Vijayaraghavan *et al.*, 2006)
Koble–Corrigan	$q_e = \frac{A C_e^n}{1 + B C_e^n}$	$\frac{1}{q_e} = \frac{1}{A C_e^n} + \frac{B}{A}$	$\frac{1}{q_e}\ vs\ \frac{1}{C_e^n}$	Biosorption of lead ion on chaff	(Han *et al.*, 2005)
Khan	$Q = \frac{Q_{max} b_K C_f}{(1 + b_K C_f)^{a_K}}$	–	–	Biosorption of nickel onto *Sargassum wightii*	(Vijayaraghavan *et al.*, 2006)
Radke–Prausnitz	$q_e = \frac{a_{RP} r_R C_e^{\gamma} R}{a_{RP} + r_R C_e^{\beta} R^{-1}}$	–	–	Biosorption of nickel onto *Sargassum wightii*	(Vijayaraghavan *et al.*, 2006)

Table 3.1 cont.: A summary of commonly used adsorption isotherms including examples of where they have been used

Multi-layer models					
Brunauer–Emmet–Teller	$q_e = \frac{q_s k_{BET} C_e}{(C_s - C_e)[1 + (C_{BET} - 1)(C_e/C_s)]}$	$\frac{C_e}{q_e(C_s - C_e)} = \frac{1}{q_s C_{BET}} + \frac{(C_{BET} - 1)}{q_s C_{BET}} \frac{C_e}{C_s}$	$\frac{C_e}{q_e(C_s - C_e)}$ vs $\frac{C_e}{C_s}$	Physical adsorption of gases on a solid surfaces	(Brunauer *et al.*, 1938)
Frenkel–Halsey–Hill	$ln\left(\frac{C_e}{C_s}\right) = -\frac{\alpha}{RT}\left(\frac{q_s}{q_e d}\right)$	–	–	Gas–solid equilibrium systems	(Foo & Hameed, 2010)
MacMillan–Teller	$q_e = q_s\left(\frac{k}{ln(C_s/C_e)}\right)^{1/3}$	–	–	Gas–solid equilibrium systems	(Foo & Hameed, 2010)

3.6 Selecting an adsorption model for PFCs

An adsorption isotherm can be defined as a realistic illustration of the relationship between the bulk activity of the adsorbate and the quantity adsorbed at invariable temperature (Stumm, 1970). There are many equilibrium isotherm models that have been developed over the years. These isotherm models are used to describe the mobility of a substance from a liquid phase to a solid phase. The selection of a model depends on the nature of the adsorption and concentration of the adsorbate (Foo & Hameed, 2010). As observed in Table 3.2, most the studies conducted on the adsorption of PFCs have used both Langmuir and Freundlich isotherms as their adsorption isotherm for PFCs onto solid matrices. One of the reasons that substantiate the choice of both Langmuir and Freundlich isotherms is that these two isotherms are used when the sorbate is in the form of a trace compound in the solution or when a very low concentration of sorbate is present. This is also one of the advantages of these two isotherms, that they can be used even when the sorbate concentration is minute (Higgins & Luthy, 2006; Herrera & Alvarez, 2008; Senevirathna *et al.*, 2010). Besides judgements based on the correlation coefficients (R^2), linearity of the PFCs' sorption is also what justifies the choice of both the Langmuir and Freundlich isotherms in adsorption studies (Higgins & Luthy, 2006; Shih & Wang, 2013).

The advantages of these two isotherms make them appropriate for certain applications. Langmuir and Freundlich isotherms suggest that adsorption may occur on the adsorbent's surface. The PFC concentration in the adsorption process is a dominant factor (Shih & Wang, 2013). The Freundlich model gives a good description of a nonlinear isotherm, which is expected once the adsorption process has been depicted between two phases (Higgins & Luthy, 2006). The Langmuir isotherm presumes that there is no interaction between molecules. As soon as the process reaches its saturation value, no further sorption occurs for both isotherms (Herrera & Alvarez, 2008), while the Freundlich isotherm describes the adsorption process onto a heterogeneous surface. It is also an empirical relationship that illustrates the adsorption of a liquid onto a solid surface (Senevirathna *et al.*, 2010). In most studies, only disadvantages of the Freundlich isotherm were noted. A limitation with regard to the Freundlich isotherm may be described in a case of adsorption occurring on a homogeneous surface, such as repulsive interaction and electro-static interaction between sorbates (Higgins & Luthy, 2006).

The Freundlich isotherm is not suitable when higher concentrations of solutes are present in solution (Senevirathna *et al.*, 2010). This disadvantage is also applicable to the Langmuir isotherm (Malik *et al.*, 2007). Additional disadvantages with regard to the Freundlich isotherm include the fact that the Freundlich equation is purely empirical and has no theoretical basis; although this was previously pointed out as an advantage, this can also

be considered a disadvantage to some extent. The equation is suitable merely up to a definite pressure and not appropriate at higher pressure. The constants *K* and *n* are also not independent of temperature (Ruthven, 1984).

Most of the sorption models discussed in this chapter heavily rely on the principles articulated in both the Langmuir and Freundlich isotherms. Therefore, it is logical to select these two models as a representative of the models used and further developed by others.

Table 3.2: Advantages, disadvantages and reasons for using Langmuir and Freundlich isotherms in PFOA and PFOS studies

Study title	Isotherm used/Reason of choice	Advantages/Disadvantages	Reference
Adsorption of PFCs on Boehmite	Langmuir and Freundlich isotherm; high correlation coefficients (R^2)	Using Langmuir and Freundlich isotherms suggests that adsorption may be taking place on the adsorbent's surface.	(Shih & Wang, 2013)
Sorption of PFCs on sediment	Freundlich isotherm; the sorption of PFCs onto sediment is non-linear	Freundlich model gives a good description of nonlinear isotherms; Freundlich isotherm as a non-linear isotherm is also expected once the process has been described to be happening between two phases; Freundlich limitation may be described in a case of adsorption occurring on a homogeneous site, such that repulsive interaction, electro-static interaction between sorbates occurs.	(Higgins & Luthy, 2006)
Sorption of PFCs onto GAC, zeolite and sludge	Langmuir and Freundlich isotherm; accurate representation of spicies' concentration in diluted solutions	Langmuir isotherm presumes that there is no interaction between molecules; as soon as the process arrives at its saturation value, no further sorption is taking place. Freundlich isotherm describes effectively adsorption phenomena for compound in form of quantities in solution.	(Herrera & Alvarez, 2008)
Adsorption of PFOS onto GAC, ion-exchange polymers and non-ion-exchange polymers	Freundlich isotherm; appropriate to describe adsorption process of compounds in diluted solutions.	Freundlich isotherm describes adsorption process onto heterogeneous surface; it is also an empirical relationship that illustrates adsorption of liquid onto solid surface; Freundlich isotherm is not suitable for higher concentration of solutes in solution.	(Senevirathna *et al.*, 2010)
Adsorption of perfluorooctane sulfonate onto minerals surface	Langmuir isotherm	Describes adsorption process for which solute is in a form of trace quantities.	(Tang *et al.*, 2010)
Adsorption of PFOA and PFOS on alumina	Langmuir and Freundlich isotherm; suitable for diluted solution and ability of evaluating the correlation coefficient (R^2)	In this study, PFOA and PFOS adsorption seems to fit better in Langmuir isotherm rather than Freundlich isotherm, based on the correlation coefficient (R^2).	(Wang & Shih, 2011)
Sorption of PFOS and PFOA on Resin	Langmuir and Freundlich isotherm; provide an accurately description of the interaction sorbate-sorbate in solution.	Langmuir isotherm has the best fit in comparison with Freundlich isotherm during the adsorption process. But the time is still considerable to reach the equilibrium.	(Yu *et al.*, 2009)
Sorption of PFOS on organo-montmorillonites	Langmuir and Freundlich isotherm	In this study, determination between Langmuir and Freundlich isotherms was difficult since each adsorbent used reacted in a different way. However, the required time was also considerable to reach the equilibrium.	(Zhou *et al.*, 2010)

3.7 Statistical analysis of adsorption kinetics data

In isotherm studies, optimisation requires the selection of an error function to be defined with the purpose of evaluating the fit of the isotherm to experimental equilibrium data (Ho *et al.*, 2002; Ng *et al.*, 2002). Among the error theories, the commonly used is the ERRSQ.

Although sum squares errors is the most extensively used error function, at the higher end of the liquid-phase concentration range, the magnitude and squares of the errors tend to increase, illustrating a better fit for the isotherm parameters derivation. It can be represented as:

$$SSE= \sum_{i=1}^{p}\left(q_{e,calc}-q_{e,meas}\right)_i^2 \qquad 3.18$$

(Foo & Hameed, 2010; Ng *et al.*, 2002; Ho *et al.*, 2002; Kumar & Sivanesan, 2006; Mane *et al.*, 2007). The SSE was determined to be a suitable error function to be used in this study.

Furthermore, a correlation coefficient which represents the percentage of variability when comparing experimental and modelled data can be used to analyse the fitting degree of the isotherm and kinetic models with the experimental data (Kumar & Sivanesan, 2006; Boulinguiez *et al.*, 2008).

CHAPTER FOUR
MATERIALS AND METHODS

4.1 Introduction

In this chapter, the materials used for the experiments are described, as well as the various methods required to obtain the necessary data to reach the aims of this study.

4.2 Sisal harvesting and processing

After sisal has reached maturity (3 years), the lower and older leaves are removed close to the head. Leaves are scraped one by one using a scraper. Following this process, the fibre is extracted, cleaned and then dried. The drying process consists of hanging the fibre in the sun, where it loses its lustre. Nevertheless, the fibre must be kept straight and clean to avoid mixing of the fibre and tuft (Conter, 1903; Chen *et al.*, 2005).

4.3 Manufacturing of activated carbon fibre (ACF)

Different reagents were sprayed onto the sisal fibres. In order to perform the spraying process, spraying bottles with a very fine nozzle were used. After spraying along the fibre length, samples were placed in an oven at a temperature of 110°C for about an hour until completely dry. The process was repeated until a total volume of 10 ml of the reagent was sprayed. Long sisal fibres were then cut to a length of 3 mm, loaded into ceramic boats, packed in a tubular furnace and pyrolysed at the required temperature under nitrogen. However, since the carbonisation and the chemical activation were combined, the purging gas (nitrogen, N_2) was switched to CO_2 when the activation temperature was reached. Once activation had taken place, a period of time elapsed, the temperature was then reduced under nitrogen to room temperature. The ACF obtained was then washed with 6 L of warm distilled water. During the washing process, bromothylmol blue was used as an indicator to assess the neutrality of the recovered rinsing water.

After washing, samples were then dried in an oven overnight. The final product (ACF) were sealed in a bag (5 x 6 cm) using heat – see Figure 4.3. The concentration of the activation reagents is shown in Table 4.2. Figure 4.2 illustrates the process followed (A) and the furnace used (B).

Table 4. 1: Concentration of different reagents used for the activation process

Activation agent	Concentration				
KOH	21.6 M	4.32 M	2.16 M	1.08 M	0.54 M
NaOH	25 M	5 M	2.5 M	1.25 M	0.625 M
$ZnCl_2$	31.8 M	6.36 M	3.18 M	1.59 M	0.795 M
H_3PO_4	14.6 M	2.92 M	1.46 M	0.73 M	0.365 M

Control pure sisal/pyrolysed sisal: KOH-121 g/100 ml at 25°C (saturated); NaOH - 100 g/100 ml at 25°C (saturated); ZnCl2 432 g/ 100 ml at 25°C (saturated); H3PO4 - Used as is and the dilution of 1/5, 1/10, 1/20, 1/40 thereafter for all of them.

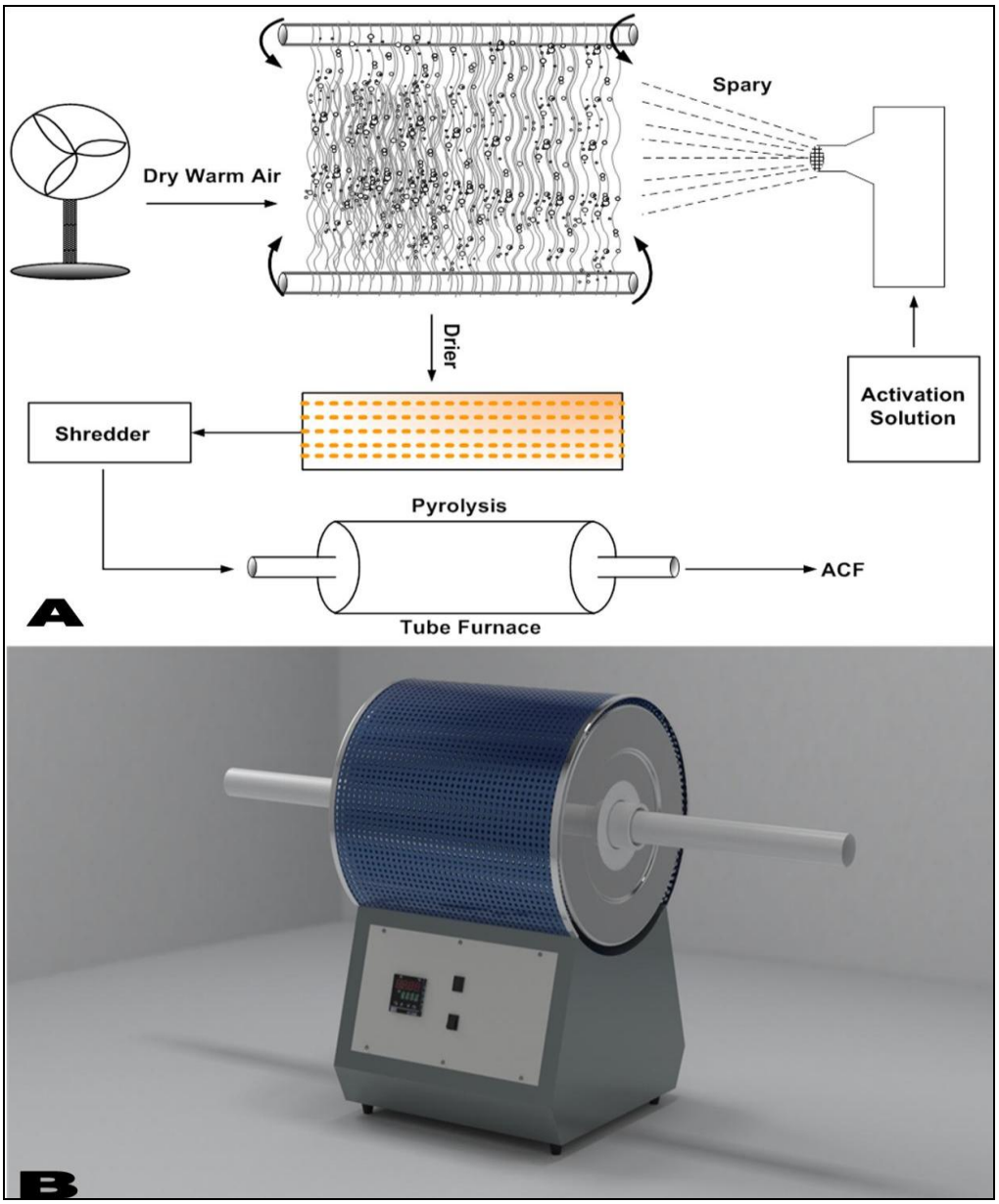

Figure 4. 1:Schematic representation of the preparation method for AFC using *Agave sisalana*

4.4 Response surface methodology

Expert Design (version 8.0.6.1, Stat-Ease, Inc.) was used as a statistical tool, for the design of experiments for the pyrolysis of *Agave sisalana* fibre based on significant factors previously identified as essential in the production of activated carbon fibre (Gassara *et al.*, 2011). As micropores are the subjects of this study, the following parameters:

1) activation time,
2) activation temperature,
3) and activation reagent concentration.

These parameters were identified as influential in the formation of the required structural distortion of the fibre. These independent factors were found to have an influence on dependent variables; of which the responses will be total surface area, activated carbon fibre yield, micropore volume, micropore surface area, total volume, micro/total volume ratio and average pore diameter. In this study, a central composite design, identified as the most suitable method among factorial designs, was used. Central composite design (CCD) is used for the fitting of a quadratic surface. It consists of 2^k factorial designs, where 2^k axial runs and nc centre runs, where k is the number of factors.

For the production of activated carbon fibre, the following factors were previously determined to be influential in pore generation using cellulosic-type fibre:

1) Activation time: the time that the temperature will be held while the activation process is taking place.
2) Activation temperature: the temperature at which the activation of fibre occurs.
3) Activation reagent concentration: the concentration of the chemical solution in which the precursor fibre will be impregnated.
4) Impregnation ratio.

Factorial designs are useful as the optimal number of runs that can be quantified if the optimisation numbers are known. In this study, 2 factors shown (Activation time and temperature). Each variable identified runs studied at these different levels (minimum, medium, maximum). The total number of experiments when using CCD was 13 (see Table 4.1). The activation reagent concentration and impregnation were assessed separately (see section 4.4) as new method had to be used to preserve the structure of the sisal fibre. This was important in order to minimise the formation of powdered debris, which can result in powdered residue, thus compromise the ease of handling, a requirement needed for large scale operations.

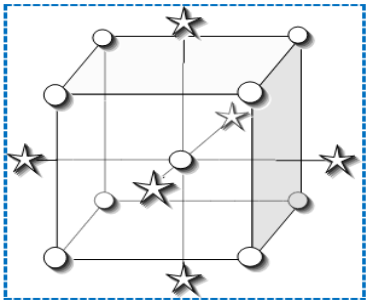

Figure 4.2: Central Composite Design (CCD) Experimental Design

Table 4.2: Experimental parameters used for the study

Run	Factor 1	Factor 2
	Activation Temperature (°C)	Activation time (min.)
1	450	45
2	650	112.5
3	650	112.5
4	367	112.5
5	850	180
6	933	112.5
7	650	112.5
8	650	17
9	850	45
10	650	208
11	450	180
12	650	112.5
13	650	112.5

4.5 Surface area characterisation

Analyses were done on a 3Flex Surface Characterization Analyzer from Micromeritics Instrument Corporation. Prior to analysis, the samples were degassed using a Vacprep 061 at 250°C for 24 hours under vacuum (Webb & Orr, 1997). CO_2 was used as the adsorbate gas at a temperature of 0°C. Table 4.3 shows different models used for surface characterisation and the surface area obtained using different feedstock. The surface area models used tend to over-estimate surface properties during analysis – see Section 5.3 (Results), therefore, the specific surface area for the ACF was quantified using the Dubinin-Astakhov isotherm with a relative pressure (P/P_0) up to 0.01. The sample mass was between 0.2 to 0.3 g. Table 4.3 list a summary of models used to determine surface area characteristics used for activated carbon using different feedstock.

Table 4.4: Summary of models used to determine surface area for activated carbon fibre from different studies

Feed Stock	Surface Area (m^2/g)	Model used *	Reference
Coconut shell	2191/2390	Brunauer–Emmet–Teller	(Hu *et al.*, 2003)
Hemp fibres	1355	Brunauer–Emmet–Teller, Dubinin–Radushkevich, Horvath–Kawazoe and Barrett–Joyner and Halenda (BJH) (used for pores distribution)	(Rosas *et al.*, 2009)
[a]Pitch	1550/1990	Barrett–Joyner and Halenda (BJH), Brunauer-Emmet-Teller	(Tamai *et al.*, 1999)
Bamboo	1896	Brunauer–Emmet–Teller	(Hameed *et al.*, 2007)
Sisal	1186	Brunauer–Emmet–Teller	(Chen *et al.*, 2005)
Piassava fibre	1190	Brunauer–Emmet–Teller	(Avelar *et al.*, 2010)
Euteromorpha prlitera	1722	Brunauer–Emmet–Teller	(Li *et al.*, 2011)
Delonix regia	2854	Brunauer–Emmet–Teller, Dubinin–Radushkevich, Horvath–Kawazoe, Barrett–Joyner and Halenda (BJH)	(Vargas *et al.*, 2010; Vargas *et al.*, 2011)
Hevea brasil-iensis (saw-dust)	1673,9	Brunauer–Emmet–Teller	(Karthikeyan *et al.*, 2005)
Cynara car-dunculus	2038	Brunauer–Emmet–Teller	(Benadjemia *et al.*, 2011)
Posidonia oceanica	1483	Dubinin–Raduschkevic	(Dural *et al.*, 2011)
Palm shell	1065	Brunauer–Emmet–Teller and Dubinin–Radushkevich	(Adinata *et al.*, 2007)
Waste tea	1157	Brunauer–Emmet–Teller, Dubinin–Radushkevich	(Yagmur *et al.*, 2008)
Hemp fibre	1350	Brunauer–Emmet–Teller, Dubinin–Radushkevich	(Rosas *et al.*, 2009)

*Equation used to calculate the apparent surface area

4.6 Preparation of POS and POFA contaminated water

A two-litre polypropylene container was washed with methanol, to avoid any PFC contamination, then rinsed with Milli-Q water (Mastalerz *et al.*, 2011). Two litres of distilled water were placed in 2 L polypropylene (P/P) bottle; 0.1 µL of PFOA and PFOS at the concentration of 2 g/L each was added into the distilled water to produce a solution of polluted water at a concentration of 100 ng/L of PFOA and PFOS. The synthetic water used, was based on raw and treated drinking assessments by Booi (2013), whereby PFC concentrations, were determined in the range upto 40 ng/L and 100 ng/L observed by Mudumbi *et al*. (2014) , in river water, for both PFOA and PFOS. The water containing a Maximum of 100 ng/L, was used for initial adsorption studies using sonication – see sections 4.7.1 and 5.2.3 including Table 5.2.3.

However, for a large scale operation, higher concentrations of polluted drinking water must be evaluated and thus both PFOA and PFOS were substantially increase to 100 mg PFC/L – see sections 4.7.2 and 5.4 including Tables 5.7 and 5.8, in order to generate appropriate adsorption profiles.

4.7 Adsorption studies

4.7.1 Physico-chemical assisted adsorption studies

Physico-chemical assisted adsorption was performed using 150 mL of the contaminated water in a 250 mL polypropylene (PP) beaker without pH adjustment; then an ACF bag containing 0.57 g of *A. sisalana* (-see Figure 4.3) was immersed into the polluted water with subsequent sonication. The sonicator was set at 20 kHz. The sonicator probe was rinsed with methanol 99% and Milli-Q water after each experiment before processing new samples. The samples were sonicated for 2 hours. Thereafter, the ACF bags were dried in the oven at 70°C while a 10 mL solution was taken from the bulk solution for analysis. The sample solution for analysis was filtered (0.22 µm polypropylene filter) and stored in the refrigerator at 4 °C prior to analysis using a SPE-LC/MS/MS.

Figure 4.3: Open and heat press sealed ACF bag

The cumulative loading for the adsorption was determined using the following mathematical expression:

$$q_{st} = \frac{X}{m} \qquad \text{with} \quad x = \frac{(C_i - C_s) * V_r}{volume\ conversion\ factor} \qquad 4.1$$

where X – is the amount of PFOA/PFOS adsorbed onto the ACF, m – is the mass of the adsorbent (ACF), C_i – is the initial concentration of PFOA/PFOS in solution, C_s – is the amount of residual PFOA/PFOS in solution, V_r – is the volume of the PFOA/PFOS contaminated water used during adsorption, and q_{st} – is the cumulative loading parameter for PFOA/PFOS adsorption.

This mathematical expression was also used for the determination of PFOA/PFOS adsorption using an Electro-physico-chemical method – see section 4.7.2.

4.7.2 Electro-physico-chemical assisted adsorption

A neckless 250 ml PP bottle (150 mL contaminated water) was used as an electrolytic - type cell, where the electrodes were 55 mm distant from each other and the ACF bag containing 0.57 g of *A. sisalana* being attached to the anode. The cathode was made of stainless steel while the an-

ode was plated with a platinum layer. The direct current used for electrolysis was 12 volt (V). During electrolysis, sonication was also applied, with samples being taken every 20 minutes for a period of 2 hours.

Figure 4. 4: Electro-physico-chemical assisted adsorption: (a) - sonicator probe, (b) - sonicator controller unit (Sonics & Materials Inc, USA), (c) - anode, (d) - cathode and (e) – electrical current adapter

4.8 FTIR analysis

In order to perform these experiments, 0.001 g from the residual ACF from the adsorption experiment was used with 0.2 g KBr. Both were mixed and crushed using a mortar and pestle until completely mixed. The mixed powder was loaded in the hydraulic press under pressure of 8 tons for about 25 minutes to form a pellet. The pellet was then placed in the spectroscopy for analysis. The objective of this experiment was to identify the existence of functional groups in the samples. This was also used to ascertain PFOA and PFOS adsorption, on to ACF.

4.9 Scanning electron microscopy analysis

Sisal fibre and ACF samples were viewed in the scanning electron microscope. Samples were glued on a pin stub then placed on the pin stub holder. The glue did not cover the sample, to allow for viewing of the sample under SEM with different magnifications.

4.10 Solid-phase extraction

A Supelco-select HLB SPE cartridges (500 mg solid phase, 12 ml tubes) were used to perform a PFC extraction from samples. Cartridges were preconditioned by eluting 5 ml of methanol (99.99%), followed by 5ml of Milli-Q water to rinse the cartridge, at a flow rate of two drops per second. Thereafter, 10 ml of the samples were loaded into the cartridge, followed with 5 ml of methanol 40 %(v/v) to wash the cartridges, then finally, 10 ml of methanol (99.99%) was loaded into the cartridges and collected in 15 ml PP sampling tubes. The volume of methanol was reduced to 1 ml by blowing nitrogen into the PP sampling tube, from which PFOA and PFOS was quantified using LC/MS/MS.

4.11 Liquid chromatography-mass spectrometry (LC-MS/MS)

LC-MS/MS was performed on a Ultimate 3000 Dionex HPLC system (Dionex Softron, Germering, Germany), equipped with a binary solvent manager and auto sampler, coupled to a Brucker ESI Ion Trap Mass Spectrometer (Bruker Daltonik GmbH, Germany). The products were separated by reversed- phase chromatography on a Waters Sunfire C18 column 5 µm, 4.6 × 150 mm (Dublin, Ireland) using gradient elution at a flow rate of 0.8 $mL.min^{-1}$, an injection volume of 10 µl and an oven temperature of 30°C. The gradient was set up as follows: 64 % A to 44 % A (12 min); 44 % A to 1 % A (12 to 13 min); 64 % A (13.1 to 20 min); solvent A – 5mM ammonium acetate in water, solvent B – acetonitrile. MS spectra were acquired in a negative mode using the full scan mode with dual spray for reference mass solution. Electrospray voltage was set to -3500 V. Dry gas flow was set at 9 $L.min^{-1}$ with a temperature of 350 °C and the nebuliser gas pressure was set to 347.96 KPa The compounds were quantified using Quant Analysis software. The operational conditions are listed in table 4.4.

Table 4. 5: Operational parameters and description of LC-MS/MS procedure.

Operational parameters	Description
1. SPE cartridge elution conditions, injection volume and final extracts volume	Elution from SPE cartridge procedure employed in this study was in accordance with that described in **USEPA Method 537-31**, although with some modifications. The details of this procedure are provided under section 4.10..
2. LC/MS/MS model used and supplier	**HPLC Model:** Ultimate 3000 Dionex HPLC system **HPLC Supplier:** Dionex Softron, Germering, Germany **MS model:** Amazon SL Ion Trap **MS supplier:** Bruker Daltonik GmbH, Bremen, Germany
3. MS/MS operational conditions and ion mode	**MS Interface**: ESI **Dry Temp**: 350°C **Nebulising pressure**: 347.96 KPa **Dry gas flow**: 9 L/min **Ionisation mode**: negative MS/MS using auto MS(n)
4. Guard column used, characteristics and supplier	No guard column used.
5. Separation column used, characteristics, supplier, temperature (i.e. operational parameters)	**Separation mode**: reversed phase chromatography **Column**: Waters Sunfire C18 column 5 µm; 4.6 × 150 mm **Supplier**: Waters, Dublin, Ireland **Column temperature used**: 30°C
6. Mobile phase constituents, concentration, flow rate, and gradient operational parameters:	**Mobile phase**: Solvent B: 100% acetonitrile; solvent A: 5mM CH_3COONH_4 in water; **Flow rate**: 0.8mL/min **Gradient**: 64 % A to 44 % A (12 min); 44 % A to 1 % A (12– 13 min); 64 % A (13.1–20 min);
7. Calibration standards used, concentration, range used, and supplier:	Calibration standards consist of the following levels: 0, 0.1, 0.2, 0.5, 1.0, 2.5 and 5.0 ppm (for other PFCx), while the calibration levels for PFOA and PFOS consist of: 0, 0.2, 0.4, 1.0, 2.0, 5.0 and 10 ppm. All standards were supplied by Sigma-Aldrich.

CHAPTER FIVE
RESULTS AND DISCUSSION

5.1 Optimum activation reagent concentration for the preparation of *Agave sisalana* activated carbon fibre

5.1.1 Introduction

Activated carbon has been widely used in the removal of dissolved pollutants in water treatment, owing to its high surface area (Selomulya *et al.*, 1999), and more especially because of its microporous structure (An *et al.*, 2011). Owing to the protection of the environment, research has focused increasingly on the manufacture of activated carbon from various plant materials. Overall, activated carbon can emanate from different sources and can be produced in several forms, such as activated carbon powder (ACP), granulated activated carbon (Ounas *et al.*) and activated carbon fibre (ACF). Among activated carbons, the activated carbon fibre has been shown to have the highest surface area (An *et al.*, 2011). *Agave sisalana* is one of the potential activated carbon precursors widely available in Africa. It was thus selected for this study due to its wide availability, as it is cheap to process, even in areas with limited technology. The experiments conducted were based on the manufacture of ACF that retained its shape and produced less powdered residue, for the adsorption of PFOA and PFOS from contaminated drinking water.

5.1.2 Aims and objectives

To achieve the goals of this study, the aims and objectives for these experiments were to:

1) determine the optimum activating reagent concentration suitable for the sisal fibre to retain its physical shape;
2) assess consistency in the formation of pores on the fibre post carbonisation treatment; and
3) quantify the activated carbon fibre yield under different conditions assessed.

To fulfil these objectives, a scanning electron microscope was also used (-for details, see-materials and methods, section 4.9).(Erkoç & Erkoç, 2001)

5.1.3 Results and discussion

5.1.3.1 Manufacturing process of activated carbon fibre (ACF)

The production of ACF from any raw material involves pre-treatment involving either physical or chemical methods or a combination of both. The activation process can occur prior to carbonisation, while carbonisation is taking place or after it has happened. In this

study, the option chosen involved chemical activation followed by the carbonization process. Sisal fibres were preliminarily treated with a chemical reagent before pyrolysis under nitrogen and carbon dioxide in a tubular furnace.

Four chemical reagents, NaOH, KOH, $ZnCl_2$ and H_3PO_4, were selected for the manufacturing process of the activated carbon. In previous studies, the sisal fibres were pre-treated by immersing or soaking the fibre into different concentrations of each of the selected chemical reagents (Adinata *et al.*, 2007; Avelar *et al.*, 2010; Benadjemia *et al.*, 2011; Vargas *et al.*, 2011). In this study, after mixing the fibres with chemical reagents diluted in distilled water, samples were removed from the solution and dried. The drying process took place in an oven overnight. Samples were then pyrolysed under nitrogen and carbon dioxide at 650°C in order to get an activated carbon fibre material. The concentration used ranged from saturation to 1/40 of the saturation concentration (see Table 4.2). Initially saturated concentration was used then progressively diluted. After samples had been removed from the oven, it was observed that some of the fibres were damaged due to the high concentrations of the activation chemicals reagents used while pre-treatment was taking place. As concentration of chemical reagents was decreased, less damage to the fibre was observed. This meant that soaking of the fibre compromised the integrity of the shape, with some fibres dissolving in the liquid containing the activation reagents, in particular, when hydroxides and phosphoric acid were used.

The second challenge faced was to regulate temperature and activation time during pyrolysis (see Table 4.1). Temperature and activation time has an influence on the yield and quality of activated carbon fibres obtained after pyrolysis. It was then observed that with a temperature increase, a lower yield percentage was achieved. A similar phenomenon was observed when activation time was increased. However, it was noted that in certain instances, the longer the activation time, with the fibre exposed at a median temperature, resulted in an increase in pore creation. However, it was also noticed that H_3PO_4 and $ZnCl_2$ protected the physical integrity of the fibres, producing fibres which retained their shape during the pyrolysis than NaOH and KOH.

Furthermore, the fibre obtained from pyrolysis for a treatment regime using each of the four reagents, was studied at a microscopic scale using different magnifications and compared with untreated sisal fibre. This fresh sisal fibre was used as a control to make a comparative analysis at different stages during ACF production (Fig. 5.1, 5.2 and 5.3).

In Figure 5.1, dried sisal was viewed under an SEM at different magnification. After mechanical preparation, that is, processing and drying of harvested leaves, it showed that dried sisal does not have pores on the surface, and this led to the presumption that the reactive surface of such a fibre was small. The surface texture of the sisal was rough, undulating and uneven, with fibre width being <100µm. The surface was covered with unidentified lump compositions which could rupture once the pyrolysis process was carried out, and as a result generate a porous structure.

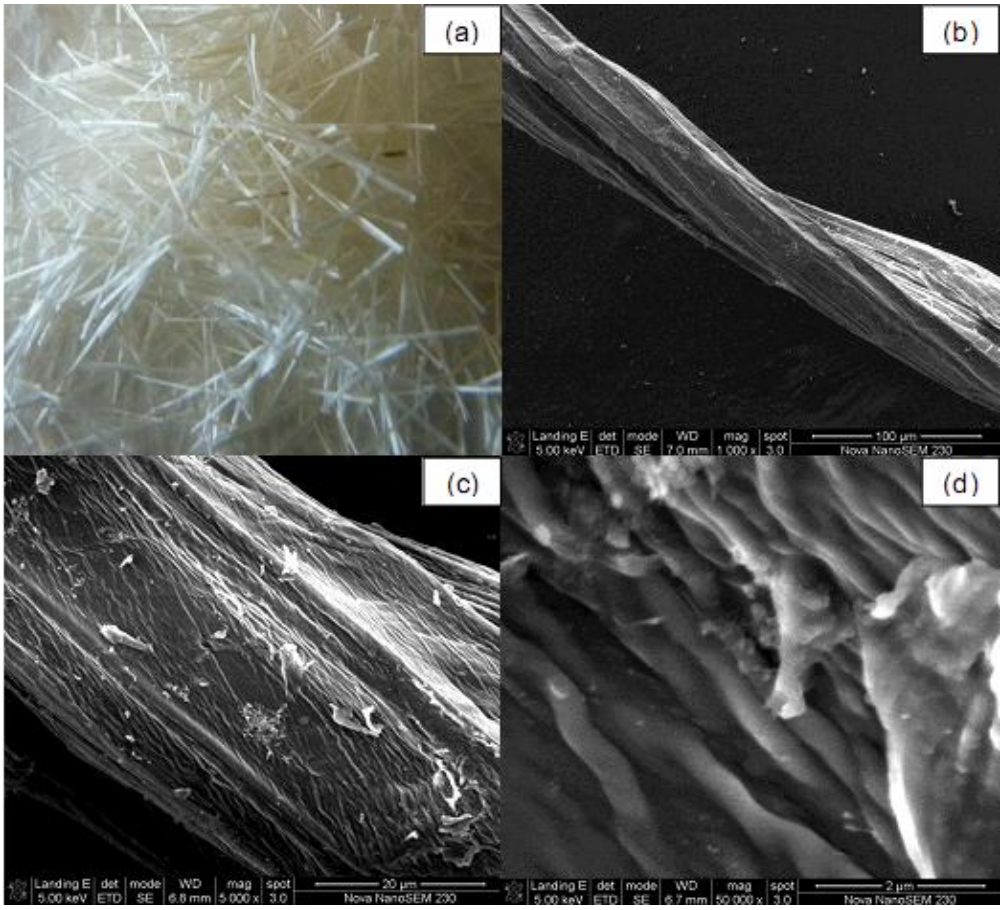

Figure 5.1: Unpyrolysed sisal fibre, after harvesting and drying, i.e. without activation. (a) standard photograph; (b) SEM micrograph (1000X); (c) SEM micrograph (5000X) and (d) SEM micrograph (50000X)

In Figure 5.2, pyrolysed sisal that has not been activated using chemical reagents is shown under an SEM at different magnitudes. This figure indicates that on the surface of the pyrolysed sisal at 650°C under nitrogen and carbon dioxide, minimal pore creation was observed. The surface texture of the sisal remained unchanged, remaining rough, undulating and uneven. This indicated that an activation process using suitable reagents was required.

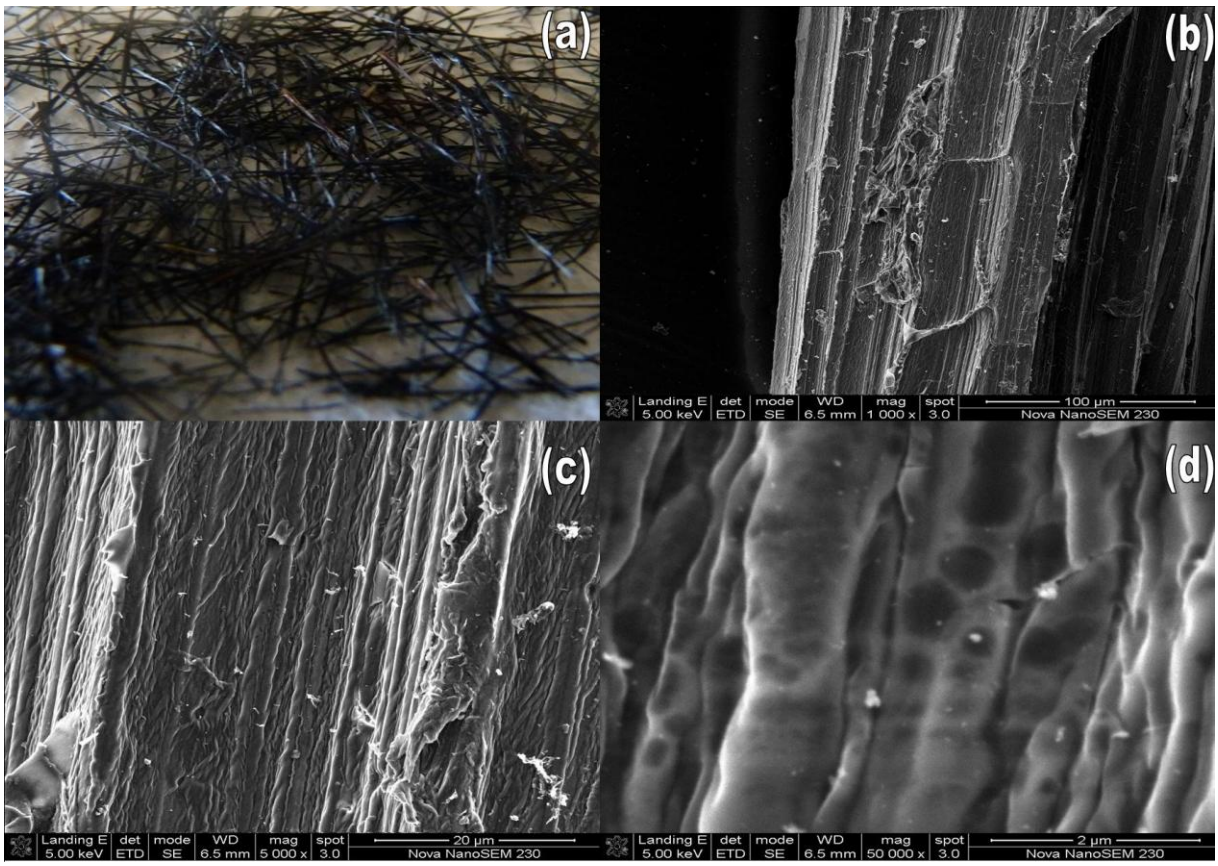

Figure 5.2: Pyrolysed sisal fibre in ACF form. (a) standard photograph; (b) SEM micrograph (1000X); (c) SEM micrograph (5000X) and (d) SEM micrograph (50000X)

As part of the objectives of this study, the production of ACF with a suitable porous structure, that is, micropores, with minimal powdered residues, was required, for easy handling including recycling of the ACF through regeneration. When a higher concentration was used, the obtained sisal fibres were mostly powdered for the four reagents used at a saturation concentration, with ash being formed. This was due to the fact that solutions of these reagents at a high concentration dissolved a large quantity of the organic matter in the fibres when under high temperature. This necessitated the reduction of the activation reagents' concentration using the dilution rates from 1/5 to 1/40 and the abandonment of the soaking method. In certain instances, even at a lower activation reagent concentration, and at a lower temperature, by also varying the ratio, chemicals/fibre, the resultant ACF formed, had a smoothed-out exterior surface without any significant porous structure as shown in the micrograph Figure 5.3.

Figure 5.3 (a, c, e, and g) displays the powdered form of ACF post pyrolysis at unsuitably high activation reagent for H_3PO_4 (Fig. 5.3a), KOH (Fig. 5.3c), NaOH (Fig. 5.3e) and $ZnCl_2$ (Fig. 5.3g), respectively. This type of activated carbon resembled the powdered form,

which was not suitable for this study. This is because in this form, it is difficult to recycle the activated powder and handling, including storage, might be difficult. Figure 5.3b, d, f, and h indicate SEM micrographs of the obtained powder. Nevertheless, when diluted concentrations were used, the integrity of the sisal fibres was maintained even at an activation temperature of 650°C using an activation time of 3 hours.

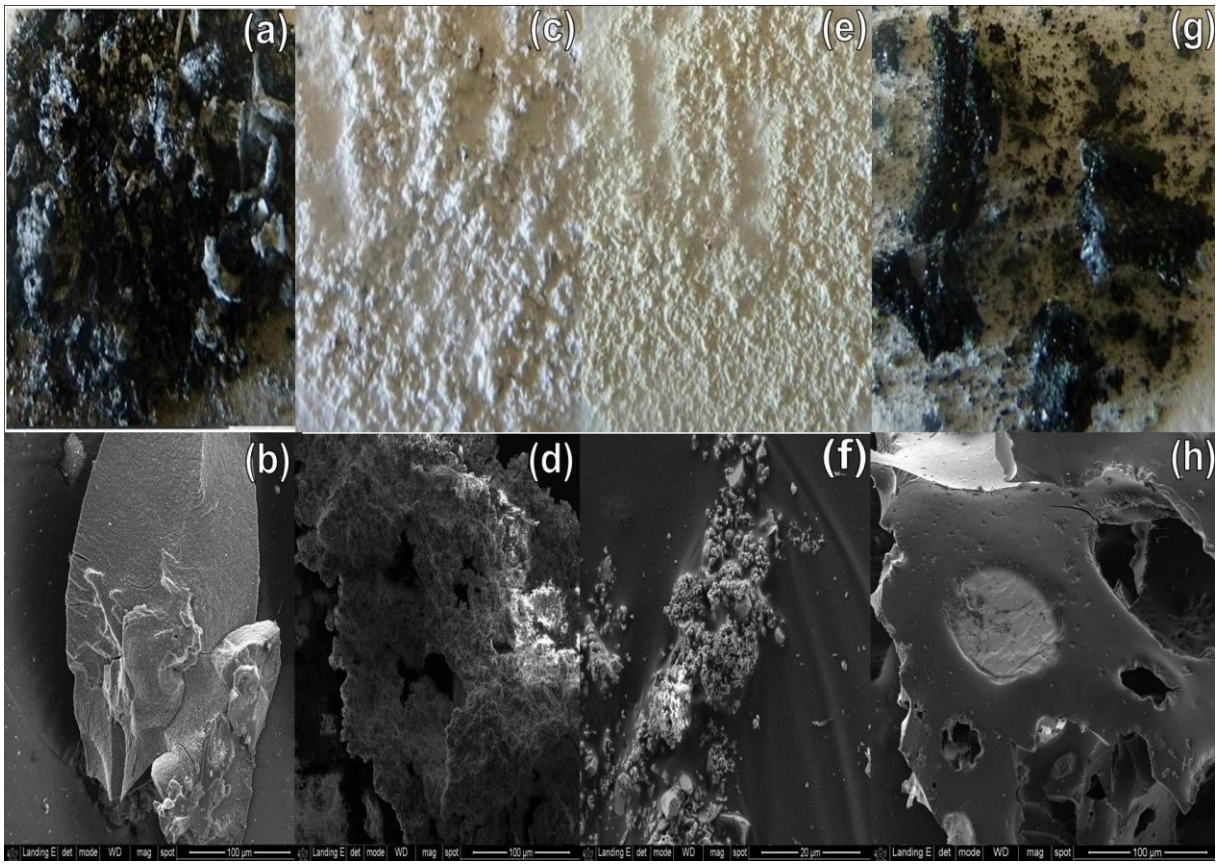

Figure 5.3: (a), (c), (e), (g) standard photograph and (b), (d), (f), (h) SEM micrograph of the sisal, after pyrolysis using high concentration activation reagents

The best results observed by visual inspection and under an SEM for samples pre-treated with H_3PO_4 were obtained at a concentration of 1.46 M and 0.73 M for H_3PO_4, corresponding to 1/10 and 1/20 dilution of the stock solution (for which 0.73 M was maintained for further experiments). Similar observations were seen for samples pre-treated with $ZnCl_2$ at a concentration of 3.18 M and 1.59 M (with 1.59 M being maintained for further experiments), while for NaOH and KOH a concentration of 1.25 M and 1.08 M achieved results deemed appropriate. However, samples pre-treated with NaOH and KOH at the above-mentioned concentration achieved a highly porous and partially powdered activated fibre, with a disintegrated structure. More than 90% of the organic matter in the raw material burnt off achieving

a low yield. Further dilution was initiated whereby a concentration of 0.625 M and 0.54 M for NaOH and KOH was used, respectively, which was maintained for further experiments.

Nevertheless, as the integrity of the fibre was of paramount importance, pre-treated samples with H_3PO_4 (0.73 M) and $ZnCl_2$ (1.59 M), respectively, indicated minimal powder formation as displayed in Figure 5.4, with Figure 5.4a and c displaying photographs, while Figure 5.4b and d represent SEM micrographs for H_3PO_4 (0.73 M) and $ZnCl_2$ (1.59 M), respectively. On closer inspection, minuscule pore structure was observed, with fragmented ash formation.

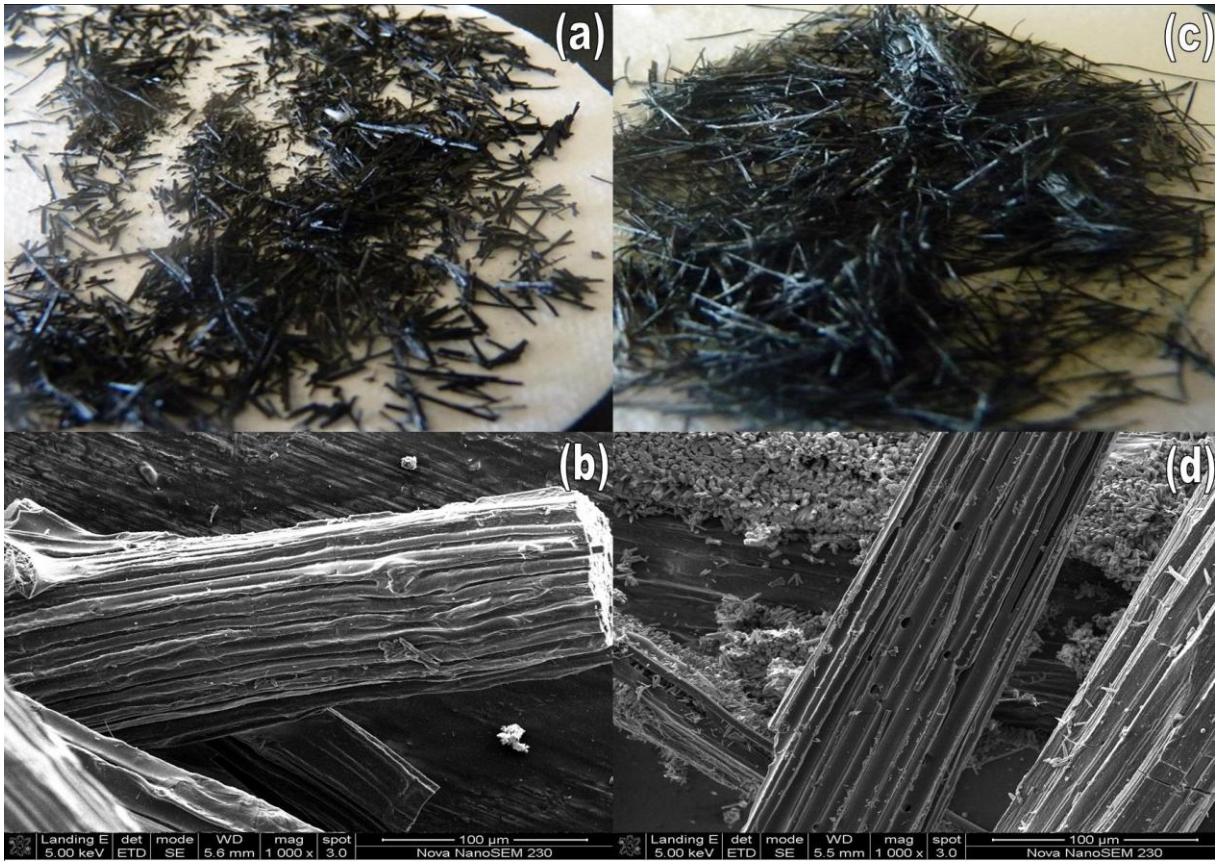

Figure 5.4: (a), (c), standard photograph and (b), (d), SEM micrograph of the sisal after pyrolysis with H_3PO_4 and $ZNCl_2$ as activating reagents at the optimum concentration

Since it was observed that the integrity of the fibres was susceptible to high temperature effects, minimising the activation reagent concentration was insufficient for the pore formation process. At this stage, it was decided that the development of a spraying technique would achieved the required pore structure on a micro-scale. The developed process was combined with an air-drying process to minimise the soaking effect for the activation process. This procedure has not been reported previously in the literature reviewed for a specific ap-

plication such as the one conducted in this study. Based on the percentage yield and the SEM images obtained, there was ample evidence that the spraying method worked better than the immersion method.

In Figure 5.5(a), (b) and (c), (d), the use of the spraying method, which soaked the fibre without a simultaneous air-drying process, resulted in a corrosive effect on the external surface area of the fibre without the creation of the required pores. Figure 5.5(a) and (b) represent samples obtained using the spray method, while (c) and (d) were obtained using the soaking (impregnation) method. Although the spray scattered the activation chemical solutions on the fibre better than impregnation, the erosive effect of the method suggests that the spray needs to be applied intermittently, with a drying effect applied for immediate drying of the droplets when they are on the surface of the sisal, resulting in the formation of pores.

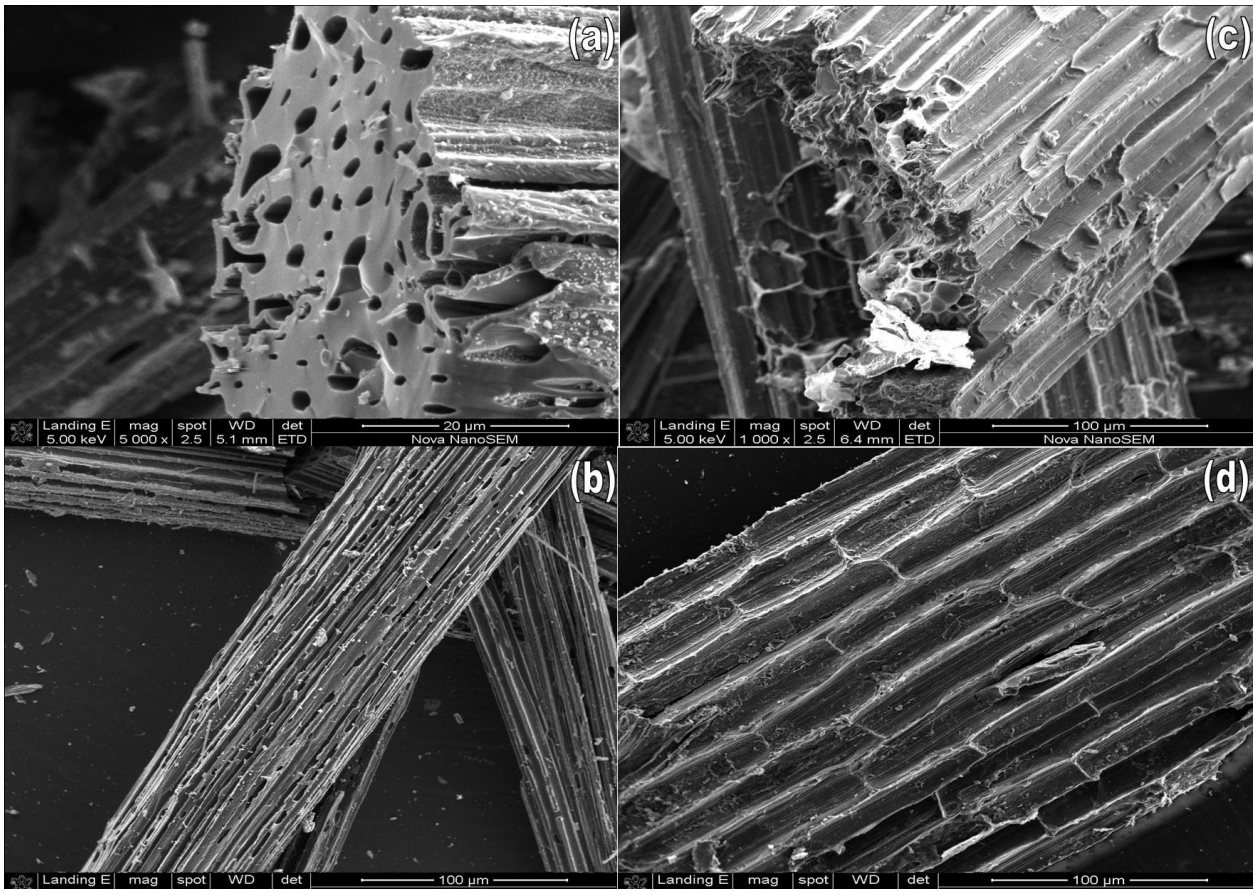

Figure 5.5: (a), (c), (b) and (d) SEM micrograph of sisal fibre after being pyrolysed with different methods of applying the activation reagents on the fibres

From this evidence, and by using different methods, a clear distinction was drawn between the two methods. Thus, based on the SEM micrographs, the evidence was that the

spray-drying method worked better than the immersion method. A comparative analysis was made using SEM monographs of the fibre obtained in this study with other SEM monographs reported in published works (Phan *et al.*, 2006; Tan *et al.*, 2007; Tan *et al.*, 2008). These samples were very similar, with the fibre obtained from this study showing a highly porous external and internal structure of the fibre. From the SEM micrographs, pores were visible, taking into consideration the fibres obtained for the control, which were the fresh sisal and pyrolysed fibre, without chemical reagent pre-treatment.

In Figure 5.6, from left to right, SEM photographs are shown for some published works, including for this study: (a) Phan *et al*., 2006; (b) current study; and (c) Tan *et al*., 2007.

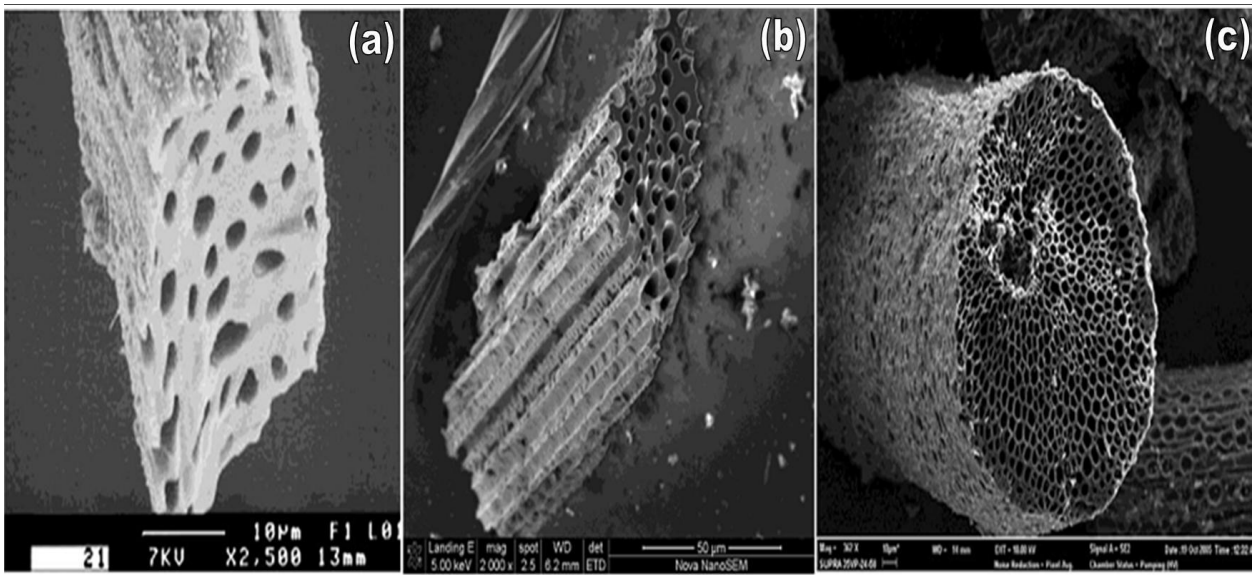

Figure 5.6: SEM photographs of published works including current study (Phan *et al.*, 2006; Tan *et al.*, 2007)

5.1.3.2 Activated carbon fibre yield from surface response methodology experiments

Because the spray-drying method had been a success thus far, a statistical method (response surface methodology) was used to optimise and assess the ACF yield under different conditions. Thus, RSM was used to design experiments to set limits for all the input variable parameters. Therefore, a temperature range between 450 °C and 950 °C and an activation time of between 45 minutes and 180 minutes were selected. These experiments were performed with regard to the previous pre-treatment conditions and the percentage yield results obtained are presented in Table 5.1. All samples obtained from the RSM experiments were used for the adsorption phase of this study. After completion of the adsorp-

tion study using a set of experiments (for which the percentage yield results are displayed in Table 5.1), samples that provided high adsorption efficiency were analysed to assess their surface properties. These samples presented high removal efficiency of both PFOA and PFOS from potable tap water, as described in detail in a subsequent section –see section 4.6.

Overall, the results obtained showed that a shorter activation time resulted in a high ACF percentage yield, with an increase in the activation temperature resulting in reduced ACF yield. See also Figure 5.7.

Table 5.1: Percentage yield for the activated carbon fibre at different activation temperatures and activation times for different activation reagents

Run	Factor 1	Factor 2	Response			
	Activation temperature (°C)	Activation time (min)	% Yield			
			NaOH	KOH	$ZnCl_2$	H_3PO_4
1	450	45	45.2	36.0	30.7	49.6
2	650	112.5	31.3	32.2	39.9	32.7
3	650	112.5	33.9	33.7	43.9	45.3
4	367	112.5	29.3	21.0	34.6	38.2
5	850	180	29.5	22.5	32.0	45.1
6	933	112.5	28.4	21.0	32.9	44.
7	650	112.5	30.8	27.0	42.6	39.1
8	650	17	27.9	13.2	30.30	39.9 1
9	850	45	28.6	16.2	nd	67.32
10	650	208	28.5	19.0	20.9	35.8
11	450	180	7.8	7.3	9.3	15.1
12	650	112.5	11.6	nd	11.5	37.0
13	650	112.5	6.4	nd	20.77	nd

*nd – not determined

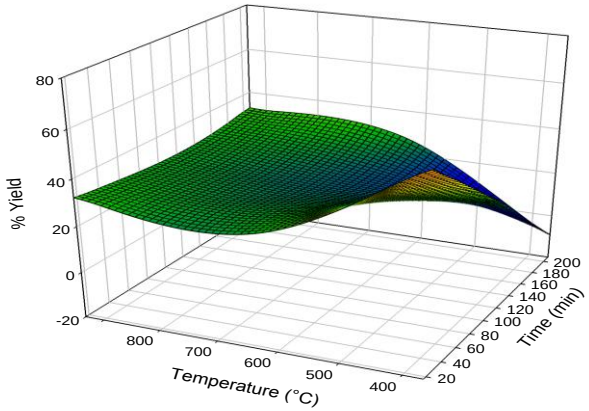

NaOH

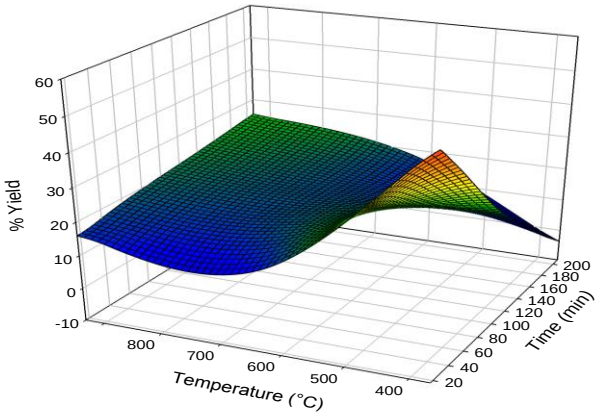

KOH

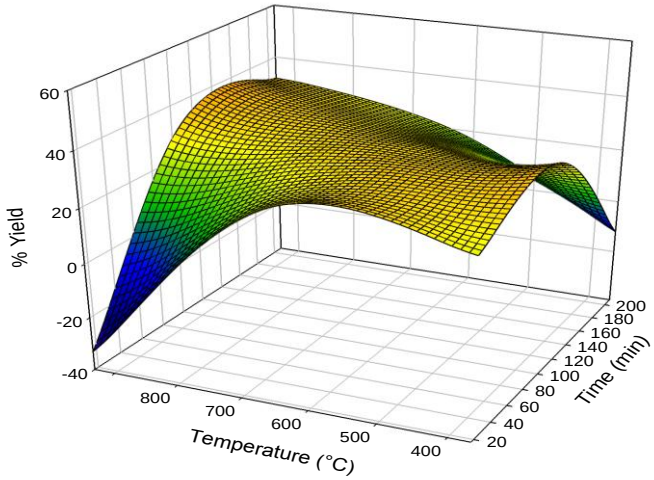

$ZnCl_2$

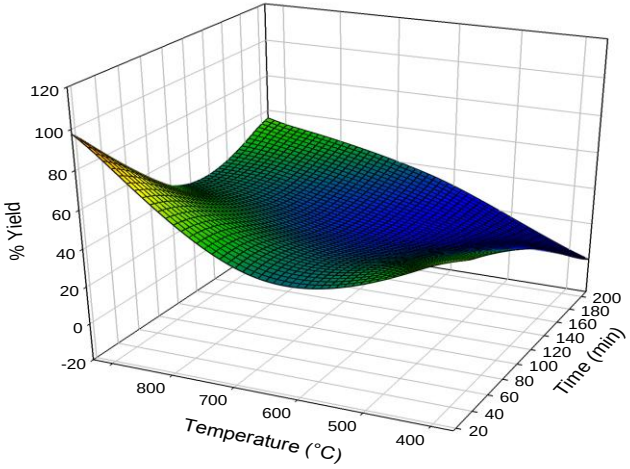

H_3PO_4

Figure 5.7: RSM plot between temperature and activation time for ACF prepared with NaOH, KOH, $ZnCl_2$ and H_3PO_4.

5.1.2.3 Summary

In this section, the primary objective was to produce a porous activated carbon fibre using *Agave sisalana*. It was observed that *A. sisalana* (sisal) was a suitable raw material for the production of activated carbon fibre. The high percentage yield was achieved at low temperature, activation reagent concentration and time. The nitrogen and carbon dioxide used during pyrolysis prevented the fibre to ashen. Once the perfect coverage of samples was ensured by activation using a newly developed praying technique, supplied at the required concentration, it ensured the integrity of the carbon fibre structure, preventing it from burning completely. Similarly, it was also noticed that these sisal fibres were damaged before the heating treatment as a result of the initial high concentration of the activation reagent. From the SEM micrographs, a similarity with other studies was observed regarding the appearance of an activated carbon fibre. In this study, the pore shape obtained was narrow and elongated.

5.2 Adsorption of PFOA and PFOS using *Agave sisalana* activated carbon fibre

5.2.1 Introduction

In recent years, research studies in the use of porous materials have increased due to their effectiveness in removing pollutant components from water (Shukla *et al.*, 2002; Mastalerz *et al.*, 2011). However, the removal of chemical substances such as oils, dyes, heavy metals and toxic salts can be performed by an organic-based biological material (Shukla *et al.*, 2002). This has opened a new era of research on different types of adsorbents from different sources which are environmentally friendly and relatively cheap. Some studies have been carried out around the world proving that PFCs are effectively removed from water using activated carbon in various forms (Yu *et al.*, 2009; Zhou *et al.*, 2010; Zhao *et al.*, 2011; Chen *et al.*, 2011). This is due to the high surface area of these materials, for which the total surface area is measured using the Brunauer-Emmett-Teller (Betts) surface area method. To some extent, it has also been proved that activated carbon fibre has a higher reactive surface area compared with activated carbon powder (Phan *et al.*, 2006). Thus, in this section of the current study, the focus was on the simultaneous removal of both PFOA and PFOS from tap water using AFC, with physic - chemical assisted adsorption; i.e. sonication.

5.2.2 Aim/Objectives

In this section, the objectives were to:

1) Remove PFOA and PFOS from contaminated water using activated carbon fibre from *Agave sisalana*. Several samples of ACF prepared with NaOH, KOH, H_3PO_4 and $ZnCl_2$ were used under different adsorption conditions, generated using design of experiment software.
2) Analyse the ACF using FTIR to identify C-F bonds in the ACF, an assessment which was used to ascertain PFOA and PFOS on to the carbonised fibre.

5.2.3 Results and discussion

5.2.3.1 PFOA and PFOS adsorption onto AFC using sonication

As adsorption can be enhanced with sonication, the physical method was used to physically assist PFOA and PFOS adsorption into the ACF pores. This phenomenon is called 'pore trapping'.

Essentially, ultrasonication can be utilised as an energy source to generate positive pressure on the reactive surface of activated carbon (Li Puma *et al.*, 2008). The use of ultrasound phenomenon has been used to hasten the adsorption process. The phenomenon responsible for this fastened adsorption is cavitation. While sequences of compression and expansion are created by acoustic waves, there is a formation of gas bubbles in the liquid that grows bigger to about 100 *μ*m in diameter. When the bubbles cross the dimension of 100 *μ*m, they become very unstable, and thus implode. As a result, high-speed micro-jets are produced, with high-pressure shock waves and strong localised heating occurring (Schueller & Yang, 2001; Zhao *et al.*, 2011). In general, sonication of water provokes the formation and collapse of millions of microscopic bubbles. As soon as these bubbles collapse, it results in the increase of the temperature of the solution and the generation of hydroxyl radicals. Thus, sonication allows a fast adsorption process of pollutants in an aqueous solution (Li Puma *et al.*, 2008). It was under these conditions that the ACF had to retain its physical properties without disintegration.

PFOA and PFOS are both anionic and have a similar molecular structure, thus a similar molecular length, which is approximate to 1 nm or 10 Å (Erkoç & Erkoç, 2001; Johnson *et al.*, 2007). This width is considered as the largest distance between atoms. In several studies it was reported that the largest distance in the PFOS's structure is 4.463 Å between carbon and sulphur atoms (Erkoç & Erkoç, 2001; Torres *et al.*, 2009). The adsorption process of PFOA and PFOS is explained when the anionic pole is attached to the positive pore on the reactive surface site of the adsorbent, which in effect results in the removal of the contaminant from the water.

During the experiments, concentrations of PFOA and PFOS in the polluted water samples were 100 ng/L and 100 ng/L, respectively. Table 5.3 displays the experimental results obtained from the adsorption of PFOA and PFOS assisted with an ultrasound probe. These experiments were performed under the following conditions: duration: 120 min; amplitude: 20 kHz; power: 28W; 220 J, with the final temperature of the water being 35°C.

Table 5.2: Adsorption of PFOA and PFOS using *Agave sisalana*

Sample ID	PFCs' Removal		Experimental Conditions for ACF production
	PFAO	PFOS	
R9 $ZnCl_2$	100%	99.55%	Temperature: 850°C; Activating time: 45 min; Concentration: 1.59M
R9 H_3PO_4	84.75%	98.79%	Temperature: 850°C; Activating time: 45 min; Concentration: 0.73M
R10 $ZnCl_2$	94.16%	99.46%	Temperature: 650°C; Activating time: 3h28min; Concentration: 1.59M
R7 KOH	84.91%	99.57%	Temperature: 650°C; Activating time: 1h53min; Concentration: 0.54M
R2 NaOH	76.22%	100%	Temperature: 650°C; Activating time: 1h53min; Concentration: 0.625M
R2 KOH	99.19%	99.74%	Temperature: 650°C; Activating time: 1h53min; Concentration: 0.54M
R2 H_3PO_4	65.55%	95.92%	Temperature: 650°C; Activating time: 1h53min; Concentration: 0.73M
R7 $ZnCl_2$	**100%**	**99.52%**	**Temperature: 650°C; Activating time: 1h53min; Concentration: 1.59M***
R5 $ZnCl_2$	**100%**	**99.64%**	**Temperature: 850°C; Activating time: 3h; Concentration: 1.59M***
R12 $ZnCl_2$	97.48%	98.41%	Temperature: 650°C; Activating time: 1h53min; Concentration: 1.59M
R13 KOH	81.49%	99.19%	Temperature: 650°C; Activating time: 1 h53min; Concentration: 0.54M
R6 $ZnCl_2$	100%	99.67%	Temperature: 933°C; Activating time: 1h53min; Concentration: 1.59M
R3 KOH	75.94%	98.74%	Temperature: 650°C; Activating time: 1h53min; Concentration: 0.54M
R5 H_3PO_4	83.64%	98.24%	Temperature: 850°C; Activating time: 3h; Concentration: 0.73M.

***low yield**

ACF prepared under different pyrolysis conditions, performed differently; however, the removal efficiency, of PFOS has been the contaminant removed consistently. Most studies reported that PFOA is largely easier to adsorb than PFOS. However, sonication could assist

the physical attachment of a contaminant to a solid matrix. Since PFOA and PFOS could attach to the surface of the ACF by physical means, the same physical forces could also result in the adsorption-desorption cyclic phenomena, for which a contaminant with weak Van der Waal's forces could largely remain within the solution in which it was initially present. As previously explained, the formation of cavitations can therefore result in the desorption of the adsorped PFCs. For this study, this removal of the two pollutants was not complete for both PFCs in the samples. This led us to presume that each ACF sample had a different affinity to PFOA and PFOS, perhaps with the reagent used for its activation playing a major role.

As Table 5.3 displays only the best results achieved with regard to the response surface methodology, it can be seen that the lowest removal percentage was 75.94% for PFOA for sample R3 KOH and 95.92% for PFOS in sample R2 H_3PO_4. In general terms, PFOS removal was high, in particular for fibre which was treated with $ZnCl_2$, H_3PO_4, and KOH, activation reagents whose concentration was diluted up to 1/40. The activation time for the ACF with the highest PFOS was 45 min at 650 °C.

Thus, of the results listed in Table 5.3, only three ACF samples were regarded as performing at the required adsorption capacity, and whose yield was actually higher than that of others observed in this study. For consistency purpose, the same amount of the adsorbent was used for all the experiments.

Table 5.3: Selection of the optimum

	Parameters/Reagents	**$^{y}ZnCl_2$**	**$^{z}H_3PO_4$**	**^{x}KOH**
% Removal	PFOA	94.2 – 100	65.55 – 84.75	75,57 – 99.19
	PFOS	98.4 – 99.7	95.92 – 98.79	98.74 – 99.74
Conditions ACF Production	Temperature	650 – 850	650 – 850	650
	Activation time	45 min – 3hrs 28 min	45 min – 3hrs	1hr 53 min
	Activation reagent conc. (M)	1.59	0.73	0.54
	% Yield	32	32.7	33.8

SEM Photographs	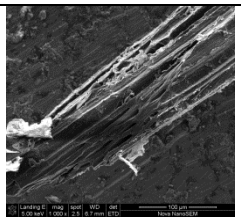	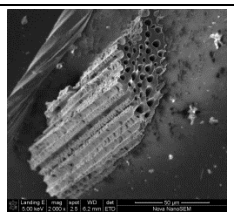	nd

y – Average of 6 samples, z - Average of 3 samples, w - Average of 1 sample and x - Average of 4 samples

Figure 5.8 shows an enlarged monograph for ACF treated with $ZnCl_2$ and H_3PO_4, under low temperature and reduced activation time. These ACF were further studied in the subsequent results section.

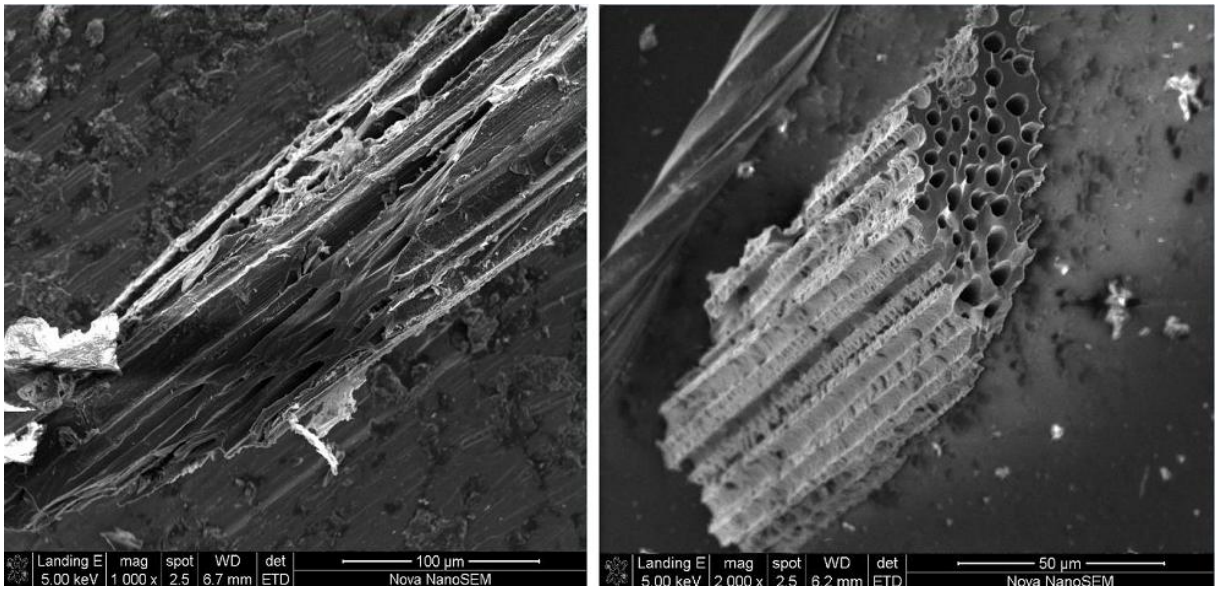

Figure 5.8: From left to right SEM photographs of sisal based ACF treated with H_3PO_4 and $ZnCl_2$ at 0.73 M and 1.59 M respectively

5.2.3.2 FTIR analysis

Assisted physical adsorption, under high-energy intensity when sonication is used, can result in the formation of vapour, particularly when the temperature of the liquid is raised. Several samples were analysed using FTIR, to ascertain that PFCs were actually adsorped to, that is, attached, to the ACF. This analysis was performed to ascertain whether or not there had been removal of PFOA and PFOS from the solution onto the ACF. The FTIR of ACF after adsorption results is illustrated in Figure 5.6 and 5.7. Repeatedly, a band appeared in all samples from adsorption experiments, which was located at 1400 cm^{-1}, a wavelength associated with C-F structural bonds. This peak was prevalent (see Figure 5.5) in all samples studied, and was repeatedly displayed in all of the ACF assessed, post adsorption.

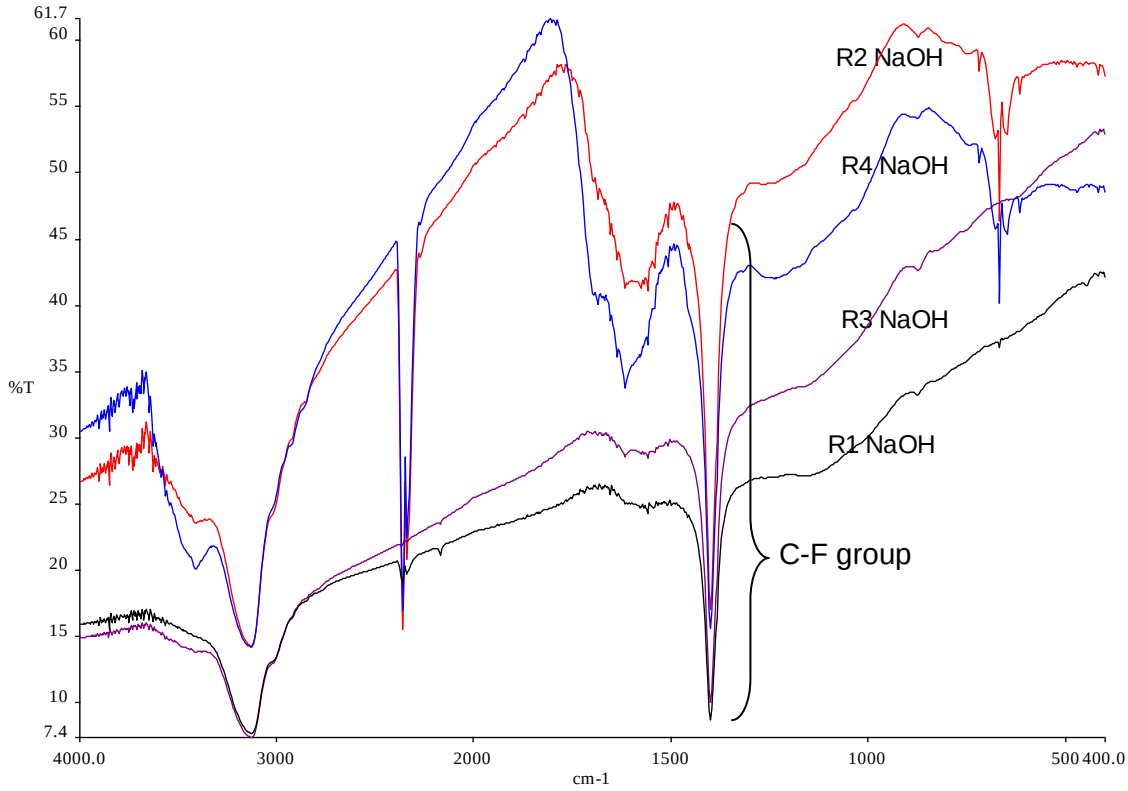

Figure 5.9: **FTIR spectra of ACFs, indicating C – F structural bonds**

Since the objective of treating the ACF was to detect if there was loading of PFOA and PFOS on to the ACF, the focus was then directed to the alkyl halides group present in the fibre. Untreated sisal was used as control to determine whether the C-F group did exist. The FTIR of one sample, named 'Dried Sisal B', which was not used for adsorption, gave a different result, where the 1400 cm^{-1} band was not present as illustrated in Figure 5.7. It was therefore justified to hypothesise that the C-F bond present in ACF used for PFC adsorption, was as a result of either PFOS or PFOA. As the C-F group was not present in the FTIR samples of the sisal fibre used in control studies. This can be used as an illustration that the successful adhesion of PFOA and PFOS can be achieved using the ACF prepared in this study.

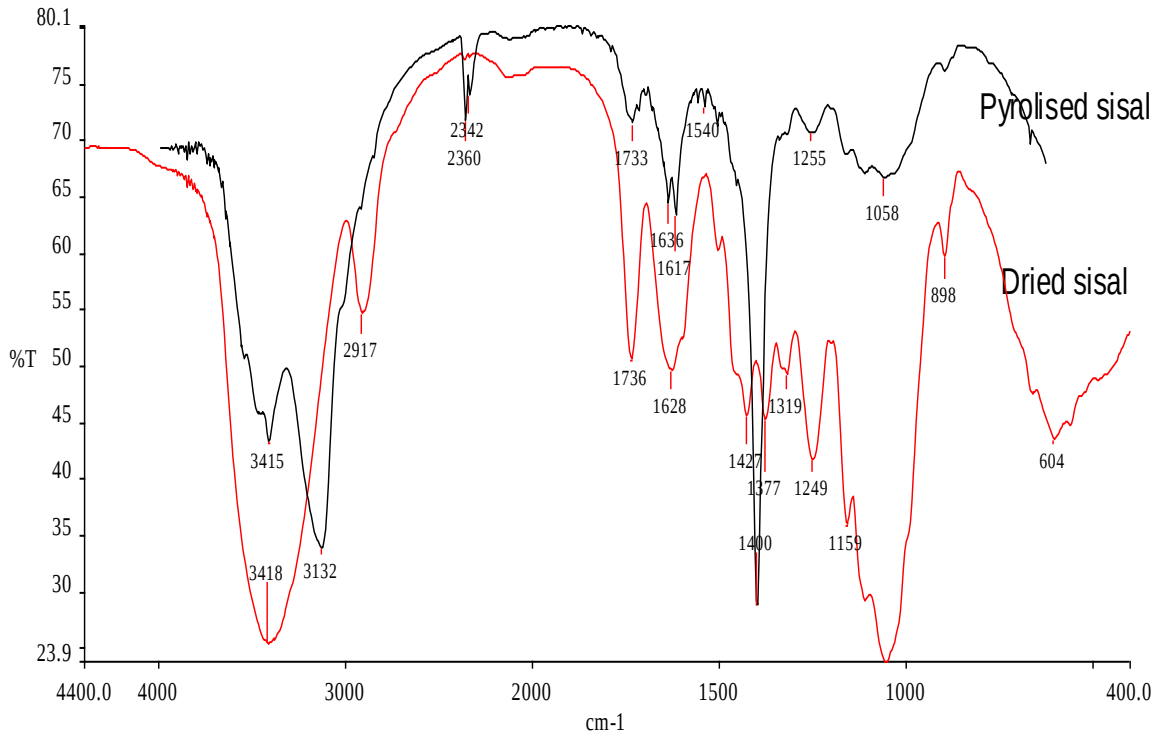

Figure 5.10: Sisal fibre FTIR patterns of ACFs

5.2.3.3 Summary

In this section, the focus was on the removal of PFOA and PFOS by adsorption using ACF produced. Analysis on the residual PFOA and PFOS was quantified in the remaining solution after adsoprtion. The results obtained proved that 14 ACF samples out of 49 samples prepared in this study could remove both PFOA and PFOS from polluted drinking water. Samples that removed PFOA and PFOS with the lowest removal rate were 75.94 (R3) and 98.74 (R3) % those with the highest removed were R5 and R7, although these samples had a low yield, respectively.

Besides analysing PFCs' concentration in the water used, including in the remaining solution after the adsorption process, an analysis with FTIR was used which showed that a 1400 cm^{-1} band appeared in all samples that underwent the adsorption process. A band at 1400 cm^{-1} is assigned to the C-F alkyl halides group and alkanes associated with PFCs, particularly as most hydrogen atoms were replaced with fluorine in PFCs to increase the stability of these compounds. Finally, it was concluded that PFOA and PFOS loading on ACF prepared under various conditions, was successfully achieved. Therefore samples R9 and R2 which indicated 100% and 99.55% for PFOA/PFOS adsorption and 99.94% and 99.74%, respectively, were used for surface area analysis – see section 4.5 for methodology. Consequently, samples R9 and R2 were used in the subsequent results section, based on 1) high yield, and 2) PFOA and PFOS removal.

5.3 Characterisation of surface properties for the *Agave sisalana*-ACF with a higher removal capacity for PFOA and PFOS

5.3.1 Introduction

Surface characterisation is a very important parameter used to analyse porous materials and is applied in numerous fields of research, in particular for adsorbents used in the removal of contaminants. Surface property characterisation of a material is a process, whereby detailed properties such as total surface area, pore diameter, and pore type (including pore distribution) are quantified. With regard to the current study, characterisation was performed on ACF, which had the best adsorbent properties for both PFOA and PFOS (see Section 5.1 and 5.2). Numerous studies have been conducted worldwide (see Table 2.5) using a variety of cellulosic feedstock pyrolysed to attain a variety of activated sorbents. The sorbents of interest were those which were converted into activated carbon (Al-Asheh *et al.*, 2000; Baquero *et al.*, 2003; Yagmur *et al.*, 2008; Mestre *et al.*, 2011; Vargas *et al.*, 2011). This section therefore presents the results of the ACF's surface area characteristics and pore properties.

5.3.2 Aims and objective

The objective for this section of the study was too primarily:

Characterise the surface properties of the sisal ACF with a higher removal of PFOA and PFOS.

5.3.3 Results and discussion

5.3.3.1 Surface area determination

With regard to the characterisation of ACF samples produced during this study, four models were used to evaluate surface area, pore size and pore volume. These models were: Brunauer-Emmett-Teller, Horvath–Kawazoe, Dubinin–Radushkevich and Dubinin–Astakhov. Based on the report of the analysis, it was found that the samples produced in this work had mostly micropores and almost no mesopores. Of the models mentioned above, the Dubinin–Astakhov isotherm was used to evaluate the micropore surface area for this study, compared with other studies where specifications were given of the stratification of AC pores, such as macropores (> 500 Å), mesepores (20 – 500 Å) and micropores (< 20 Å) (Pelekani & Snoeyink, 1999), with sizing related to the pore's diameter. In order to perform this analysis, low pressure CO_2 adsorption at 0°C was used to describe the pore size and surface characteristics of the ACF. The Dubinin–Astakhov equation can be used to linearize adsorption data

that generate curved Dubinin–Astakhov plots. Micropore volumes found using the Dubinin–Astakhov equation agreed with the total volume generated by the nitrogen adsorption method which occurs at - 196°C for all activated carbon studies (Ghosal & Smith, 1996).

The ACF prepared with $ZnCl_2$ at the concentration of 1.59M had a micropore surface area of 1036 m^2/g with a limiting volume of 0.32 cm^3/g while the one prepared with KOH at the concentration of 0.54M had a micropore surface area of 1285m^2/g with a limiting volume of 0.39 cm^3/g. In a study on the production of activated carbon from olive industry waste using NaOH, Na_2CO_3, HCl, H_2SO_4, H_3PO_4 and KOH, H_3PO_4 and KOH, KOH was reported to be the best activation reagent when it comes to the adsorption of trace contaminants in water (Ounas *et al.*, 2009). In this study the focus was on ACF made from KOH, which was then used for, electro-physico-chemical adsorption kinetics – see Section 5.4. The physical properties of the ACF in this section of the study are listed in Table 5.4. – See table 5.2 and section 5.2.3.3 for the reasons associated with the selection of these ACFs.

Table 5.4: Physical properties of *Agave sisalana* ACF

Property	$ZnCl_2$ [1.59 M] (R9)	KOH [0.54 M] (R2)
Surface area (m^2g^{-1})*	1036.76	1285.83
Micropore volume (cm^3g^{-1})	0.097	0.13
Total pore volume (cm^3g^{-1})	0.32	0.39
Microporosity (%)	30.36	34.16
Average micropore width (Å)	(3.7 – 8.04)	(3.7 – 8.21)

*Determined using Dubinin – Astakhov Isotherm

Activated carbon fibre emanating from sisal prepared with $ZnCl_2$ and KOH provided micropores with a suitable width for the adsorption of PFOA and PFOS. In this study, ACF from sisal produced a micropore- material with a distribution pore of about 8 Å, which was reported in another study by Chen *et al.* (2005), who achieved an ACF with a similar pore diameter.

The well-known method of measuring surface area on porous material is by using the BET isotherm, which is based on physical adsorption and/or entrapment of gases onto pores on solid matrices. However, BET doesn't respond very well when it comes to the measurement of microporous materials. There are other models that give a better fit on characterisation of micropores, such as the MP, Dubinin–Radushkevic, Dubinin–Astakhov, and Horvath–Kawazoe isotherms. In this study the method that provided the best result was the Dubinin–Astakhov isotherm which is associated with Density Functional Theory (DFT) which is a porosity distribution method which confirms the presence of micropores (Webb & Orr, 1997).

DFT is a molecular model of adsorption which provides an accurate description of adsorption phenomenon. This model is based on the intermolecular potentials of fluid-fluid and fluid-solid interactions thus allow the construction of the adsorption isotherms in model pores (Ravikovitch, 1998). The density functional theory is used in adsorption to incorporate a random distribution of pore wall thickness in the solid (Bhatia, 2002).

The reason for using the CO_2 method was that all the samples produced at the beginning of this study and analysed with the N_2 method were providing a very small surface area with inconclusive results, and P/P_0 profiles which have been observed and or reported in any other study before. While proceeding with the analysis of samples, the equilibrium could not be reached after an extended period of time. For this study, the adsorption of CO_2 and N_2 on organic matter (sisal before ACF), took six weeks to reach the equilibrium and the surface area evaluated was low. It was confirmed that the diffusion rate of N_2 molecules into micropores was incredibly slow and it seems that under those conditions the pores were inaccessible to N_2 molecules. This proved N_2 was not a suitable gas to analyse materials with smaller pore sizes, while CO_2 was determined to be the best alternative (De Jonge & Mittelmeijer-Hazeleger, 1996; Ghosal & Smith, 1996; Webb & Orr, 1997; Lu & Sorial, 2004). Additionally, the usefulness of CO_2 at 0°C for the characterisation of the porous carbons indicated that surface characterisation using N_2 at - 196°C presented an impossibility of obtaining an isotherm that could be used to quantify the required surface characteristic parameters, owing to the size of the pores and their narrow shape. In other studies, CO_2 was recommended for characterisation of microporous materials (Lozano-Castelló *et al.*, 2004). Some studies have used the CO_2 method at 0°C instead of N_2 for the characterisation of the pores (micropores). It was decided to adapt the CO_2 method for this study, as it had also been used in other similar studies (De Jonge & Mittelmeijer-Hazeleger, 1996). Additionally McLaughlin (from Micrometrics Analytical Service, personal communication) supported the hypothesis that N_2 cannot be distributed into micropores when compared with CO_2 at 0°C. Figure 5.11 illustrates an adsorption profiles obtained.

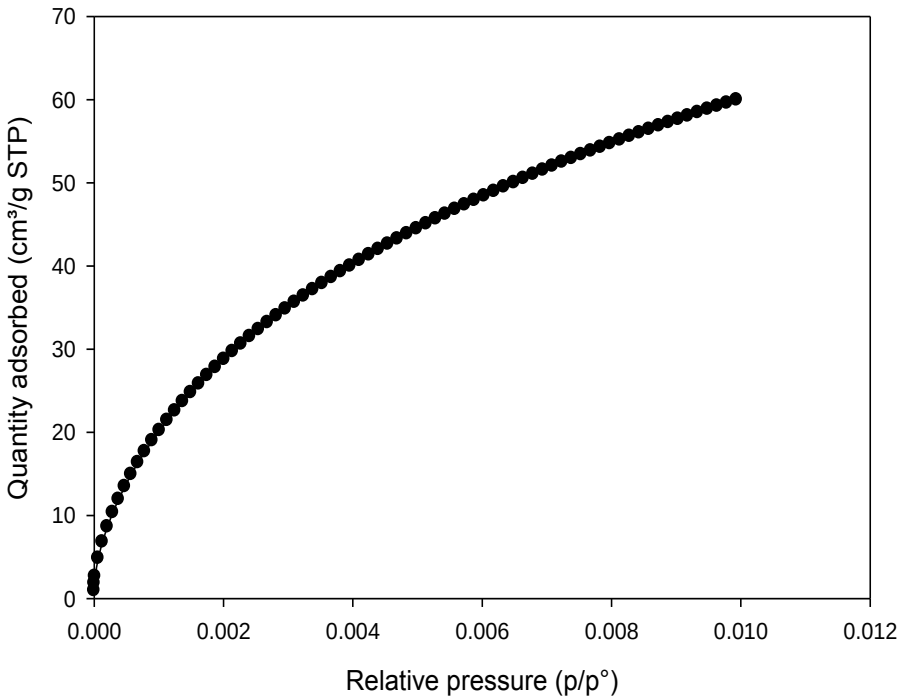

KOH [0.54 M]

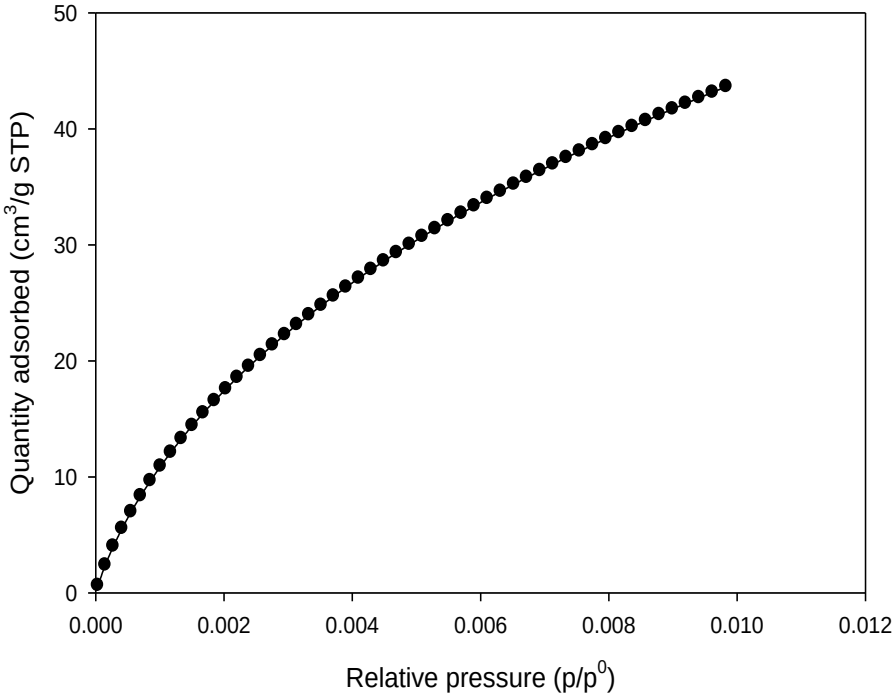

$ZnCl_2$ [1.59 M]

Figure 5.11: CO_2 adsorption isotherm at 0°C for AFC treated with 0.54 M KOH and 1.59 M $ZnCl_2$

Among the CO_2 methods mentioned above, Dubinin–Radushkevich and Dubinin–Astakhov are similar; however, the Dubinin–Astakhov method linearised the adsorption data better than the Dubinin–Radushkevich, for which the correlation coefficient (R^2) was 0.99 in this study. Looking at the plot displayed in Figure 5.11, it can be seen that the CO_2 used generated Type I isotherm as explained in Chapter 3. The figure 5.11 adsorption isotherm of the form Type I, is a characteristic representation of a microporous material (Lozano-Castelló *et al.*, 2004). The curve of the isotherm suggested that shapes of pores are slits and not cylindrical or narrow. On the other hand, CO_2 seems to be well adsorbed by the ACF as the energy requirements for adsorption increased even at lower pressure. Table 5.5 lists all surface characterisation conditions and results from generated instrumentation reports.

Table 5.5: Surface characterisation conditions and results

Conditions:	
Adsorptive gas: CO_2	
Bath temperature: 0 °C	
Method used to calculate total surface area: Dubinin–Ashakhov Isotherm*	
Sample 1: Feedstock – *Agave sisalana*	Activation reagent $ZnCl_2$ [1.59 M]:
Surface area (m^2/g):	1036.7592
Equivalent pore width (range):	8.415906 – 10.958997Å*
Roasting time (min):	45
Temperature (°C):	850
Sample mass (g):	0.2767
Cold free space (cm^3):	23.3755
Warm free space (cm^3):	22.2096
Low pressure dose (mmol/g):	0.04461
Equilibrium intervals (second):	15
Sample density (g/cm^3):	1
Sample 2: Feedstock – *Agave sisalana*	Activation reagent KOH [0.54 M]:
Surface area (m^2/g):	1285.8333
Equivalent pore width (range):	10.031130 – 10.967264 Å*
Roasting time (min):	113
Temperature (°C):	650
Sample mass (g):	0.1997
Cold free space (cm^3):	22.8056
Warm free space (cm^3):	21.6984
Low pressure dose (mmol/g):	0.04461
Equilibrium intervals (seconds):	15
Sample density (g/cm^3):	1

*Pore sizes suited for PFOA and PFOS adsorption (Erkoç & Erkoç, 2001)

5.3.4 Summary

In this section the characterisation of the adsorbent produced during this study was investigated. Information regarding the shape, pore volume, pore-size distribution and sur-

face area was quantified. The ACF produced provided a very high surface area and was determined to be suitable.

5.4 Removal of PFOA and PFOS from drinking water using *Agave sisalana* activated carbon fibre: an electro-physico-chemical adsorption method

5.4.1 Introduction

In the last decade, PFCs have become a general concern for environmentalists worldwide; they result in environmental deterioration, as they have been observed to be potential sources of contamination throughout the food chain. They are found in trace quantities in the environment, because they emanate from a chain of various industrial processes. PFCs, PFOA and PFOS, including other well-known contaminants, were targeted POPs for various studies, in particular, their removal from water, as these compounds are very difficult to remove from water using conventional treatment systems.

In order to remove these pollutants from a water system, many methods have been used; only adsorption has provided a good rate of removal to date. Additionally, activated carbon has proved to have the best adsorbent with excellent removal rates. However, when activated carbon was used for PFOA and PFOS removal, the rates were poor, both when electrolysis and sonication were used. There have been no studies on the removal of PFOA and PFOS using an electrolytic cell in combination with sonication simultaneously, a process described as electro-physico-chemical adsorption in this study.

In this section, the focus was on the removal of PFOA and PFOS using sisal-based activated carbon fibre produced in this study as an adsorbent in an electro-physico-chemical system. Samples with better surface area properties, i.e. R2 (KOH – 0.54 M) was used – see section 5.1 to 5.3 for reasons associated with the selection of this sample.

5.4.2 Aims and objective

The objective for this section of the study was to:

- Model adsorption kinetics and determine associate model parameters for PFOA and PFOS adsorption on to the sisal-based ACF using an electro-physico-chemical adsorption method for rapid removal of PFOA and PFOS from drinking water.

5.4.3 Results and discussion

The adsorptive capacity of the commercial activated carbon and ACF was assessed by fitting experimental data to Langmuir and Freundlich isotherms. These isotherms were explained in detail in Chapter 3. The correlation co-efficient showed that the adsorption of PFOA and PFOS from polluted tap water using ACF and activated carbon, fitted the Freundlich model better with $R^2 = 0.99$, while the fit with the Langmuir model had $R^2 = 0.83$ to 0.95. The related model parameters are listed in Table 5.6.

The adsorption of PFOS can be described as a chemisorption type based on the value of exponent *n* obtained when assessing the kinetic parameters using the Freundlich isotherm. This type of sorption mechanism involves a chemical reaction between the adsorbent and the adsorbate. It was previously suggested that fluorinated materials can decompose when in an electrolytic cell, particular when appropriate electrodes are used. Although gas samples were not collected, it is highly unlikely that the defluorination of PFOS occurred, as gaseous by-products in the form of bubbles were not observed at either electrodes used. Furthermore, when a chemisorptions kinetic mechanism occurs, it is likely that the reusability of the adsorbent might be hampered due to the binding energy required to be overcome in order to desorp the PFCs from the adsorbent such that the adsorbent can be reused.

In this study, PFOS had a higher adsorption affinity when compared to PFOA both when ACF as well as ACP are used. However, it was observed from the ACF plot that the equilibrium was reached at 60 min with minor increases observed thereafter.

Activated carbon presented a higher adsorption capacity compared with the ACF produced in this study as displayed in Table 5.6 and 5.7 and in Figure 5.14 and 5.15. It was clearly visible that there were two types of adsorption isotherms taking place on the sorbents, a single layer (ACF) and a multilayer (commercial AC). This phenomenon is similar to that observed by Philip (2006). However, the adsorption process was rapidly achieved using ACF when compared with previous studies, with equilibrium being reached after 60 min. Previously (-section 5.4/Table 5.6), it was demonstrated the PFOS/PFOA concentrations being observed in Western Cape Drinking Water Treatment Plants can be successfully removed by the ACF produced. This is because the generated adsorption profiles indicated a favourable adsorption profiles, an indication that, even at lower PFC concentrations, a higher quantity of the pollutants can be adsorbed onto the ACF.

Table 5.6: Adsorption kinetics and model parameters determined using the linearised Langmuir and Freudlich isotherms

Adsorption kinetics

Activated carbon fibre

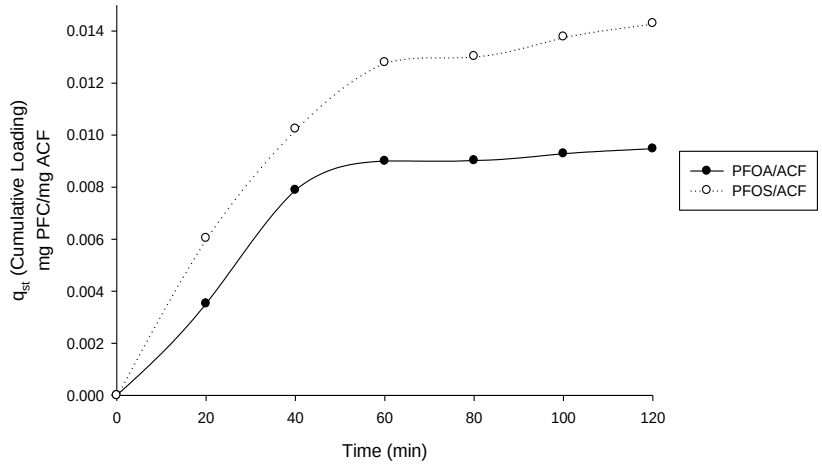

Figure 5.12: Cumulative loading profile for ACF

Activated carbon powder

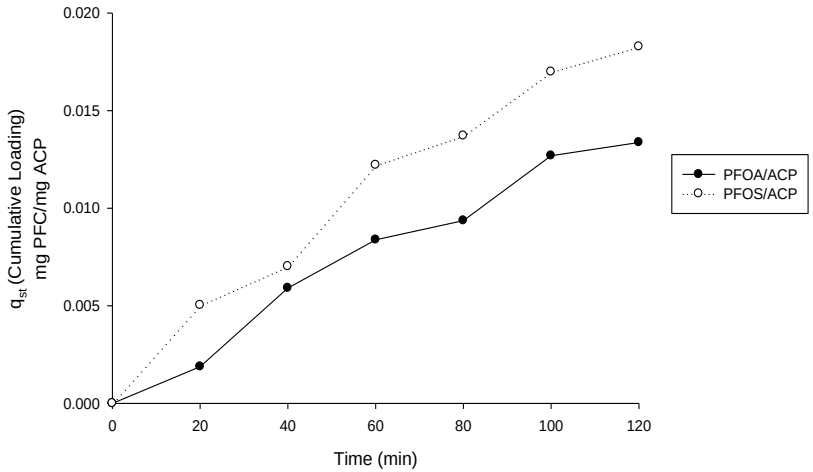

Figure 5.13: Cumulative loading profile for ACP

Adsorption kinetic parameters

Langmuir

ACF				ACP			
Contaminants	**b [mg^{-1}]**	**Q_0**	**R^2**	**Contaminants**	**b [mg^{-1}]**	**Q_0**	**R^2**
PFOA	0.011	0.051	0.87	**PFOA**	n/d	n/d	n/d
PFOS	0.019	0.043	0.95	**PFOS**	0.064	0.005	0.99

Freundlich

ACF				ACP			
Contaminants	**K_F**	**n**	**R^2**	**Contaminants**	**K_F**	**n**	**R^2**
PFOA	0.0000031	0.54	0.83	**PFOA**	0.000014	0.63	0.99
PFOS	0.0003	1.03	0.95	**PFOS**	0.00098	1.4	0.99

In other studies, similar adsorption kinetics were obtained with a similar PFOA and PFOA concentration being adsorbed only after >120 min. A larger quantity of ACF can then be used under similar adsorption conditions using an electro-physico- chemical cell for high concentrations of PFCs and to process a larger volume of water. From the observations, the monolayer adsorption achieved using ACF, occurred on a certain number of sites available, when compared with the commercial ACP, which might have had a higher surface area. After adsorption, the remaining solution from the commercial AC sample contained a black residue which required centrifugation and filtration to take samples for further analysis; whilst this was not observed for ACF samples.

Thus the higher removal percentage for commercial activated carbon compared with ACF was hypothesised as due to the fact that the sonication was continuously breaking the AC into finer particulate matter, thus making more sites available for the adsorption of both PFOA and PFOS. This also explains why a multilayer profile was obtained. This meant that the retainment of the structural integrity of the ACF could result in the definite number of sites being available for which there was no further adsorption occurring. In addition, the q_s value which justifies the adsorption capacity supports the hypothesis that PFOS has a higher affinity for both sorbents used in this study ($q_{s/PFOS} > q_{s/PFOA}$). There was confirmation that this kind of phenomenon is fairly common, as a study that was carried out on the sorption of several PFCs in the presence of an ultrasound obtained similar results whereby $q_{e/PFOS} > q_{e/PFOA}$, even in the presence of other PFCs (Zhao *et al.*, 2011).

Overall, it was clear that using a larger quantity of ACF achieved suitable sorption rates, with greater than 53% being adsorbed using ACF.

Table 5.7: Percentage removal of PFOA and PFOS from tap polluted water with ACF

Sample Name	PFOA		PFOS		Time	% removal	
	Calc. Conc.		Calc. Conc.		(min)	PFOA	PFOS
KFP0	106.141167	mg/L	100.144789	mg/L	0	0	0
KF1	92.838803	mg/L	77.36552	mg/L	20	12.53271	22.74633
KF2	76.391983	mg/L	61.523586	mg/L	40	28.02794	38.56536
KF3	72.185936	mg/L	52.785909	mg/L	60	31.99063	47.29041
KP4	72.090836	mg/L	51.891404	mg/L	80	32.08023	48.18362
KF5	71.110049	mg/L	49.070465	mg/L	100	33.00427	51.00048
KF6	70.388271	mg/L	47.126637	mg/L	120	33.68429	52.9415

Table 5.8: Removal of PFOA and PFOS from tap polluted water with granulated activated powder

Sample Name	PFOA		PFOS		Time	% removal	
	Calc. Conc.		Calc. Conc.		(min)	PFOA	PFOS
KFP0	106.141167	mg/L	100.144789	mg/L	0	0	0
KP1	99.052947	mg/L	81.175934	mg/L	20	6.678106	18.94143
KP2	83.874524	mg/L	73.663673	mg/L	40	20.97833	26.44283
KP3	74.525731	mg/L	54.104199	mg/L	60	29.78621	45.97402
KP4	70.837118	mg/L	48.420205	mg/L	80	33.26141	51.6498
KP5	58.279195	mg/L	36.087935	mg/L	100	45.09275	63.96424
KP6	55.718786	mg/L	31.216978	mg/L	120	47.50502	68.82816

5.4.4 Summary

In this section, experimental data for adsorption kinetics proved that PFOA and PFOS were removed from polluted water using commercial activated carbon and ACF produced from *Agave sisalana* treated with KOH. Both sorbents showed an ideal fit when the Freundlich isotherm was used in comparison to the Langmuir isotherm. On the other hand, the cumulative loading of PFOA and PFOS was also explored. It was hypothesised that the prevalence of PFOS adsorption might have been due to a chemisorption phenomena taking place on a reactive surface (ACF).

CHAPTER 6
OVERALL DISCUSSION AND CONCLUSION

6.1 Overall discussion

The study set out to explore the concept of *Agave sisalana* being used as raw material for the production of activated carbon fibre for the removal of PFOA and PFOS. The investigation has offered a different perspective on the feasibility of removing PFCs and PFOA/PFOS simultaneously, using a new electrolyte sonication for rapid adsorption of these common water contaminants.

Among existing methods for the manufacture of activated carbon, chemical activation combined with carbonisation was used. The selection of activation reagent was done, based on four reagents, NaOH, KOH, H_3PO_4 and $ZnCl_2$, substantiated by the literature reviewed. Experiments revealed that the activation process took place when these reagents were used. However, the concentration and application of the chemicals to the sample was not a success, particularly at high concentrations. It was therefore decided to select a concentration that could maintain the carbon skeleton of the sisal intact through the carbonisation and activation process on the one hand. On the other hand, the application method of the activation chemicals used (soaking, impregnating, immersing, etc.) didn't work. Another technique that was used, which was the spray method, provided suitable formation of the pore profile required in comparison with the impregnation previously used. To the best of the researcher's knowledge, spraying as a method of applying chemicals for the activation process in activated carbon manufacturing has not yet been reported. A similarity in the pore distribution in the results was observed regarding the concentrations used for NaOH and KOH, as well as H_3PO_4, based on the SEM micrographs. The adequate concentration for NaOH, KOH, H_3PO_4 was 0.625 0.54, 0.73 and 1.59 M respectively.

Agave sisalana has been used to manufacture activated carbon in several studies around the world. It was proved in these studies that ACF based on sisal was able to remove pollutants from water. To the best of the researcher's knowledge, ACF-based sisal hasn't been reported for the removal of PFCs in general and PFOA and PFOS in particular. In this study, it was proved that ACF-based sisal produced in this work removed PFOA and PFOS from water. The removal rates were above 98% for both PFOA and PFOS under sonication conditions.

The adsorption of PFOA and PFOS was observed on both commercial activated carbon and ACF. However, commercial activated carbon presented a high removal percentage for PFOA and PFOS, in comparison with ACF when adsorption was used with sonication in

an electrolytic cell. The data profile indicated that different types of adsorption took place on commercial activated carbon and ACF. On commercial activated carbon, a multi-layer type of adsorption occurred, while on ACF, a monolayer type was observed. This substantiates the fact that there is more loading of PFOA and PFOS on commercial activated carbon compared with ACF. However, the affinity of PFOA and PFOS was similar, whereby the adsorption of PFOS was greater compared with PFOA.

The samples that provided the highest percentage removal for both PFOA and PFOS were then characterised. Generally, characterisation of porous materials is done with N_2 at 0°C, but where the pore size couldn't allow for gas adsorption in the pores, an alternative method was developed and used to overcome this constraint. CO_2 at 0°C was a better option that provided properties of the ACF produced. ACF produced in this work provided a very high micropore structure. The Dubinin–Astakhov model was used to determine micropore size and micropore diameter respectively. The ACF sample prepared with KOH at the concentration of 0.54 M with a micro-surface area equivalent to 1285 m^2/g and pore width between 3.7 and 8.21 with 35% microporosity, was determined to be the best sorbent.

After isolating the best sorbent, a kinetics study was performed for both commercial activated carbon and ACF. The most used isotherm to determine the adsorption ability of a material is Langmuir and Freundlich isotherms. Based on experimental data, both models seemed to work and described the adsorption occurring on the sorbents used in this study. However, the Freundlich presented the best fit with R^2 being ~1.

6.2 Overall conclusion

The manufacture of activated carbon by chemical activation requires the use of chemicals. In order for these chemicals to operate as expected by creating pores, this research provided an adequate concentration for the chemical reagents selected. Samples prepared with KOH present the best percentage removal for PFOA and PFOS, where the satisfactory concentration for KOH was 0.54 M.

In spite of diverse chemical reagents used for the chemical activation process of sisal while producing activated carbon fibre for this study, this research reported that PFOA and PFOS were effectively removed from polluted tap water. This study demonstrated that an activated carbon fibre based *Agave sisalana* successfully removed PFOA and PFOS.

Several samples of ACF were generated based on the chemical reagent and conditions of manufacturing (temperature and activation time); thus subsequent to adsorption process one sample was selected among numerous others. The selected sample was

treated with KOH under the following conditions: 0.54 M, 650 °C and 1hr 53 minutes of activation time. Analysed in a porosimeter with CO_2 at 273 K, the ACF produced in this study was reported to be mostly microporous. Dubinin–Astakhov and Horvath–Kawazoe models were used to determine microporous surface area (1285m^2/g) and a suitable pore diameter was achieved.

The adsorption process is based on mathematical models that predict the type of adsorption that is taking place. Generally, adsorption is represented by Langmuir and Freundlich models for most of the research reported in the literature. The sorbent generated in this study provided the best fitting with the Langmuir model in comparison with the Freundlich model, with R^2 equivalent to 1 and 0.9863. In addition, ACF allowed a monolayer-type adsorption to be observed.

The contribution to the advancement of knowledge in this area of research is as follows:

1) Manufacture of sisal ACF (OD < 100 µm) with a porous structure.
2) Development of a method for the analysis of surface characteristics for the sisal-based ACF, using CO_2 at 0°C, a method scarcely reported in literature.
3) Design and operation of an electrolytic-sonication cell for rapid PFOA and PFOS.

6.3 Recommendation

The scale of this investigation is therefore extensive and multifaceted. To generate achievable improvement with regard to the assortment of the research, further research may be initiated by exploring the following aspects:

1) Temperature of the batch while adsorption is taking place.
2) Removal of other PFCs than PFOA and PFOS.
3) Investigation of the possibility of the removal of PFCs in solution in the presence of metals.
4) Evaluation of the removal affinity with other organic pollutants.
5) Improvement of the properties of ACF.

REFERENCES

Adinata, D., Wan Daud, W. M. A. and Aroua, M. K. 2007. Production of carbon molecular sieves from palm shell based activated carbon by pore sizes modification with benzene for methane selective separation. *Fuel Processing Technology,* 88: 599-605.

Al-Asheh, S., Banat, F., Al-Omari, R. and Duvnjak, Z. 2000. Predictions of binary sorption isotherms for the sorption of heavy metals by pine bark using single isotherm data. *Chemosphere,* 41: 659-665.

Ali, I. and Gupta, V. K. 2007. Advances in water treatment by adsorption technology. *Nature Protocols,* 1: 2661-2667.

Amankwah, K. and Schwarz, J. 1995. A modified approach for estimating pseudo-vapor pressures in the application of the Dubinin-Astakhov equation. *Carbon,* 33: 1313-1319.

An, H., Feng, B. and Su, S. 2011. CO_2 capture by electrothermal swing adsorption with activated carbon fibre materials. *International Journal of Greenhouse Gas Control,* 5: 16-25.

Appleman, T. D., Dickenson, E. R., Bellona, C. and Higgins, C. P. 2013. Nanofiltration and granular activated carbon treatment of perfluoroalkyl acids. *Journal of Hazardous Materials,* 260: 740-746.

Atkins, G. L. 1973. A simple digital-computer program for estimating the parameters of the Hill equation. *European Journal of Biochemistry,* 33: 175-180.

Avelar, F. F., Bianchi, M. L., Gonçalves, M. and Da Mota, E. G. 2010. The use of piassava fibers (*Attalea funifera*) in the preparation of activated carbon. *Bioresource Technology,* 101: 4639-4645.

Baquero, M. C., Giraldo, L., Moreno, J. C., Suárez, G., amp, x, a, F., Martı, nez-Alonso, A. and Tascón, J. M. D. 2003. Activated carbons by pyrolysis of coffee bean husks in presence of phosphoric acid. *Journal of Analytical and Applied Pyrolysis,* 70: 779-784.

Bartell, S. M., Calafat, A. M., Lyu, C., Kato, K., Ryan, P. B. and Steenland, K. 2010. Rate of decline in serum PFOA concentrations after granular activated carbon filtration at two public water systems in Ohio and West Virginia. *Environmental Health Perspectives,* 118: 222–228.

Benadjemia, M., Millière, L., Reinert, L., Benderdouche, N. and Duclaux, L. 2011. Preparation, characterization and methylene blue adsorption of phosphoric acid activated carbons from globe artichoke leaves. *Fuel Processing Technology,* 92: 1203-1212.

Betts, K. S. 2007. Perfluoroalkyl acids: what Is the evidence telling us? *Environmental Health Perspectives,* 115: A250–A256.

Booi, X. 2013. *Perfluorinated compounds and trihalomethanes in drinking water sources of the Western Cape, South Africa.* Unpublished Masters Dissertation, Cape Peninsula University of Technology.

Boulinguiez, B., Le Cloirec, P. and Wolbert, D. 2008. Revisiting the determination of Langmuir parameters application to tetrahydrothiophene adsorption onto activated carbon. *Langmuir,* 24: 6420-6424.

Breitbach, M. and Bathen, D. 2001. Influence of ultrasound on adsorption processes. *Ultrasonics Sonochemistry,* 8: 277-283.

Brunauer, S., Deming, L. S., Deming, W. E. and Teller, E. 1940. On a theory of the van der Waals adsorption of gases. *Journal of the American Chemical Society,* 62: 1723-1732.

Brunauer, S., Emmett, P. H. and Teller, E. 1938. Adsorption of gases in multimolecular layers. *Journal of the American Chemical Society,* 60: 309-319.

Carrott, P. J. M., Nabais, J. M. V., Ribeiro Carrott, M. M. L. and Pajares, J. A. 2001. Preparation of activated carbon fibres from acrylic textile fibres. *Carbon,* 39: 1543-1555.

Chen, P., Zhang, C., Chen, Q. and Zhou, Q. 2011. Effect factor of perfluorooctane sulfonate adsorbed on granular activated carbon in aqueous. Proceedings of the 5th International Conference on Bioinformatics and Biomedical Engineering (ICBBE), Place. IEEE: 1-4.

Chen, S., Liu, J. and Zeng, H. 2005. Structure and antibacterial activity of silver-supporting activated carbon fibers. *Journal of Materials Science,* 40: 6223-6231.

Cheng, L. S. and Yang, R. T. 1995. Predicting isotherms in micropores for different molecules and temperatures from a known isotherm by improved Horvath-Kawazoe equations. *Adsorption,* 1: 187-196.

Conter, F. E. 1903. *The cultivation of sisal in Hawaii*, Hawaiian Gazette Company.

De Jonge, H. and Mittelmeijer-Hazeleger, M. C. 1996. Adsorption of CO_2 and N_2 on soil organic matter: nature of porosity, surface area, and diffusion mechanisms. *Environmental Science and Technology,* 30: 408-413.

Deng, S., Niu, L., Bei, Y., Wang, B., Huang, J. and Yu, G. 2013. Adsorption of perfluorinated compounds on aminated rice husk prepared by atom transfer radical polymerization. *Chemosphere,* 91: 124-130.

Dural, M. U., Cavas, L., Papageorgiou, S. K. and Katsaros, F. K. 2011. Methylene blue adsorption on activated carbon prepared from *Posidonia oceanica* (L.) dead leaves: kinetics and equilibrium studies. *Chemical Engineering Journal,* 168: 77-85.

Erkoç, Ş. and Erkoç, F. 2001. Structural and electronic properties of PFOS and LiPFOS. *Journal of Molecular Structure,* 549: 289-293.

Foo, K. Y. and Hameed, B. H. 2010. Insights into the modeling of adsorption isotherm systems. *Chemical Engineering Journal,* 156: 2-10.

Fu, R., Liu, L., Huang, W. and Sun, P. 2003. Studies on the structure of activated carbon fibers activated by phosphoric acid. *Journal of Applied Polymer Science,* 87: 2253-2261.

Fu, R., Zeng, H., Lu, Y., Lai, S. Y., Chan, W. H. and Ng, C. F. 1995. The reduction of Pt(IV) with activated carbon fibers—An XPS study. *Carbon,* 33: 657-661.

Gassara, F., Brar, S. K., Tyagi, R., John, R. P., Verma, M. and Valero, J. 2011. Parameter optimization for production of ligninolytic enzymes using agro-industrial wastes by response surface method. *Biotechnology and Bioprocess Engineering,* 16: 343-351.

Ghosal, R. and Smith, D. 1996. Micropore characterization using the Dubinin-Astakhov equation to analyze high pressure CO_2 (273 K) adsorption data. *Journal of Porous Materials,* 3: 247-255.

Gil, A. and Grange, P. 1996. Application of the Dubinin-Radushkevich and Dubinin-Astakhov equations in the characterization of microporous solids. *Colloids and Surfaces A: Physicochemical and Engineering Aspects,* 113: 39-50.

Gil, A. and Grange, P. 1997. Comparison of the microporous properties of an alumina pillared montmorillonite and an activated carbon from nitrogen adsorption at 77 K. *Langmuir,* 13: 4483-4486.

Gil, A., Korili, S. and Cherkashinin, G. Y. 2003. Extension of the Dubinin–Astakhov equation for evaluating the micropore size distribution of a modified carbon molecular sieve. *Journal of Colloid and Interface Science,* 262: 603-607.

Good-Avila, S. V., Souza, V., Gaut, B. S. and Eguiarte, L. E. 2006. Timing and rate of speciation in *Agave (Agavaceae*). *Proceedings of the National Academy of Sciences,* 103: 9124-9129.

Hameed, B. H., Din, A. T. M. and Ahmad, A. L. 2007. Adsorption of methylene blue onto bamboo-based activated carbon: kinetics and equilibrium studies. *Journal of Hazardous Materials,* 141: 819-825.

Han, R., Zhang, J., Zou, W., Shi, J. and Liu, H. 2005. Equilibrium biosorption isotherm for lead ion on chaff. *Journal of Hazardous Materials,* 125: 266-271.

Hanssen, L., Rollin, H., Odland, J. O., Moe, M. K. and Sandanger, T. M. 2010. Perfluorinated compounds in maternal serum and cord blood from selected areas of South Africa: results of a pilot study. *Journal of Environmental Monitoring,* 12: 1355-1361.

Herrera, O. V. and Alvarez, S. R. 2008. Removal of perfluorinated surfactants by sorbtion onto granular activated carbon, zeolite and sludge. *Chemosphere,* 72: 1588 - 1593.

Higgins, C. P. and Luthy, R. G. 2006. Sorption of perfluorinated surfactants on sediments. *Environmental Science and Technology,* 40: 7251-7256.

Ho, Y., Porter, J. and McKay, G. 2002. Equilibrium isotherm studies for the sorption of divalent metal ions onto peat: copper, nickel and lead single component systems. *Water, Air and Soil Pollution,* 141: 1-33.

Hofmeyr, J.-H. S. and Cornish-Bowden, H. 1997. The reversible Hill equation: how to incorporate cooperative enzymes into metabolic models. *Computer Applications in the Biosciences,* 13: 377-385.

Hu, Z., Guo, H., Srinivasan, M. P. and Yaming, N. 2003. A simple method for developing mesoporosity in activated carbon. *Separation and Purification Technology,* 31: 47-52.

Hu, Z., Srinivasan, M. and Ni, Y. 2001. Novel activation process for preparing highly microporous and mesoporous activated carbons. *Carbon,* 39: 877-886.

Huang, H., C., H., Wanga, L., Ye, X., Bai, C., Simonich, M. L., Tanguay, R. T. and Dong, Q. 2010. Toxicity, uptake kinetics and behavior assessment in zebrafish embryos following exposure to perfluorooctane sulphonic acid (PFOS). *Aquatic Toxicology,* 2: 139-147.

Jain, A. K., Suhas and Bhatnagar, A. 2002. Methylphenols removal from water by low-cost adsorbents. *Journal of Colloid and Interface Science,* 251: 39-45.

Jin, H. Y., Liu, W., Sato, I., Nakayama, F. S., Sasaki, K., Saito, N. and Tsuda, S. 2009. PFOS and PFOA in environmental and tap water in China. *Chemosphere,* 77: 605-611.

Johnson, R. L., Anschutz, A. J., Smolen, J. M., Simcik, M. F. and Penn, R. L. 2007. The adsorption of perfluorooctane sulfonate onto sand, clay, and iron oxide surfaces. *Journal of Chemical and Engineering Data,* 52: 1165-1170.

Karthikeyan, T., Rajgopal, S. and Miranda, L. R. 2005. Chromium(VI) adsorption from aqueous solution by *Hevea Brasilinesis* sawdust activated carbon. *Journal of Hazardous Materials,* 124: 192-199.

Keller, J. U. and Staudt, R. 2005. *Gas adsorption equilibria: experimental methods and adsorptive isotherms*, Springer.

Kim, J.-H., Lee, C.-H., Kim, W.-S., Lee, J.-S., Kim, J.-T., Suh, J.-K. and Lee, J.-M. 2003. Adsorption equilibria of water vapor on alumina, zeolite 13X, and a zeolite X/activated carbon composite. *Journal of Chemical and Engineering Data,* 48: 137-141.

Kissa, E. 2001. *Fluorinated surfactants and repellents,* New York, Marcel Dekker.

Kongsuwan, A., Patnukao, P. and Pavasant, P. 2009. Binary component sorption of Cu(II) and Pb(II) with activated carbon from *Eucalyptus camaldulensis* Dehn bark. *Journal of Industrial and Engineering Chemistry,* 15: 465-470.

Kumar, K. V. and Sivanesan, S. 2006. Pseudo second order kinetics and pseudo isotherms for malachite green onto activated carbon: comparison of linear and non-linear regression methods. *Journal of Hazardous Materials,* 136: 721-726.

Kunacheva, C. 2009. *Study on contamination of perfluorinated compounds (PFCs) in water environment and industrial wastewater in Thailand.* Unpublished-PhD thesis, Kyoto University.

Langmuir, I. 1916. The constitution and fundamental properties of solids and liquids. *American Chemestry Society,* 11: 2221-2295.

Lee, J.-W., Kang, H.-C., Shim, W.-G., Kim, C. and Moon, H. 2006. Methane adsorption on multi-walled carbon nanotube at (303.15, 313.15, and 323.15) K. *Journal of Chemical and Engineering Data,* 51: 963-967.

Lein, N. P. H., Fujii, S., Tanaka, S., Nozoe, M. and Tanaka, H. 2008. Contamination of perfluorooctane sulfonate (PFOS) and perfluorooctanoate (PFOA) in surface water of the Yodo River basin (Japan). *Desalination,* 226: 338-347.

Lemal, D. M. 2004. Perspective on fluorocarbon chemistry. *The Journal of Organic Chemistry,* 69: 1-11.

Li Puma, G., Bono, A., Krishnaiah, D. and Collin, J. G. 2008. Preparation of titanium dioxide photocatalyst loaded onto activated carbon support using chemical vapor deposition: A review paper. *Journal of Hazardous Materials,* 157: 209-219.

Li, Y., Du, Q., Liu, T., Qi, Y., Zhang, P., Wang, Z. and Xia, Y. 2011. Preparation of activated carbon from *Enteromorpha prolifera* and its use on cationic red X-GRL removal. *Applied Surface Science,* 257: 10621-10627.

Lin, A. Y.-C., Panchangam, S. C., Chang, C.-Y., Hong, P. and Hsueh, H.-F. 2012. Removal of perfluorooctanoic acid and perfluorooctane sulfonate via ozonation under alkaline condition. *Journal of Hazardous Materials,* 243: 272-277.

Lozano-Castelló, D., Cazorla-Amorós, D. and Linares-Solano, A. 2004. Usefulness of CO_2 adsorption at 273 K for the characterization of porous carbons. *Carbon,* 42: 1233-1242.

Lu, Q. and Sorial, G. A. 2004. Adsorption of phenolics on activated carbon: impact of pore size and molecular oxygen. *Chemosphere,* 55: 671-679.

Lu, X., Jiang, J., Sun, K. and Xie, X. 2014. Preparation and characterization of sisal fiber-based activated carbon by activation with zinc chloride. *Bulletin of the Korean Chemical Society,* 35: 103.

Malik, R., Ramteke, D. and Wate, S. 2007. Adsorption of malachite green on groundnut shell waste based powdered activated carbon. *Waste Management,* 27: 1129-1138.

Mall, I. D., Srivastava, V. C., Agarwal, N. K. and Mishra, I. M. 2005. Removal of congo red from aqueous solution by bagasse fly ash and activated carbon: kinetic study and equilibrium isotherm analyses. *Chemosphere,* 61: 492-501.

Mane, V. S., Deo Mall, I. and Chandra Srivastava, V. 2007. Kinetic and equilibrium isotherm studies for the adsorptive removal of Brilliant Green dye from aqueous solution by rice husk ash. *Journal of Environmental Management,* 84: 390-400.

Mastalerz, M., Schneider, M. W., Oppel, I. M. and Presly, O. 2011. A salicylbisimine cage compound with high surface area and selective CO_2/CH_4 adsorption. *Angewandte Chemie International Edition,* 50: 1046-1051.

Melzer, D., Rice, N., Depledge, M. H., Henley, W. E. and Galloway, T. S. 2010. Association between serum perfluorooctanoic acid (PFOA) and thyroid disease in the NHANES study. *Environmental Health Perspectives,* 118: 686–692.

Mestre, A. S., Bexiga, A. S., Proença, M., Andrade, M., Pinto, M. L., Matos, I., Fonseca, I. M. and Carvalho, A. P. 2011. Activated carbons from sisal waste by chemical activation with K_2CO_3: kinetics of paracetamol and ibuprofen removal from aqueous solution. *Bioresource Technology,* 102: 8253-8260.

Midasch, O., Drexler, H., Hart, N., Beckmann, M. and Angerer, J. 2007. Transplacental exposure of neonates to perfluorooctanesulfonate and perfluorooctanoate: a pilot study. *International Archives of Accupational and Environmental Health,* 80: 643-648.

Moore, B. 2010. Overview of perfluorooctanoic acid. Proceedings of the Annual International Conference on Soils, Sediments, Water and Energy, Place.: 32.

Mudumbi, J. 2012. *Perfluorooctane sulfonate and perfluorooctanoate contamination of riparian wetlands of the Eerste, Diep and Salt Rivers.* Unpublished Masters Dissertation, Cape Peninsula University of Technology.

Mudumbi, J. B. N., Ntwampe, S. K. O., Muganza, M. F. and Okonkwo, J. O. 2014. Perfluorooctanoate (PFOA) and perfluorooctane sulfonate (PFOS) in South African river water. *Water Science and Technology,* 69: 185-194.

Ng, J. C. Y., Cheung, W. H. and McKay, G. 2002. Equilibrium studies of the sorption of Cu(II) ions onto Chitosan. *Journal of Colloid and Interface Science,* 255: 64-74.

Nikam, T., Bansude, G. and Aneesh Kumar, K. 2003. Somatic embryogenesis in sisal (*Agave sisalana* Perr. ex. Engelm). *Plant Cell Reports,* 22: 188-194.

Noel, M., Suryanarayanan, V. and Chellammal, S. 1997. A review of recent developments in the selective electrochemical fluorination of organic compounds. *Journal of Fluorine Chemistry,* 83: 31-40.

Ochiai, T., Iizuka, Y., Nakata, K., Murakami, T., Tryk, D. A., Fujishima, A., Koide, Y. and Morito, Y. 2011. Efficient electrochemical decomposition of perfluorocarboxylic acids by the use of a boron-doped diamond electrode. *Diamond and Related Materials,* 20: 64-67.

Oguzie, E. and Ebenso, E. 2006. Studies on the corrosion inhibiting effect of Congo red dye-halide mixtures. *Pigment and Resin Technology,* 35: 30-35.

Oguzie, E., Unaegbu, C., Ogukwe, C., Okolue, B. and Onuchukwu, A. 2004. Inhibition of mild steel corrosion in sulphuric acid using indigo dye and synergistic halide additives. *Materials Chemistry and Physics,* 84: 363-368.

Organisation Economic co-operation and Development (OECD). 2002. *Co-operation existing chemicals hazard assessment of perfluorooctane sulfonate (PFOS) and its salts.* ENV/JM/RD(2002)17/Final. Paris.

Parsons, J. R., Sáez, M., Dolfing, J. and Voogt, P. 2008. Biodegradation of perfluorinated compounds. *Reviews of Environmental Contamination and Toxicology Vol 196*: 53-71.

Pelekani, C. and Snoeyink, V. L. 1999. Competitive adsorption in natural water: role of activated carbon pore size. *Water Research,* 33: 1209-1219.

Pereira, M. M. and Faria, J. 2008. *Catalysis from theory to application*, *Imprensa da Universidade de Coimbra*.

Phan, N. H., Rio, S., Faur, C., Le Coq, L., Le Cloirec, P. and Nguyen, T. H. 2006. Production of fibrous activated carbons from natural cellulose (jute, coconut) fibers for water treatment applications. *Carbon,* 44: 2569-2577.

Philip, L. 2006. Water and wastewater engineering. Madras: Indian Institute of Technology.

Plumlee, M. H., Larabee, J. and Reinhard, M. 2008. Perfluorochemicals in water reuse. *Chemosphere,* 72: 1541-1547.

Qiu, Y. 2007. *Study on treatment technologies for perfluorochemicals in wastewater.* Unpublished PhD thesis, Kyoto University.

Rampey, A. M., Umpleby, R. J., Rushton, G. T., Iseman, J. C., Shah, R. N. and Shimizu, K. D. 2004. Characterization of the imprint effect and the influence of imprinting conditions on affinity, capacity, and heterogeneity in molecularly imprinted polymers using the Freundlich isotherm-affinity distribution analysis. *Analytical chemistry,* 76: 1123-1133.

Renner, R. 2001. Growing concern over perfluorinated chemicals. *Environmental Science and Technology,* 35: 154A-160A.

Rosas, J. M., Bedia, J., Rodríguez-Mirasol, J. and Cordero, T. 2009. HEMP-derived activated carbon fibers by chemical activation with phosphoric acid. *Fuel,* 88: 19-26.

Ruthven, D. M. 1984. *Principles of adsorption and adsorption processes*.

Schueller, B. S. and Yang, R. T. 2001. Ultrasound enhanced adsorption and desorption of phenol on activated carbon and polymeric resin. *Industrial and Engineering Chemistry Research,* 40: 4912-4918.

Selomulya, C., Meeyoo, V. and Amal, R. 1999. Mechanisms of Cr(VI) removal from water by various types of activated carbons. *Journal of Chemical Technology and Biotechnology,* 74: 111-122.

Senevirathna, S., Tanaka, S., Fujii, S., Kunacheva, C., Harada, H., Shivakoti, B. and Okamoto, R. 2010. A comparative study of adsorption of perfluorooctane sulfonate (PFOS) onto granular activated carbon, ion-exchange polymers and non-ion-exchange polymers. *Chemosphere,* 80: 647-651.

Shih, K. and Wang, F. 2013. Adsorption behavior of perfluorochemicals (PFCs) on Boehmite: influence of solution chemistry. *Procedia Environmental Sciences,* 18: 106-113.

Shuixia, C., Changqing, W. and Hanmin 1998. Study on the adsorption of dyes on sisal-based activated carbon fibres. *China Synthetic Fibre Industry,* 5: 21-29.

Shukla, A., Zhang, Y.-H., Dubey, P., Margrave, J. L. and Shukla, S. S. 2002. The role of sawdust in the removal of unwanted materials from water. *Journal of Hazardous Materials,* 95: 137-152.

Skutlarek, D., Exner, M. and Färber 2006. Perfluorinated surfacts in surface and drinking waters. *University of Bonn, Institute of Hygiene and Public Health,* 13: 149-158.

Steenland, K., Tinker, S., Shankar, A. and Ducatman, A. 2010. Association of perluorooctanoic acid (PFOA) and perfluorooctane sulfonate (PFOS) with uric acid among adults with elevated community exposure to PFOA. *Environmental and Health Perspectives,* 118: 229-233.

Stumm, W. 1970. *Aquatic chemistry; an introduction emphasizing chemical equilibria in natural waters.*, New York, Wiley-Interscience.

Suzuki, M. 1994. Activated carbon fiber: Fundamentals and applications. *Carbon,* 32: 577-586.

Tamai, H., Yoshida, T., Sasaki, M. and Yasuda*, H. 1999. Dye adsorption on mesoporous activated carbon fiber obtained from pitch containing yttrium complex. *Carbon,* 37: 983-989.

Tan, I. A. W., Ahmad, A. L. and Hameed, B. H. 2008. Adsorption of basic dye using activated carbon prepared from oil palm shell: batch and fixed bed studies. *Desalination,* 225: 13-28.

Tan, I. A. W., Hameed, B. H. and Ahmad, A. L. 2007. Equilibrium and kinetic studies on basic dye adsorption by oil palm fibre activated carbon. *Chemical Engineering Journal,* 127: 111-119.

Tang, C. Y., Shiang Fu, Q., Gao, D., Criddle, C. S. and Leckie, J. O. 2010. Effect of solution chemistry on the adsorption of perfluorooctane sulfonate onto mineral surfaces. *Water Research,* 44: 2654-2662.

Tongpoothorn, W., Sriuttha, M., Homchan, P., Chanthai, S. and Ruangviriyachai, C. 2011. Preparation of activated carbon derived from Jatropha curcas fruit shell by simple thermo-chemical activation and characterization of their physico-chemical properties. *Chemical Engineering Research and Design,* 89: 335-340.

Torres, F., Ochoa-Herrera, V., Blowers, P. and Sierra-Alvarez, R. 2009. *Ab initio* study of the structural, electronic, and thermodynamic properties of linear perfluorooctane sulfonate (PFOS) and its branched isomers. *Chemosphere,* 76: 1143-1149.

Tzong-Horng, L. 2011. Development of mesoporous structure and high adsorption capacity of biomass-based activated carbon by phosphoric acid and zinc chloride activation. *Chemical Engineering Journal,* 158: 129-142.

Vargas, A. M. M., Cazetta, A. L., Garcia, C. A., Moraes, J. C. G., Nogami, E. M., Lenzi, E., Costa, W. F. and Almeida, V. C. 2011. Preparation and characterization of activated carbon from a new raw lignocellulosic material: Flamboyant (*Delonix regia*) pods. *Journal of Environmental Management,* 92: 178-184.

Vargas, A. M. M., Garcia, C. A., Reis, E. M., Lenzi, E., Costa, W. F. and Almeida, V. C. 2010. NaOH-activated carbon from flamboyant (*Delonix regia*) pods: Optimization of preparation conditions using central composite rotatable design. *Chemical Engineering Journal,* 162: 43-50.

Verreault, J., Berger, U. and Gabrielsen, G. W. 2007. Trends of perfluorinated alkyl substances in herring gull eggs from two coastal colonies in Northern Norway: 1983−2003. *Environmental Science and Technology,* 41: 6671-6677.

Vijayaraghavan, K., Padmesh, T. V. N., Palanivelu, K. and Velan, M. 2006. Biosorption of nickel(II) ions onto Sargassum wightii: Application of two-parameter and three-parameter isotherm models. *Journal of Hazardous Materials,* 133: 304-308.

Wang, F. and Shih, K. 2011. Adsorption of perfluorooctanesulfonate (PFOS) and perfluorooctanoate (PFOA) on alumina: influence of solution pH and cations. *Water Research,* 45: 2925-2930.

Wang, Y., Zhang, P. Y., Pan, G. and Chen, H. 2008. Photochemical degradation of environmentally persistent perfluorooctanoic acid (PFOA) in the presence of Fe(III). *Chinese Chemical Letters,* 19: 371-374.

Webb, P. A. and Orr, C. 1997. *Analytical methods in fine particle technology*, Micromeritics Norcross, GA.

Whitacre, D. M. (ed.) 2010. *Reviews of Environmental Contamination and Toxicology Volume 208: Perfluorinated alkylated substances*: Springer.

Xiao, F., Simcik, M. F. and Gulliver, J. S. 2013. Mechanisms for removal of perfluorooctane sulfonate (PFOS) and perfluorooctanoate (PFOA) from drinking water by conventional and enhanced coagulation. *Water Research,* 47: 49-56.

Yagmur, E., Ozmak, M. and Aktas, Z. 2008. A novel method for production of activated carbon from waste tea by chemical activation with microwave energy. *Fuel,* 87: 3278-3285.

Ylinen, M., Hanhijärvi, H., Peura, P. and Rämö, O. 1985. Quantitative gas chromatographic determination of perfluorooctanoic acid as the benzyl ester in plasma and urine. *Archives of Environmental Contamination and Toxicology,* 14: 713-717.

Yu, Q., Zhang, R., Deng, S., Huang, J. and Yu, G. 2009. Sorption of perfluorooctane sulfonate and perfluorooctanoate on activated carbons and resin: kinetic and isotherm study. *Water Research,* 43: 1150-1158.

Zhao, D., Cheng, J., Vecitis, C. D. and Hoffmann, M. R. 2011. Sorption of perfluorochemicals to granular activated carbon in the presence of ultrasound. *The Journal of Physical Chemistry A,* 115: 2250-2257.

Zhou, Q., Deng, S., Yu, Q., Zhang, Q., Yu, G., Huang, J. and He, H. 2010. Sorption of perfluorooctane sulfonate on organo-montmorillonites. *Chemosphere,* 78: 688–694.

Zhou, Q., Pan, G. and Zhang, J. 2013. Effective sorption of perfluorooctane sulfonate (PFOS) on hexadecyltrimethylammonium bromide immobilized mesoporous SiO_2 hollow sphere. *Chemosphere,* 90: 2461-2466.

Zhuo, Q., Deng, S., Yang, B., Huang, J., Wang, B., Zhang, T. and Yu, G. 2012. Degradation of perfluorinated compounds on a boron-doped diamond electrode. *Electrochimica Acta,* 77: 17-22.